REPORT NR. 29

# Geographical Report of the GeoArk expeditions to North-East Greenland 2007 and 2008

Aart Kroon, Bjarne Holm Jakobsen, Jørn Bjarke Torp Pedersen, Laura Addington, Laura Kaufmann, Bjarne Grønnow, Jens Fog Jensen, Mikkel Sørensen, Hans C Gulløv, Mariane Hardenberg, Anne Birgitte Gotfredsen, Morten Meldgaard

SILA – THE GREENLAND RESEARCH CENTRE AT THE NATIONAL MUSEUM OF DENMARK 2009

**To this edition of the report**
This is the preliminary edition and will be published in the Report series of SILA, The Greenland Research Centre at the National Museum of Denmark in spring 2009 under Report nr. 29.

Questions or comments about the report can be addressed to:

Department of Geography and Geology,
University of Copenhagen
Øster Voldgade 10
1350 Copenhagen, Denmark

Aart Kroon, e-mail: ak@geo.ku.dk
Bjarne Holm Jakobsen, e-mail: bhj@geo.ku.dk
Jørn Bjarke Torp Pedersen, e-mail: jtp@geo.ku.dk

**Acknowledgements**

The GeoArk team greatly acknowledges all the support they have had during the expeditions in 2007 and 2008. Special thanks go to Danish Polar Center, National Environmental Research Institute and Greenland Commando ('Forsvaret, Grønlands Kommando': 'Vædderen' and 'Slædepatruljen Sirius') for their logistic support. The financial support of the Commission for Scientific Research in Greenland and several private funds are highly appreciated.

## Contents

## 1. Introduction

The GeoArk project explores which climatic, environmental and cultural preconditions favored the initial colonization by the Inuit people of the Thule Culture around 1400 AD and which factors triggered their disappearance around 1850 AD. Most of the former Thule settlements are located in specific coastal environments. The area of focus is North-East Greenland, at about 74-75$^0$ NB (Fig. 1.1). We try to map and correlate the geomorphologic and geologic setting with the spatial patterns of the settlements. We also try to understand in which way and at what time the regional climatic changes, indicated by changes in wind regimes, temperatures and precipitation, have determined substantial changes in snow- and ice coverage and polynya during the Thule era. Sediment cores of the upper layers in small lakes, lagoons, and on the coastal shelf are used to extract a regional climate record over the last part of the Holocene.


*Figure 1.1 Map of the area where the GeoArk expeditions in 2007 and 2008 occurred.*

A modern satellite image (Fig. 1.2), showing the characteristic mid summer coastal landscape of the study area in North East Greenland, clearly illustrates that snow and ice coverage and duration are dominating and controlling factors, influencing basic landscape geomorphology and biota, and determining conditions given immigrating Inuit's in their need for access to sufficient game species in the ice free coastal landscapes and in near coastal waters. This concept of a primarily snow and ice controlled landscape ecosystem for the understanding of the North East Greenland

cultural history governs the main topics and research questions in the geography part of the GeoArk project.

The Key Issues are:

- What are the basic geomorphology and the morphodynamics in coastal landscape in the studied region in North East Greenland?
- What are the basic environmental dynamics in the coastal ice free landscapes and in near coastal waters in North East Greenland during the Holocene with special focus on the late Holocene cultural era?
- In which way and at which time did regional climatic changes – primarily in temperatures, precipitation and wind regimes - determine changes in snow and ice coverage, ice margins and polynya during the late Holocene cultural era?
- Which relative sea level changes in the region are generally observed for the Holocene, and how did sea level changes during the cultural era of the latest 4500 years influence on coastal landscapes and Inuit settlements?

The geographers in the GeoArk team were in 2007 focused on the coastal areas where the settlements were found and they tried to reconstruct climate conditions of the area over the last centuries. The coastal morphology of the south and east coast of Clavering showed pocket beaches with actual and recent beach ridges between basaltic headlands, alternated with small deltas. Leveling surveys were made to quantify its dimensions and to reconstruct beach ridge positions and old shorelines. These data were also used to study spatial and temporal variability in erosion and accumulation patterns along the shores. Locations with recent periglacial processes around the settlements were mapped. The climate conditions of the area largely influenced the availability and accessibility of natural resources to Eskimos. The sedimentary history of small basins like lagoons, lakes and nivation niches was studied to reconstruct variations in climatic parameters. These parameters included the general temperature, especially of the summer, the snow cover, and the ice coverage in the coastal waters. Field samples of fossil soils were sampled on sites along the south coast of Clavering Ø, including cores from lakes at Eskimonæs and from the hinterland near Dahls Skær. These samples were further analyzed and dated in the laboratory. Soil samples from excavations at Fladstrand were gathered in order to correlate archaeological and geomorphologic phases at the site.

In 2008, the geographers in the team were again specifically interested in the coastal areas where the settlements were found and they tried to reconstruct climate conditions of the area over the last centuries. Many coastal settlements in different morphological settings were visited and described, like pocket beaches with actual and Holocene beach ridges between headlands at Clavering Ø, gravel spits and lagoons on Hvalros Ø, and the present day delta of Zackenberg on Wollaston Foreland. Leveling surveys and echosoundings were made to quantify the dimensions of the morphological features at land and on sea, to reconstruct beach ridge positions and to map the old and present day shorelines. These data were used to study spatial and temporal variability in erosion and accumulation patterns along the shores. Besides, they were used together with maps of solifluction lobes and other dynamic periglacial features, to understand recent changes in

and around the settlements. The climate conditions of the area largely influenced the availability and accessibility of natural resources to the Eskimo population. The sedimentary history of small basins like lagoons, lakes and nivation niches was studied to reconstruct variations in climatic parameters. These parameters included the general temperature, especially of the summer, the snow cover, and the ice coverage in the coastal waters. Field samples of fossil soils were sampled on sites along the south coast of Clavering Ø near for example Eskimonæs. Cores were taken in different lakes, like shallow bottom frozen lakes (in winter) near Revet, and deep non-bottom frozen lakes at Eskimonæs on Clavering Ø and at Germania Havn on Sabine Ø. The cores were further analyzed and dated in the laboratory with XRF scanning and other methods. Soil samples from excavations at Eskimonæs were gathered in order to correlate archaeological and geomorphologic phases at the site. Additional cores were taken on the seaward slope of the Clavering Sound off Hvalros Ø close to the location of a polynya with the help of the Danish Marine vessel 'Vædderen'. These cores will also be used to study the climate conditions over the Holocene in more detail.

The aim of this report is to describe the geographical topics that were covered in the successive expeditions. We will also give an overview of data gathered during the 2007 and 2008 GeoArk expeditions.

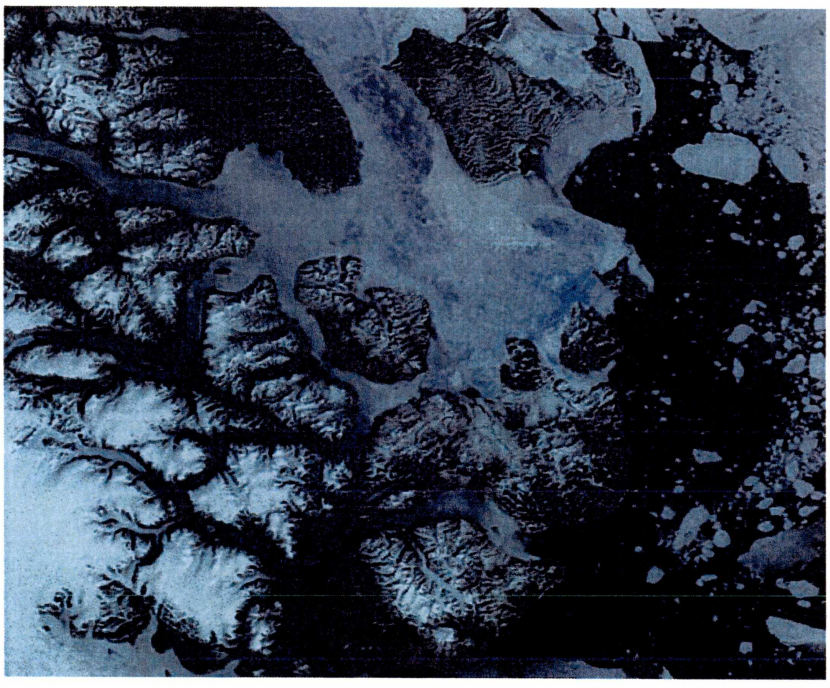

*Figure 1.2. Satellite image of the study area at Clavering Island, Wollaston Forland and Sabine Island, late July 1994. Landfast ice is still covering the outer parts of some fjords and large quantities of pack ice are drifting southward along the coast carried by the East Greenland Currrent. The pack ice plays an important role in damping the effect of swells from the North Atlantic on the coast.*

## 2. Description of the expedition area: Clavering Ø, Wollaston Forland, Sabine Ø and Hvalros Ø

### *2.1 Introduction*

The coastal areas in Northeastern Greenland have traditionally been the areas where Paleo-Eskimos and the Inuit of the Thule Culture settled in the past 4500 years. The coastal areas offered opportunities to use natural resources, like peat and stones, and offered easy accessibility to both the land-based and sea/ice-based yacht activities. The actual locations of former settlements were thus closely coupled to both ice-and-snow landscapes in the winter and coastal landscapes in summer. The local geology, upland geomorphology, and especially coastal morphology of Clavering Ø, Wollaston Forland, Sabine Ø and Hvalros Ø are outlined in this section.

### *2.2 Geology*

The geology of Clavering Ø is divided in three regions: a westerly region, a central region, and an eastern region (Fig. 2.1 after Koch and Haller, 1971). The boundary between the western and central region is formed by the valley Granatdalen in the south and Louises Elv in the north, and the boundary between the central and eastern region is formed by the valley Baesdalen in the south and Dolomit Dalen in the north. Rock formations and sediments in the western region are of carbonate origin with basaltic cores from Cretaceous-Tertiary eruptives, forming the top of the mountain ridges. The carbonate rocks of the Lower Cretaceous period are not very resistant against erosion and many small rivers deliver the weathered sediments towards the coastal zone. The rocks in the central region consist of the more resistant gneiss and granite formations of Caledonian Crystalline complexes (Migmatite Gneiss, Mica-Schist and Biotite Gneiss, and Quartzite Schist to Gneiss, Koch and Haller, 1971). The relief of this region is much more pronounced than that of its neighbors: mountains are higher and steeper and the upper parts of the mountains are covered by glaciers. Most of these glaciers constantly feed rivers in the larger valleys in summer and discharge water and sediments towards a couple of larger deltas at the end of glacial-shaped river valleys (e.g., deltas at Dødemandsbugten and Baesedalen). The Finsch Øer just south of Clavering Ø is of similar origin.
The rock formations and sediments in the eastern region have again a Cretaceous origin with basaltic intrusions from Cretaceous-Tertiary eruptives (Fig. 2.1). The mountains and valleys in the cretaceous rocks are less pronounced, but the basaltic intrusions are more resistant against erosion and form prominent cliffs and headlands in the coastal areas.

The local geology of eastern Wollaston Forland, Sabine Ø and Hvalros Ø is comparable to the eastern region of Clavering Ø. The rock formations and sediments have a Cretaceous origin with basaltic intrusions from Cretaceous-Tertiary eruptives (Fig. 2.1). The mountains and valleys in the cretaceous rocks are less pronounced, but the basaltic intrusions are more resistant against erosion and form prominent cliffs and headlands in the coastal areas. The coastal plain along southern Wollaston Forland and

Sabine Ø does have Quaternary deposits (e.g., moraines). The northeastern part of Wollaston Forland and Hvalros Ø almost solely consist of basaltic deposits.

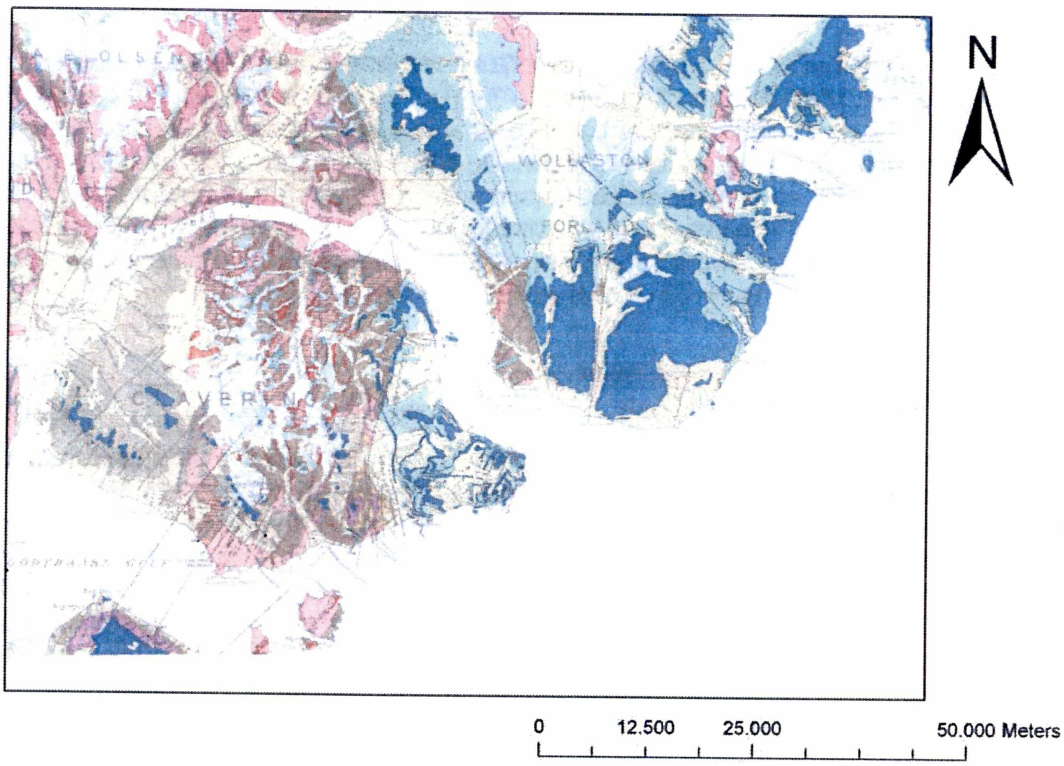


*Figure 2.1. Geological regions of Clavering Ø, Wollaston Forland, Sabine Ø and Hvalros Ø. Geological Map of East Greenland $72^0$-$76^0$ Northern Latitude (scale 1:250.000; Koch and Haller, 1971). Note three regions at Clavering Ø: 1) western region, 2) central region, 3) eastern region. Quaternary sediments (yellow), Basalt (blue), Cretaceous rocks (green), Carbonate rocks (brown) and Gneiss (pink).*

### *2.3 Geomorphology*

The geomorphology at Clavering Ø is closely related to the geological substrate (Fig. 2.2). The western and eastern regions of Clavering Ø are characterized by a number of small rivers, draining the upland area, delivering sediment towards the coastal zone, and creating mildly sloping topography in the coastal area. The hard-rock relief of the uplands in these areas is moderate and there is a lot of sediment in glacial landforms like moraines in the river valleys and coastal areas. Recent glacial and periglacial processes are all over the place. Nivation processes and the periglacial process solifluction (mass movements along the slopes, due to thaw and freeze cycles over permafrost layers), occur on many slopes and influence the local slope stability.
The relief in the central region is much more pronounced. Mountains are glaciated, the slopes of the valleys are steep and typically U-shaped (glacial). Many of the mountains in this area fringe the fjords and in most locations there is hardly any space to build up a coastal plain.

A number of deltas occur in the area (e.g., Dødemandsbugten, Lerbugten, Zackenberg, and Fig. 2.2). These deltas are formed by the water and sediment discharge from rivers and wave and ice reworking at their shoreline fringes. The selected deltas in Fig. 2.2 all match the following criteria: 1) their river system is connected to the glacier or higher regions of the area; 2) their river system has a substantial drainage basin, almost always with many tributaries in the upper area; and 3) their rivers have a substantial sediment delivery to the coastal zone. The latter creates depositional coastal features along the delta fringes like beach ridges and spits. Wave processes tend to build up elongated sandy beaches, which can be seen along the southwest and southeast coast of Clavering Ø and the southern shore of Wollaston Foreland, Close to the major river outflows, the delta often shows characteristic channel lobe switching which highly influence the erosion/accretion patterns along the shore and makes the area too dynamic for settlements.

Coastal plains are especially present at the western and eastern regions of Clavering Ø, at the Zackenberg delta and at the southern part of Wollaston Forland and Sabine Ø (Fig. 2.2). The northern central part of Clavering Ø and the southern shore of AP Olsenland is too steep and the steep slopes of the mountains are almost vertically continued into the fjords. The southern shore of region 2 (Fig. 2.2) has many capes in gneiss and granite materials. The coastal areas have not a lot of sediments available, there is mainly small influx from creeks with a limited drainage basin, quite often steep alluvial fans. There are thus pocket beaches and small creeks between the capes in gneisses and most of these pocket beaches are hanging on the steep slopes of the fjord. The northeastern part of the Wollaston Forland shore does have a large basalt outcrop and the whole shoreline is formed by a cliff without any significant coastal plain in front.

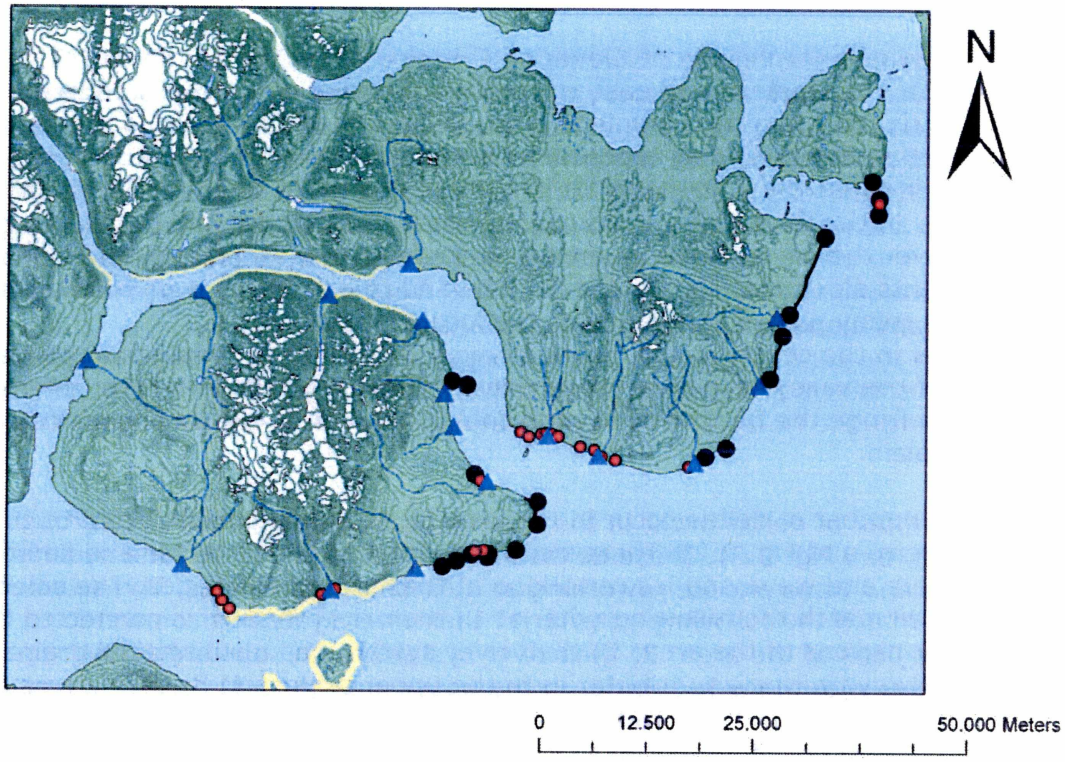


*Figure 2.2. Geomorphologic map of the area with major deltas: major deltas (blue triangle), beach ridge system (red dot), pocket beaches fringing gneiss formations (yellow line), basalt capes (black dots), and basalt cliffs (black line).*

### *2.4 Climate*

The area has a High Arctic climate with an averaged temperature during the warmest summer month below +6 °C (Hansen et al., 2008; Fig. 2.3). At the same time, the midnight sun in summer lasts 106 days and the highest temperature can be over +20 °C. In winter, a polar night of 89 days occurs and the temperature is often below -30 °C. The yearly precipitation is about 260 mm. Most of this precipitation is in the form of snow: about 10% falls as rain (Hansen et al., 2008; Fig. 2.4). The wind speed and direction shows a clear seasonality (Hansen et al., 2008; Fig. 2.5): The largest wind speeds occur in winter and come from the North. In summer, wind speeds are less and mainly come from southeasterly directions.

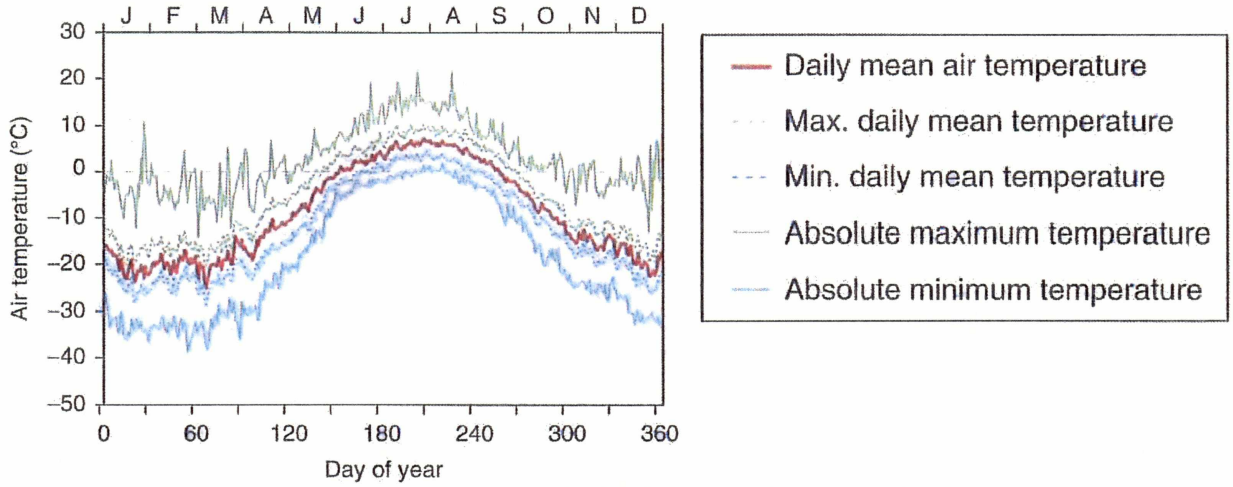


*Figure 2.3 Daily mean temperatures and absolute maximum and minimum temperatures at Zackenberg over the period 1996-2005 (Hansen et al., 2008).*

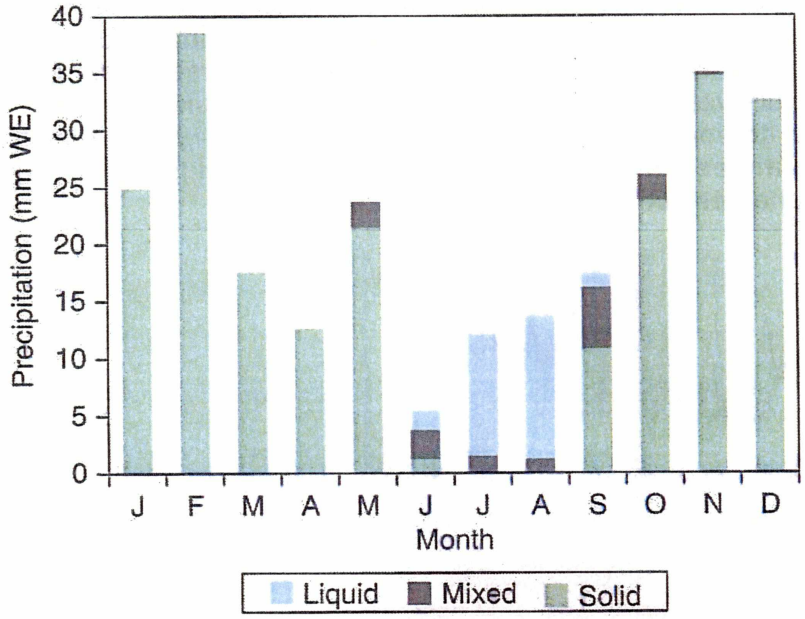


*Figure 2.4 Monthly mean precipitation at Zackenberg over the period 1996-2005 (Hansen et al., 2008). Liquid is rain and solid is snow.*

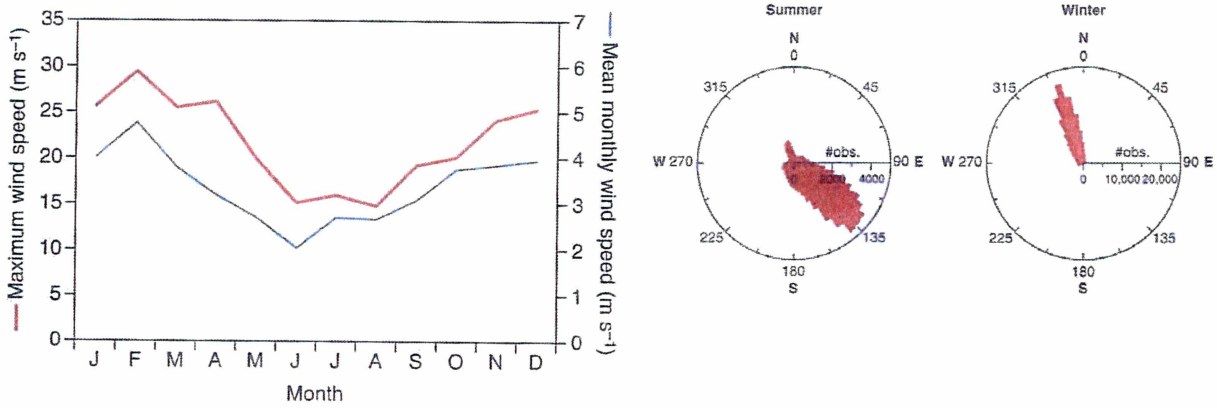


*Figure 2.5. Monthly distribution of wind speed and wind direction at Zackenberg over the period 1996-2005 (left panel), and wind roses for summer and winter conditions (right panels) (Hansen et al., 2008).*

The snow coverage on land and the ice coverage in the fjords and at the open sea have an important impact on the availability of natural recourses and the existence of people and animals in the area. Overall, most of the snowfall occurs when warm and moist air masses arrive in winter (Fig. 2.6). Large amounts of snowfall in winter can result in a shorter summer season without snow coverage, and the potential formation of ice layers in the snow pack during warm spells further makes it difficult for mammals like reindeer and musk ox to survive. Hence, snow rich periods generally makes it more difficult for flora and fauna to flourish. On the other hand, cold and dry winters might make it easier the large mammals to feed during winter and result in longer snow free land areas in summer with a positive effect for flora and fauna.

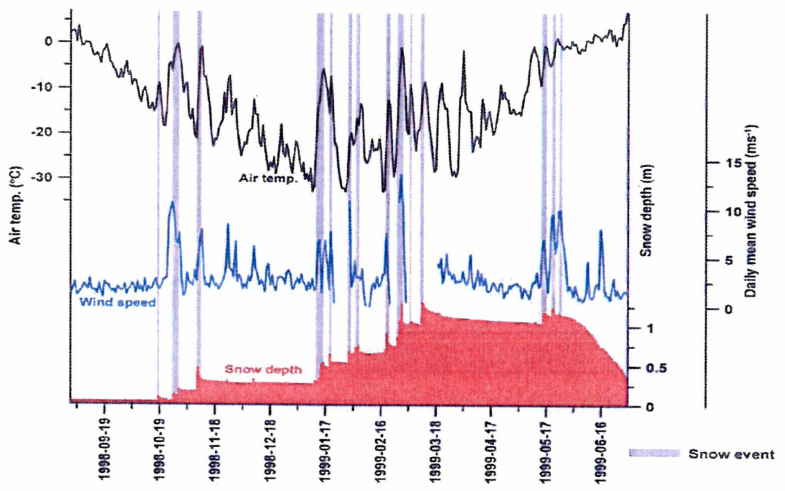


*Figure 2.6. Air temperature, daily mean wind speed and snow depth over the winter season 1998-1999 at Zackenberg (Hinkler, unpublished).*

Preliminary results in the Zackenberg area, central positioned in the area (see Fig. 1.1) show an inverse relationship between the sea ice coverage and the snow depth (Fig. 2.7) especially in the area of the triangle in Fig. 2.8.

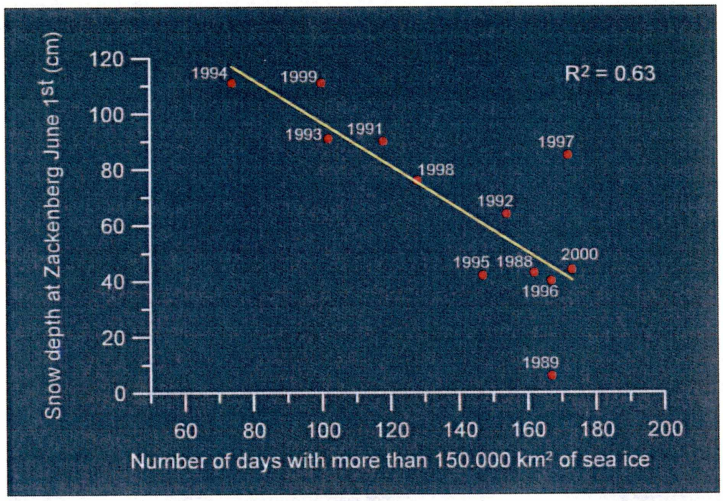


*Figure 2.7. Relationship between sea ice coverage in the Greenland Sea and snow depth at Zackenberg over the period 1988-2000 (Hinkler, unpublished data).*

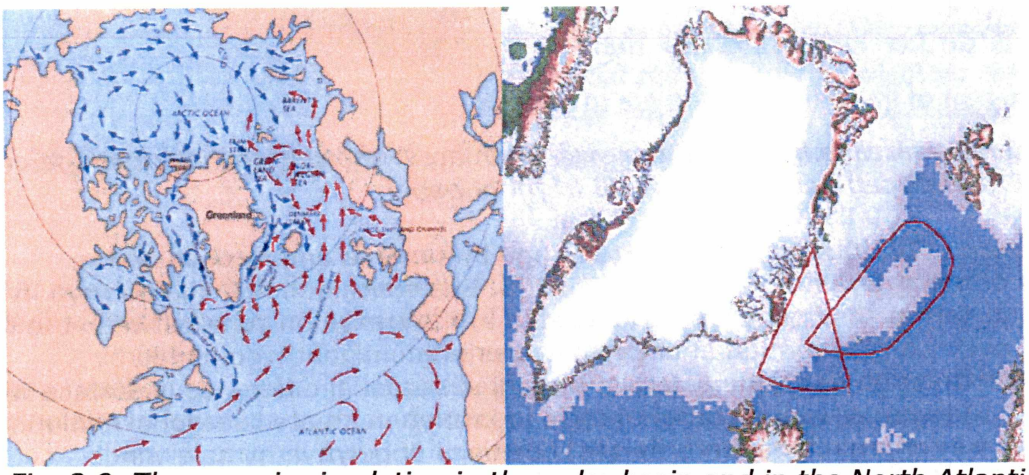

*Fig. 2.8. The oceanic circulation in the polar basin and in the North Atlantic (left) a general outline of winter ice coverage around Greenland. The polygon to the right indicates the current driven ice rich 'Odden area', and the triangle shows the area, where ice coverage has the strongest negative correlation with snow coverage in studied coastal landscapes (Hinkler, unpublished data).*

### *2.5 Ice coverage and polynya*

The ice in the fjords is almost permanently present from the end of September until July. On sea and at the mouth of the fjords, the ice is more dynamic (more periods with ice drift) over the winter months. Quite often, open water areas exist, the so called polynya. Ice coverage in the expedition area on two moments in shown in Fig. 2.9. Based on these observations, the type and thickness of the ice was classified and presented in Ice Charts (Fig. 2.10). Polynya can clearly be identified near Hvalros Ø in the North and near Kap Breusing at the mouth of the Young Sund in the central area.

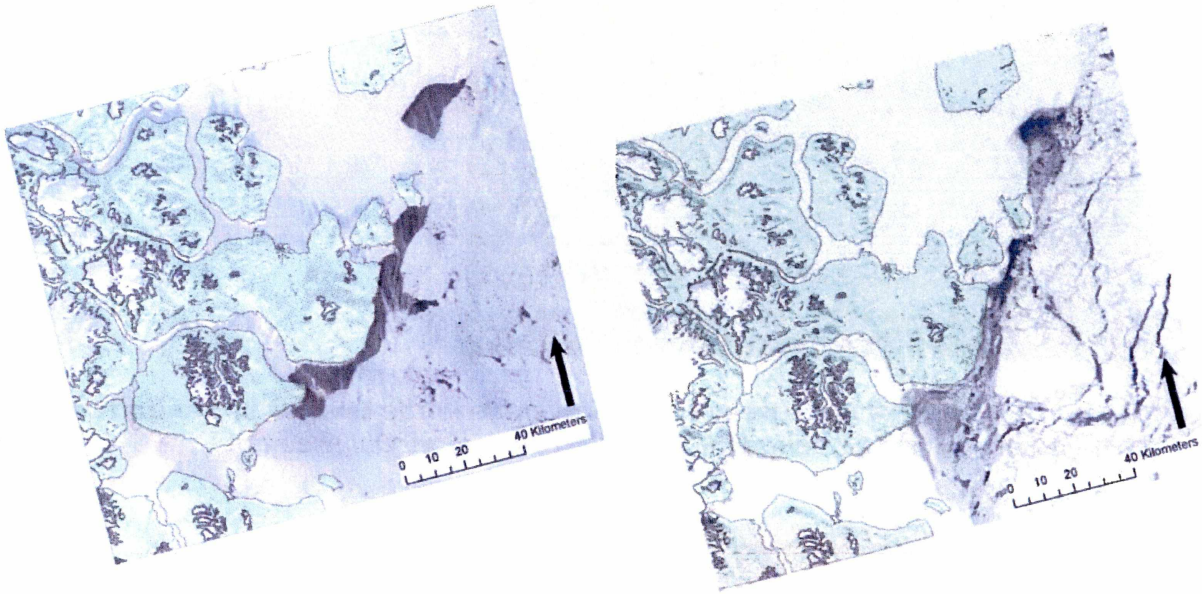


*Figure 2.9. Modis satellite images of the expedition area, showing the ice coverage on 29 February 2008 (left panel) and 29 April 2008 (right panel).*

Kaufmann (2009) studied the ice coverage in the area and focused on the persistency of polynya over the years 2007-2008. She concluded that the polynya in the area are wind-driven shelf water polynya located in the transition zone between the fast ice and the pack ice. The formation of polynya was predominantly governed by mechanical forcing due to northerly gales. A marked seasonal difference in surface wind fields (Fig. 2.5) together with a seasonal cycle in insolation created seasonal evolution of polynya. The winter regime had intermittent openings of polynya by gale winds alternating with periods of more calm weather allowing an advancement of the fast ice edge and growing ice cover in the polynya. This is expressed in Fig. 2.11 where the size of the open water areas in spring 2008 is coupled to the wind speed and temperature. Over summer, most of the ice disappeared in the area due to southeasterly winds and significant higher insolation rates.

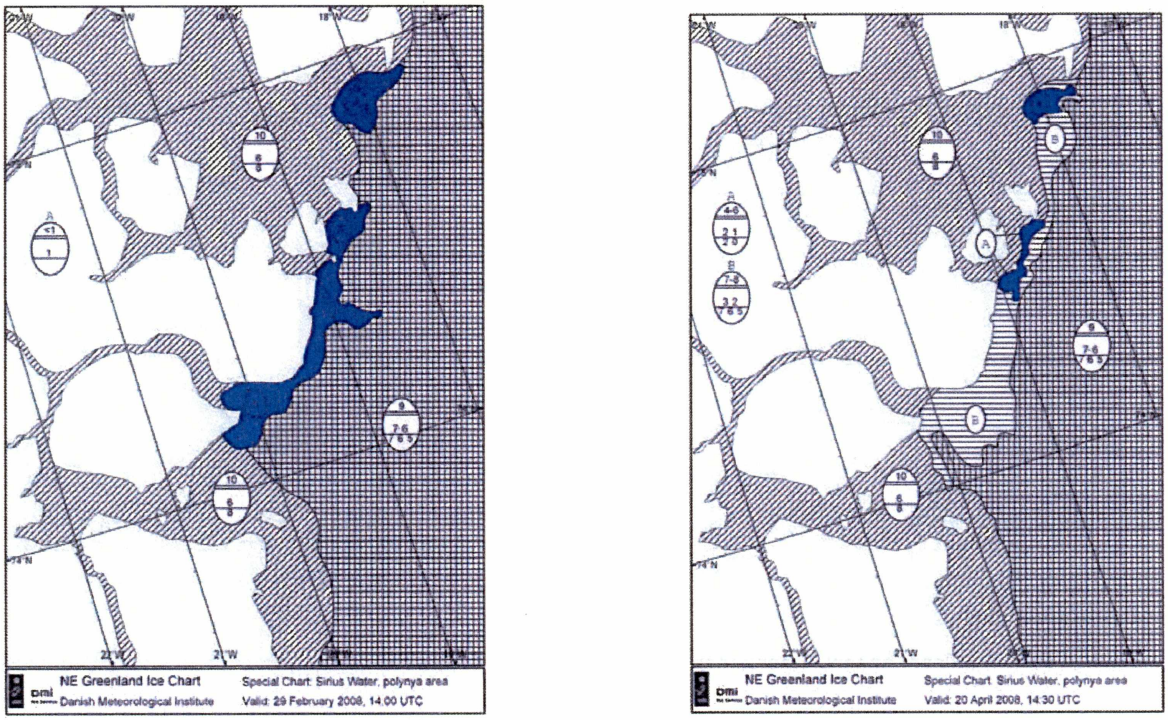


*Figure 2.10. Ice charts of 29 February 2008 (left panel) and 29 April 2008 (right panel).*

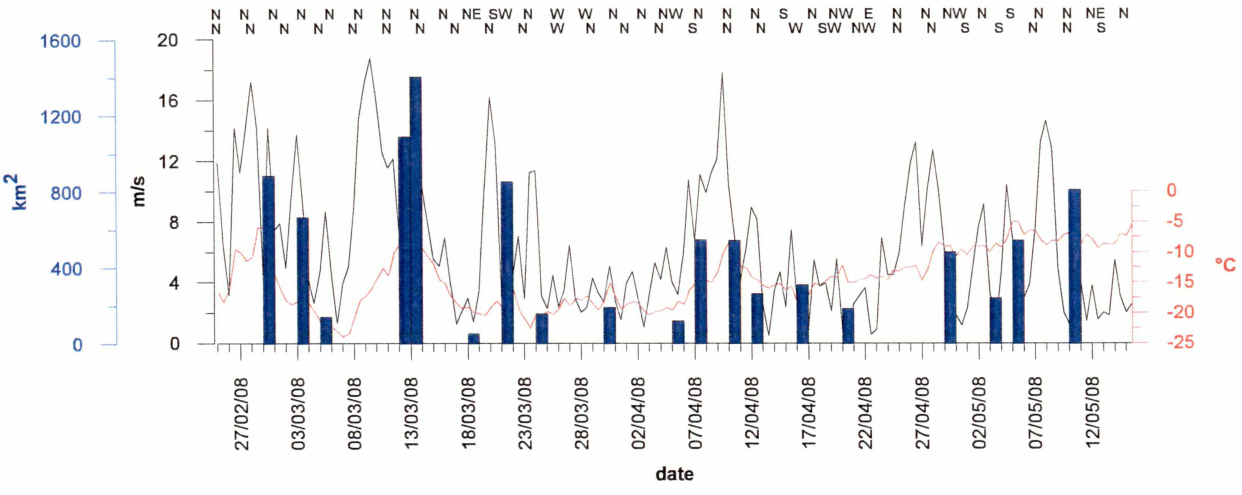


*Figure 2.11. Open water area, wind speed, wind direction and air temperature in the expedition area (see Fig. 2.10) over winter and spring 2008.*

# 3. Geographical topics in the Geoark project

## 3.1 Morphology and morphodynamics of coastal environments

### *Coastal Geomorphology*

Sandy and gravelly dominated sedimentary features like spits and beach ridges alternate with headlands in hard rock along the shores of Clavering Ø (Fig. 2.2: granites and gneisses in the central region; basalt in the eastern regions). The size and extension of these features strongly depend on the availability of sediment. A lot of small rivers feed the coastal area with sediments from the interior and from the eroded glacial deposits in the western and eastern regions. This leads to the formation of beach ridges near the water line. The central region has only major coastal features along the fringes of deltas, formed at the end of a limited number of large rivers draining the hinterland (see Fig. 2.3). Pocket beaches are located between two headlands and can especially be found in the central and eastern regions (example in Fig. 3.1). Most often, these pocket beaches have a closed sediment budget and beach ridges are formed by the reworking of glacial deposits. Major sources of sediment delivery are lacking: no sediment influx along the headlands by alongshore currents, neither from the hinterland by rivers or from the fjord by incoming skewed waves and ice over the seaward slope of the fjord. The latter slope is often much too steep, especially in the central region.

*Figure 3.1. Pocket beach between Fladstrand and Eskimonæs, central region Clavering Ø. Most sediment on these pocket beaches are of local origin.*

Many beaches on Clavering Ø have ridges near the high-tide waterline and/or near a storm surge level (Fig. 3.2). In general, these beach ridges are formed along the waterline by swash processes due to waves. The velocity and transport capacity of the onshore directed swash run-up is often much stronger than the offshore directed back-wash on coarse-grained sandy or gravelly beaches, because much of the run-up percolates into the beach which weakens the backwash. Variations in high-tide levels (e.g., spring-tide neap-tide variations) or storm levels can further stimulate the present beach ridge formation. Interestingly, the morphodynamics of beach ridges on arctic

beaches like those at Clavering Ø do include additional process-characteristics by ice. Firstly, sediment-laden ice masses, often icebergs, transport additional sediments towards the shore. Secondly, drifting ice may push up sediments towards the shore while grounding on the slope (Fig. 3.3), and finally ice masses in the fjord can fix the melt water discharge of rivers in spring along the shore and might thus increase alongshore currents and local water levels.

*Figure 3.2. Active sandy beach ridge at the coastal plain near Eskimonæs, Clavering Ø.*

*Figure 3.3. Active beach ridge in gravel with ice-pushed lunar shaped curves half way the beach, Store Finsch Ø.*

Some of the beaches show a number of beach ridges on their upland slope. These beach ridges were formed in the past in periods with a higher relative sea level. In areas with an isostatic uplift of the land masses and a relative sea level fall, the older beach ridges are on the highest levels on the slope and the successive beach ridges down the slope are younger (Fig. 3.4). This is probably the case for Clavering Ø. The observed locations of beach ridge complexes above the present-day level of the Fjord may reflect the relative sea level variations over the Holocene. The oldest ridges on Clavering Ø are now at about 30 m above present sea level. Quite often, the sloping beach ridge plain is reworked by solifluction processes: the beach ridge will loose its original shape (becomes more pronounced) and will move in a downslope direction. Solifluction of beach ridge

plains were observed on almost every location along the southern shore (example see Fig. 3.5). However, it was most intense on the poorly draining flat sloping plains in the eastern region. Nowadays, we observe the largest beach ridges near the present water line. This might be an indication for a stand-still or even transgressive phase in the area induced by rising sea-levels.

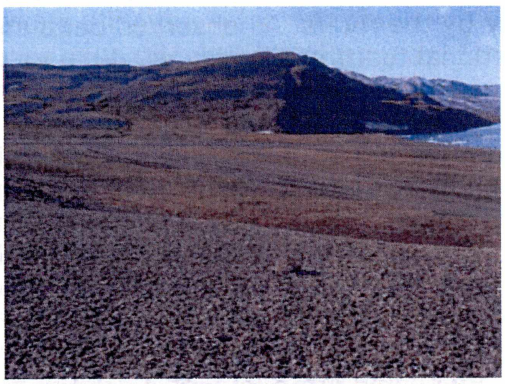

*Figure 3.4. Beach ridges on a coastal plain, Grønnedalen, Clavering Ø. The upper beach ridge is about 30 m above the present water level in the Young Sound.*

*Figure 3.5. Transformed beach ridge due to solifluction, Dahls Skær, Clavering Ø. Mind the steep slope of the ridge towards the fjord (left in the photo) and the high water levels at the landward site of the ridge (right in the photo).*

There is a distinct spatial pattern of morphological features along a delta front. This spatial pattern is caused by a balance of processes: between river discharge rates at the delta mouth and wave and ice action along the delta fringes. Elongated sand and gravel bars along the levees of the main discharge channel on the delta plain can extend into the fjords. In this case, the river outflow processes dominate over the re-shaping processes by waves and ice. Sediments are deposited at the delta mouth and an underwater delta is built up. However, further off the main discharge channels, the wave action may dominate and recent beach ridges are formed along the delta fringes. The sediments in these ridges are cross-shore delivered from the underwater delta by skewed

waves and/or alongshore transported by wave-induced alongshore currents. Nice examples of the spatial patterns in delta-fringe morphologies are observed along the many deltas in the Young Sound area (e.g., Zackenberg delta, Fig. 3.6 and Store Stromdalen, Fig. 3.7).

Erosional and accretional patterns along the shoreline with deltas are also showing similar spatial variability. The sediment availability on almost all deltas is abundant, due to the sediment supply by the rivers. All observed delta shorelines close to actual river mouths do show accretional features like ridges, do have mildly sloping underwater slopes of the delta front, and often show a plume of suspended sediment that can be seen far off the delta mouth (e.g., Zackenberg delta). However, further off the actual river mouth, on adjacent coastal stretches, the sediment availability might be limited and the impact of waves can be even more pronounced because the underwater delta slope is much steeper or even lacking. In these cases erosional features like shoreline cliffs are observed. The sediment availability on a specific place along the delta fringe also changes in time. In general, delta lobe switching or channel lobe switching is often observed over decadal time-scales. An example of the first is observed in Zackenberg ('old delta' and 'recent delta'); examples of the second are observed on other delta plains in the Young Sound area. Switching often implies a change from an accretional towards an erosional shoreline trend or vise versa in a specific coastal stretch. These major changes can also induce an erosion of old Eskimo settlements, like those close to Henning Elv (Fig. 3.8). Observations of the spatial variability of accretional and erosional features are essential before a general coupling between features and overall change in relative sea-level can be made.

*Figure 3.6. Delta morphology in the Young Sound area: Zackenberg delta. Recent delta mouth shows elongated bars pointing into the Young Sound, while the old delta mouth has a wave-formed spit on its old delta front. Adjacent shoreline just east of the old delta front is eroding (left in the photo), probably because the waves are locally more dominant now and more intense over the reduced (?) delta front.*

*Figure 3.7. Delta morphology in the Young Sound area: Store Strømdalen, Clavering Ø. One delta system: recent delta mouth shows elongated bars pointing into the Young Sound.*

*Figure 3.8. Erosion of the actual shoreline near Henning Elv. The present delta lobe is further to the west. Erosion can be caused by a channel lobe switch of the Henning Elv or a general relative sea-level rise in the area.*

The coastal geomorphology of Hvalros Ø showed a lot of beach ridges (Fig. 3.9). Most of these beach ridges were built with local debris: basalt pebbles. The highest beach ridges occurred at about 30 m a.s.l. and are now located in the central area of the island. The coastal plain was dipping towards the west and the successive beach ridges were at lower elevations. The western central part also showed an enclosure of an embayment (remnant can now be seen as a large lake). First, a couple of spits migrated into this area and finally the whole embayment was closed by a beach ridge. Seaward of this ridge were about four other ridges, successively formed under falling mean sea levels. The north western part of the island showed a number of spits who looked like beach terraces. These spits changed their alignment since the area filled up under falling sea levels in the Holocene.

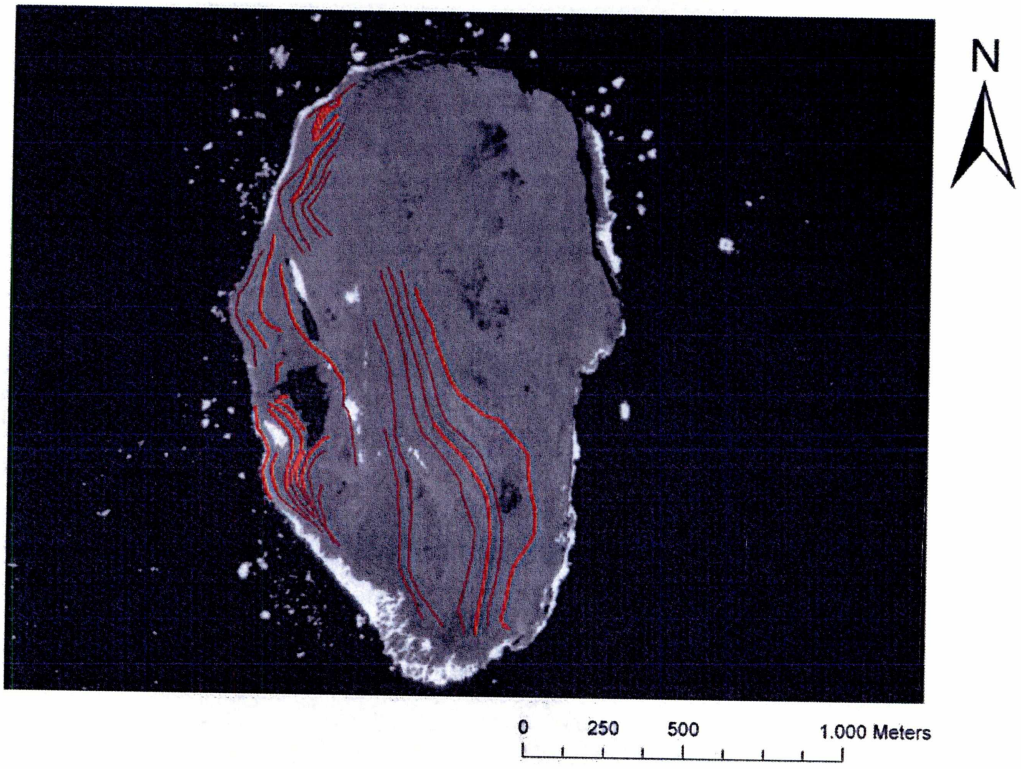


*Figure 3.9 Beach ridges on Hvalros Ø (Thick lines are also measured with dGPS).*

### *Geomorphology and Thule Culture settlements*

In general, we observed some preferred coastal landscapes that determine the spatial distribution of settlements, like Thule Culture winter houses. These winter houses are often found along the central part of the southern shoreline of Clavering Ø and on the basalt headlands (Fig. 3.10). These pocket beaches and headlands on the southern shore may be good for winter settlement because:

- The substrate is quite stable;
- Small creeks are relatively stable and have produced peat;
- The headlands and pocket beaches do not show large dynamic changes by enormous amounts of sediment delivery (only very limited amount of major deltas, with strongly different character: Dødemandsbugten and Lerbugten);
- Solifluction processes are present, but less than in the other areas, because there is also less loose sediment;
- The coastal area is relatively well protected against the dominant winds from north.

The areas between the basalt capes have a lot of sediment, but this sediment is highly mobile and influenced by solifluction processes and draining water from snow patches (see Fig. 3.11). With enough sediment delivery, many coastal features could develop on accreting coastal plains (see especially southern Wollanston Forland). These coastal features, like beach ridges could be less influenced by solifluction processes, because they are close to the well drained levees of the creeks/rivers (example south coast Wollaston Forland, but also Dahls Skær). For this reason, the capes and occasionally the beach ridges are the only stable parts in the areas.

The areas close to deltas could be too dynamic to settle. A nice example of a very dynamic delta is Grønnedal, where the creeks on the present delta have shifted its courses several times in the last centuries. Thule Culture winter settlements are however found close to the basalt cape in the most western part of the beach plain. Other less permanent settlements are sporadically found on the more stable and well drained moraines and on the beach ridges (Fig. 3.12).

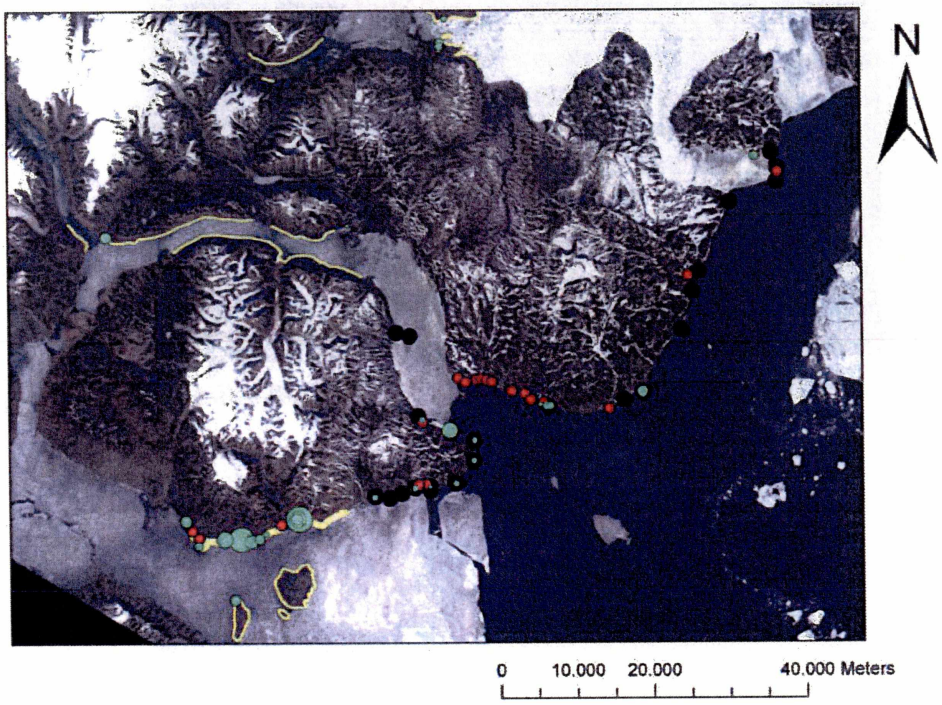


*Figure 3.10. Geomorphologic map with distribution of Thule Culture winter houses. Legend: winter house (green dot), beach ridge system (red dot), pocket beach fringing gneiss formations (yellow line), and basalt capes (black dots).*

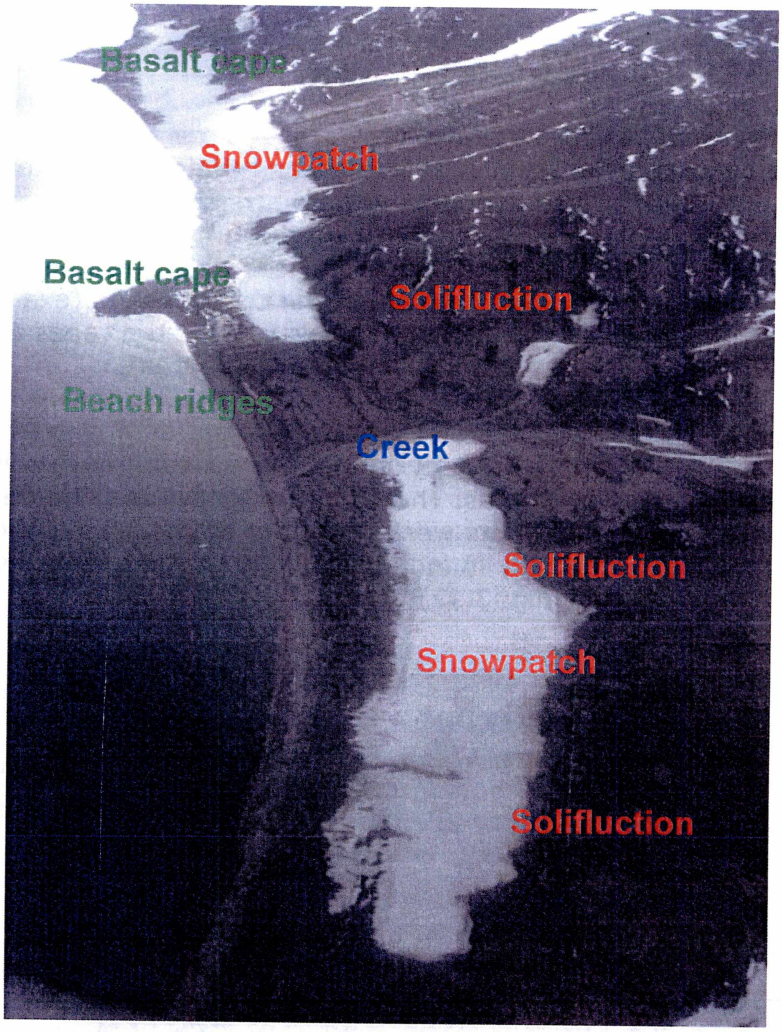


*Figure 3.11. Geomorphologic processes and features at Dahls Skær, eastern southern shore of Clavering Ø.*

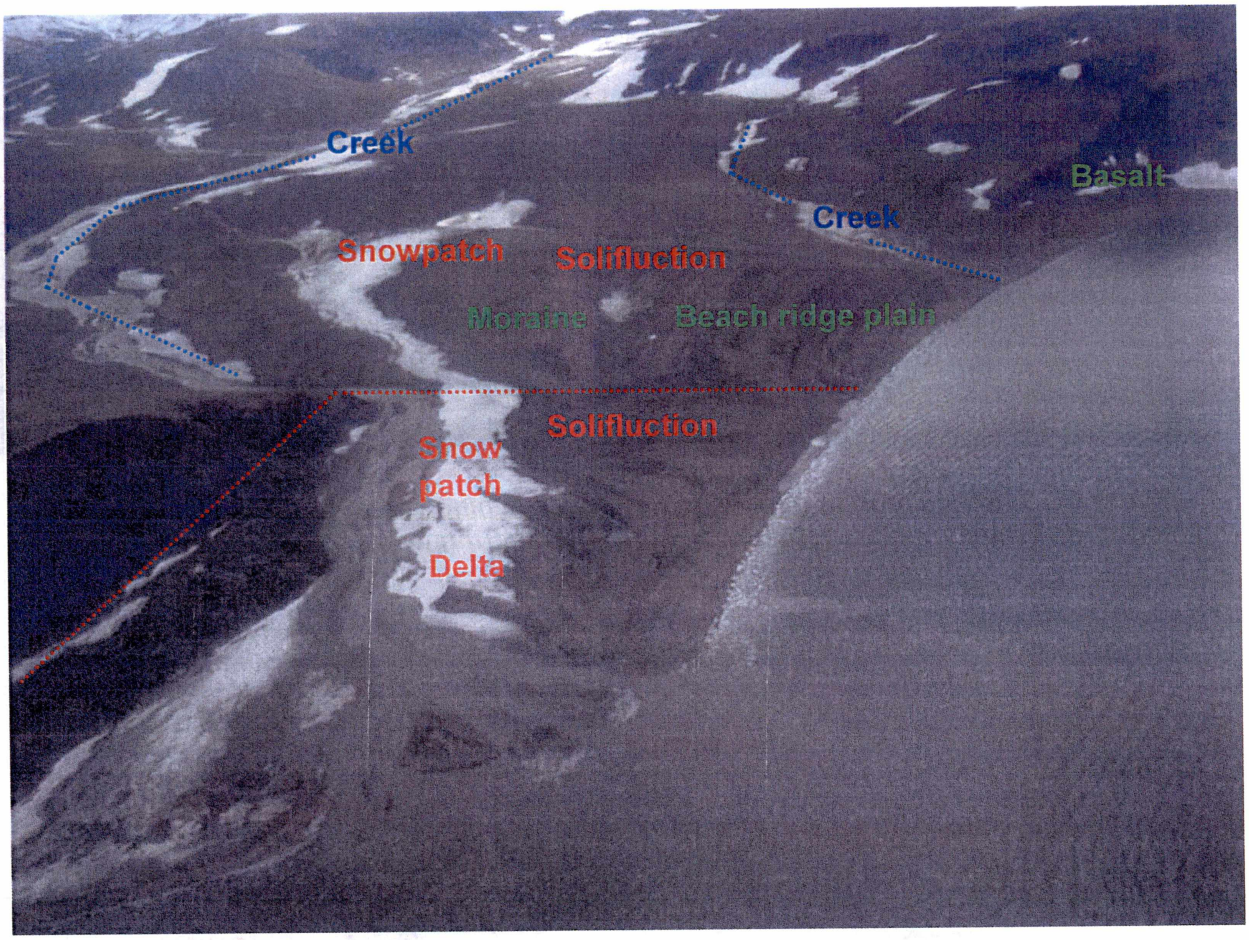


*Figure 3.12. Geomorphologic processes and features at Grønnedal, eastern northern shore of Clavering Ø.*

Coastal, fluvial and periglacial processes and morphologies are studied in more detail around some specific Thule Culture settlements. Estimations of the maximum size of the settlement, in order to predict the amount of Eskimos that have lived on a location, may be underestimated because of beach erosion, switching creek distributaries, solifluction lobes or mass movements by falling and sliding rocks. An example of the restriction of a settlement size by a solifluction lobe and by a switching creek on the alluvial fan is Eskimovig (see Figs. 3.13 and 3.14).

*Figure 3.13. Solifluction lobe (left panel) and a switching creek on an alluvial fan (right panel) at Eskimovig, central southern shore of Clavering Ø.*

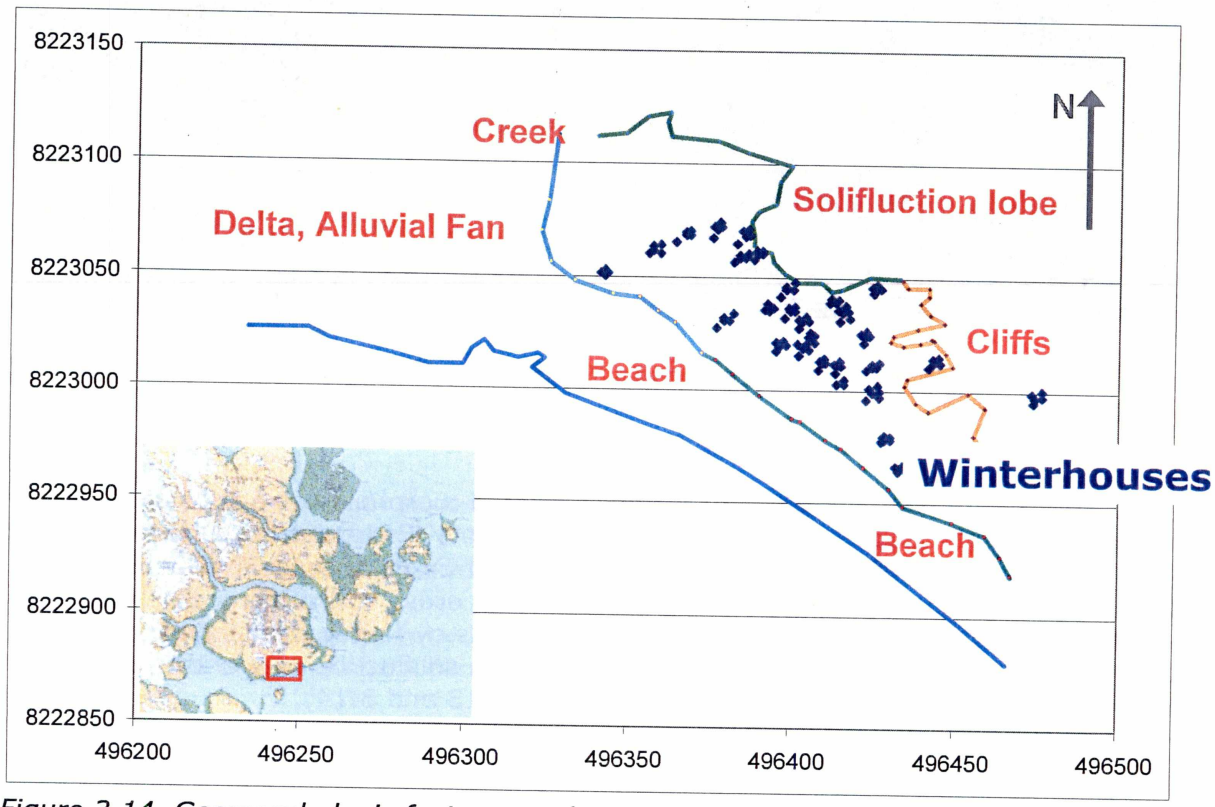


*Figure 3.14. Geomorphologic features and processes mapped at Eskimovig, central southern shore of Clavering Ø.*

## 3.2 Relative sea level variations, paleo climate and climatic changes in the Holocene

### *Reconstructions of former sea levels*

The beach ridge plain at Grønnedal (see Fig. 3.12) was used to study former sea level stages. A total of over 25 ridges were observed and measured at this location, with the highest ridge at about +30 m above present sea-level. Seven prominent beach ridges in this sequence were selected for OSL dating (see Fig. 3.15). At Eskimonæs, a present day bar at the beach has been migrated onshore over an older seaward dipping coastal plain. At this location, we dated some older organic samples just beneath the bar and dated some levels in the sandy bar deposits with OSL (Fig. 3.16). Finally, a pit was dug in a lagoon infill behind a gravel barrier at Strandengnæs, southern shore of Clavering Ø. There was a whole succession of sandy layers with inclusion of peat and organic material. Several layers in this pit were dated, mainly on C-14 content in organic material, and gave an idea of the infill history of this depression over the last part of the Holocene (see Fig. 3.17).

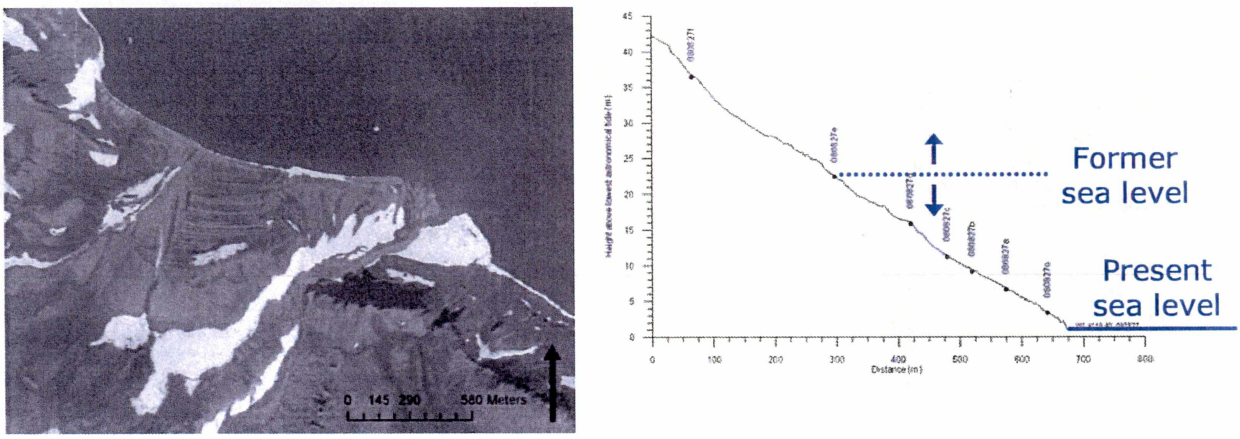


*Figure 3.15. Plain view (left panel) and cross-shore profile (right panel) of the Grønnedal beach ridge plain.*

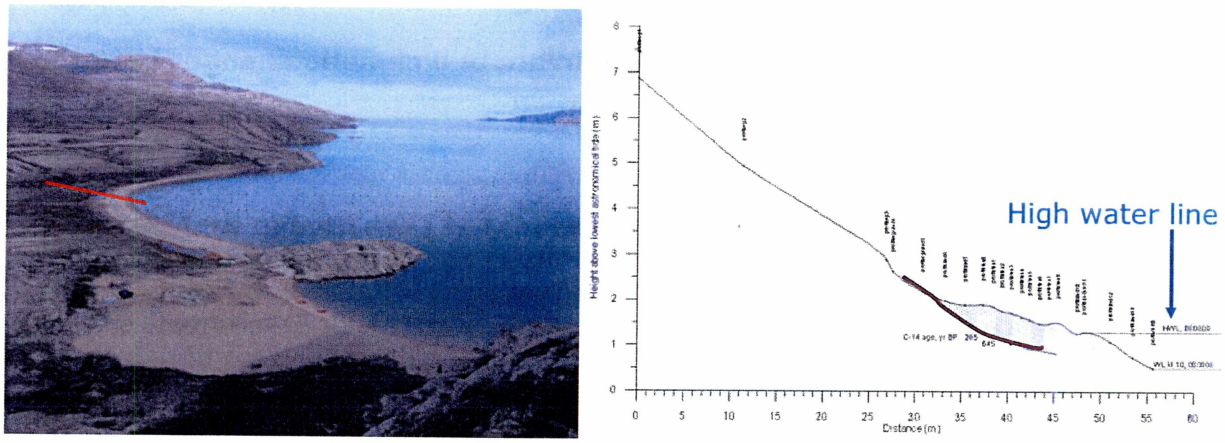


*Figure 3.16. Oblique view (left panel) and cross-shore profile (right panel) of the coastal area at Eskimonæs.*

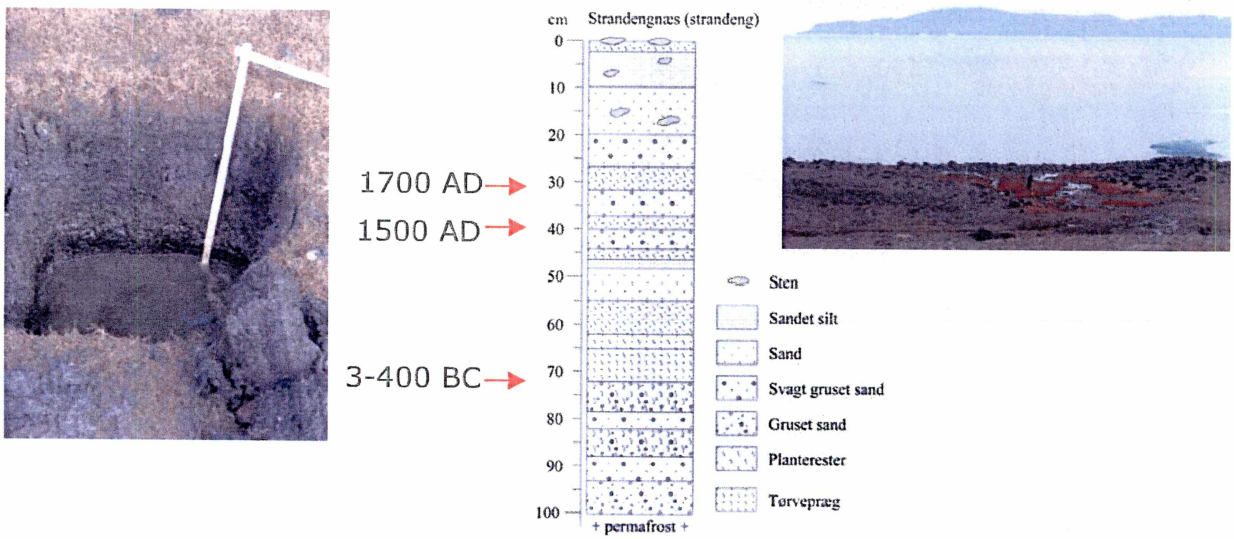


*Figure 3.17. Oblique view (left panel), cross-section of the pit (central panel) and interpretation of the pit layers (right panel) at the filled lagoon of Strandengnæs.*

A preliminary relative sea level curve over the Holocene (Fig. 3.18) was based on all these datings. As in other curves for North-East Greenland, there is a rapid sea level fall in the first part of the Holocene until about 3500 BP, where after the sea level remains more or less stable. The impact of the relative sea level can also be seen in the settlements of the different inhabitants. The oldest paleo houses are mostly found on the higher levels in the coastal environments, where the younger Dorset and Thule Culture houses are situated much closer to the present day sea level. Nice examples of this segregation of settlements are found on Hvalros Ø (Fig. 3.19).

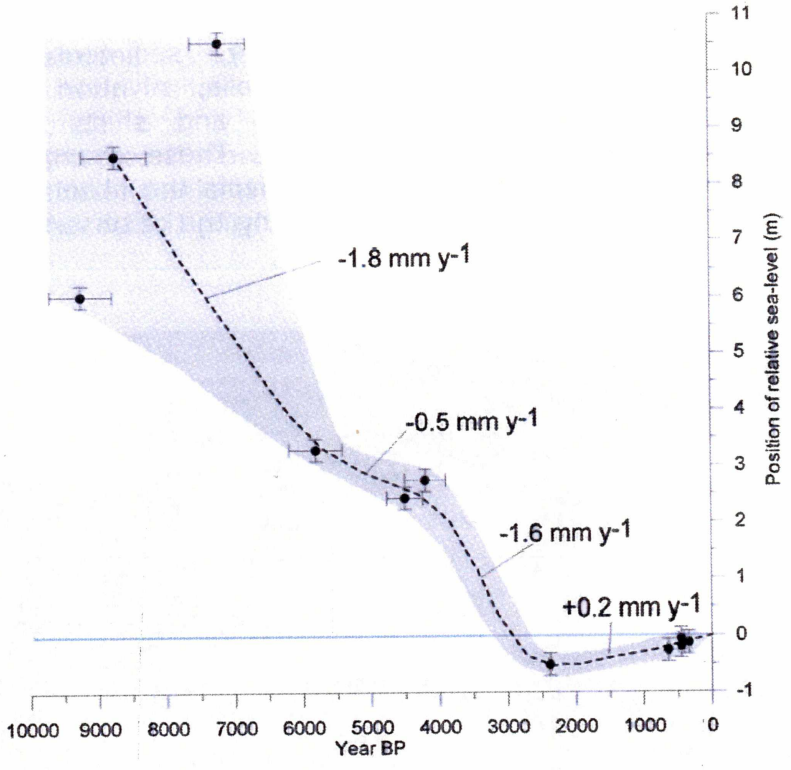


*Figure 3.18. Relative sea level curve and sea level change rates for North-East Greenland, based on GeoArk datings. Culture period started at about 4500 BP.*

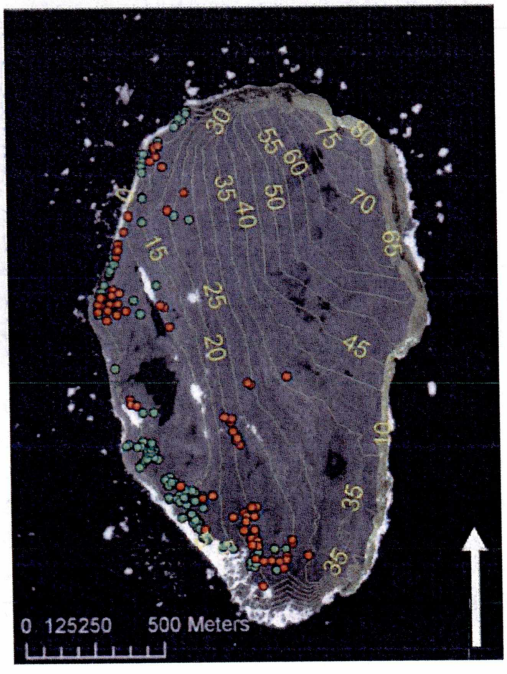


*Figure 3.19. Map of Hvalros Ø with the locations of the paleohouses (orange dots) and Thule Culture tent rings (green dots).*

## *Reconstruction of palaeo climate and climatic changes in the Holocene*

Geomorphological evidence, e.g. the stratigraphy, sedimentology and geobiochemical characteristics of polysequent palaeo soils, nivation and lake sediments indicate substantial environmental variability and shifts in coastal landscapes of Northeast Greenland during the Holocene. These changes appear basically to be orbitally driven (Fig. 3.20), which also explains the observed overall and continued climatic cooling during the Holocene underlying the observed shifts and variability (Fig. 3.21).

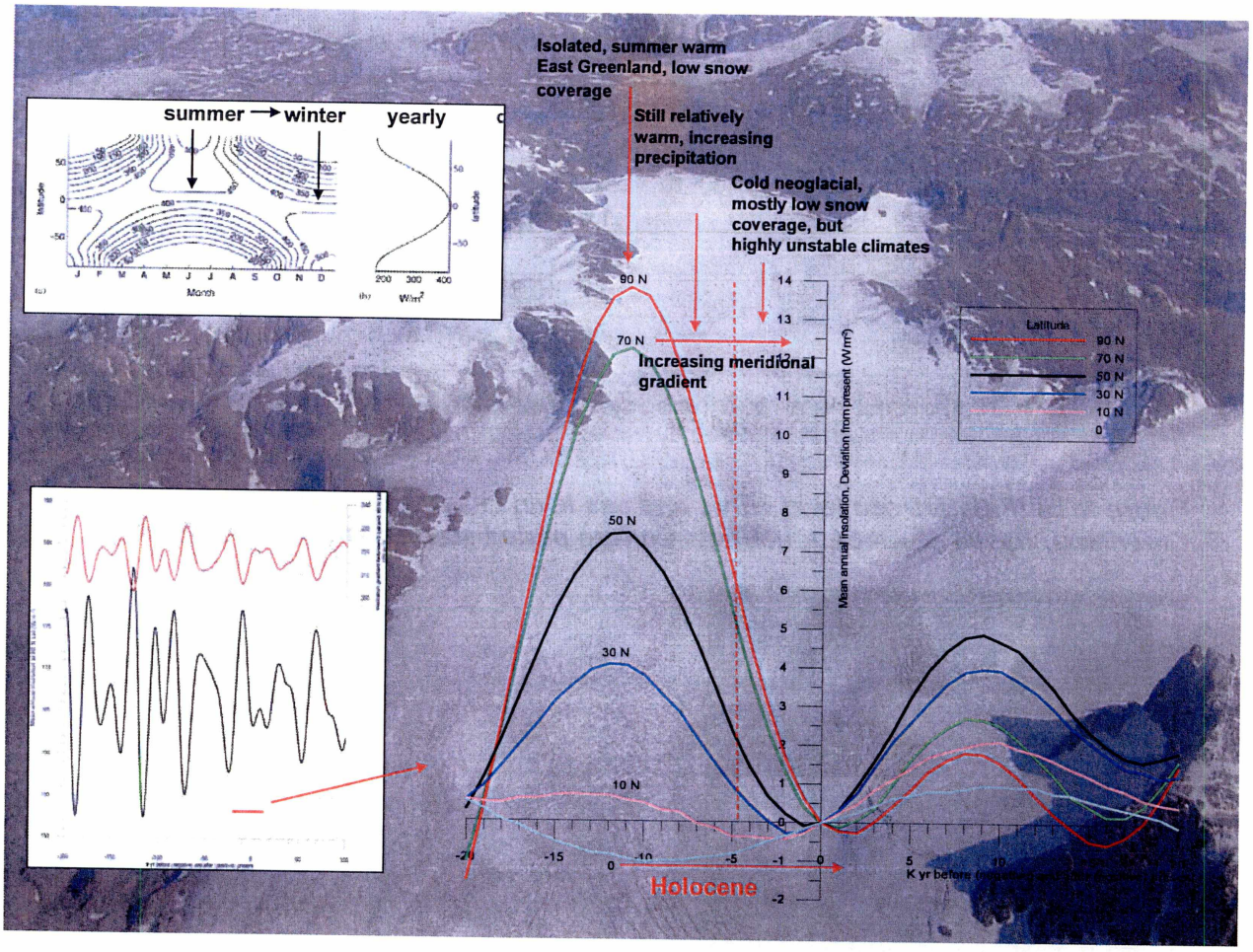


*Figure 3.20. Meridional variations in annual insolation in W/m² from 20 KYBP to 20 KYAP. Lower left figure shows the variations in insolation from 200 KYBP to 100 KYAP and insolation gradient changes from lower to higher latitudes (red curve). Upper left figure shows yearly insolation variations at different latitudes. Insolation changes both drive changing regional climate systems as the warming in high latitude environments, and determine the changing meridional energy gradients influencing the meridional atmospheric circulation and exchange of energy and moisture from lower to higher latitudes.*

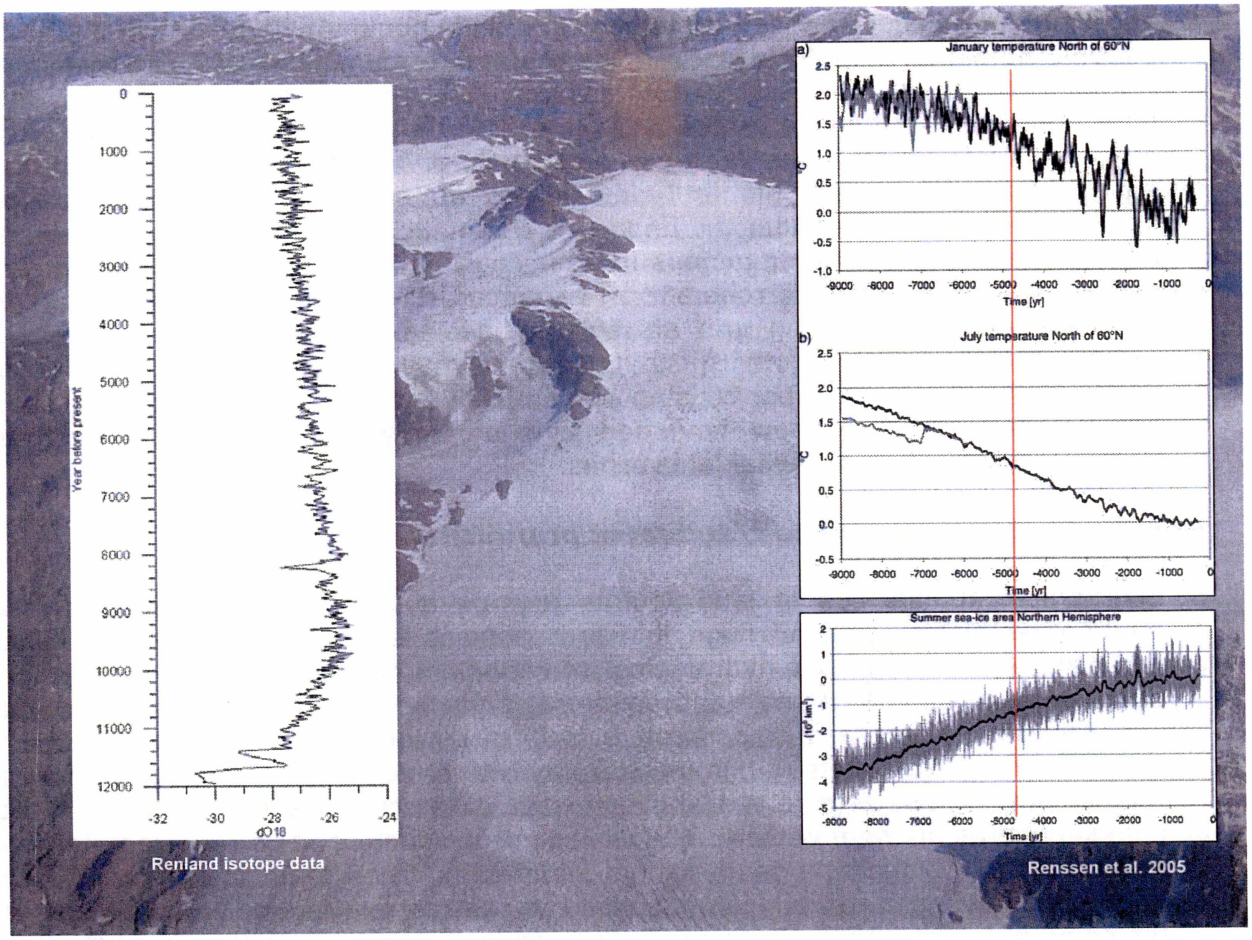


*Figure 3.21. Holocene oxygen isotope record from the Renland ice core, situated at low elevation close to the coastal landscapes in the Scoresby Sund area in central East Greenland. Low values indicate warmer climates (left). Simulated Holocene climate evolution at northern high latitudes using a coupled atmosphere-sea ice-ocean-vegetation model (right)*

The early Holocene, starting about 11.500 BP and following the Younger Dryas cooling, is concurrent with and following the final postglacial melting of glaciers in coastal landscapes of East Greenland. This early era appears to have experienced the warmest Holocene summer conditions, a continental climate, thin snow covers and ice-free seas during the summer. The climatic situation seems to a considerable extent to have been based on internal regional meteorological processes and largely without strong and regular cyclonic impacts from lower latitudes. Generally, decreasing summer and annual insolation at higher latitudes during the Holocene, a still colder landscape and near coastal sea, further cooled by the negative albedo feedback from snow and ice, have increased a periodic and gradient driven atmospheric circulation of heat and moisture northwards in the western part of the North Atlantic. Counteracting this southerly influx of heat and moisture, will be the blocking effect of a cold, snow and ice-covered region. A conceptual model could be outlined to understand the observed cyclic and chaotic environmental fluctuations during a still colder Holocene in East Greenland, from periods of relatively seen colder and ice rich conditions to periods of relatively seen warmer and snow rich conditions,

and to understand the observed major climatic shift about 4500 BP. At that time a possible fundamental shift took place in the climatic framework of East Greenland, at a time also globally showing marked changes in many different ecosystems. At that time, still lower insolation values and increasing negative albedo effects causes the basis for a neoglaciation in the ice free landscapes, and the basis for a still stronger energy gradient towards higher latitudes driving atmospheric circulations into the region. After 4500 BP and under the impact of a neoglacial development and more ice rich conditions during summer periods in near coastal waters, geomorphological and sedimentological indicators corroborate an enhanced climatic instability characterized by a basic continued cooling and strongly increasing summer sea ice coverage, frequently interrupted by both spells and somewhat longer periods of stronger southerly atmospheric influxes, causing somewhat warmer conditions, less sea ice, higher precipitation and snow coverage and probably stronger and dominating northerly winds in ice free coastal landscapes.

***Lake sediment cores and soil/sediment profiles.***

Stratigraphical analyses of lake sediments provide a wealth of information about environmental history, and through interpretations it is possible in many cases to reconstruct past climate and hydrological conditions. Characteristics of specific lake settings, such as catchment size and shape, and the geology and geomorphology of the catchment, influence the particulate and dissolved inputs to the lakes (the allogenic fraction). Lake settings, in interplay with climatic and hydrological regimes in the catchment, also determine the biogeochemical state of the lake water body and of lake sediments at the lake bottom. The organic productivity and the precipitation and flocculation of biogenic and inorganic sedimentary materials inside the lake (the endogenic fraction) are strongly influenced by the thermal regime and structure of the water body and of the vertical mixing processes in the lake. With regard to the final appearance of lake sediment sequences, it also has to be taken into consideration how the mentioned lake water body properties influence the final trapping and possible return of chemical elements at the water sediment interface, thus determining the authigenic fraction of lake sediments.

The thermal regime and stratification of lake waters basically show three different water bodies. Warmer and lighter water is found near the surface, colder and heavier water stays at the bottom of the lake and in between, the water forms a zone of thermal transition. In addition to external factors, such as wind and fluvial input, temperature controlled changes in density determine lake water mixing. In lakes under arctic climates, spring warming and autumn cooling can give rise to a diving of water reaching its maximum density at 4°C. In addition, fluvial influxes from cold precipitation or snow melt can lead to the mixing of waters during spring and summer. If mixing processes are incomplete or weak, the deepest part of the lake can hold stable and oxygen depleted waters, having significant influence on both the endogenic and authigenic sedimentary fractions accumulating on the lake bottom.

Obviously, changing climatic conditions, primarily changing temperatures, precipitation and snow and ice coverage will influence sedimentary conditions in lakes and thereby be recorded in lake sediments. But, independent of climatic changes, lake sediments also represent a record of a lake life cycle, or a part of it. Most lake sediment sequences, especially in former glaciated landscapes, show early sediments accumulated under eutrophic conditions and initially dominated by allogenic materials,

whereas later stages normally document a relative increase in endogenic sediment fractions and mostly also more oligotrophic conditions.

In arctic landscapes, lakes are covered by ice and snow for most of the year, often more than 10 months. Therefore, the length of the ice- and snow-free period and the amount of runoff from the catchment during the short arctic summer has a strong influence on sedimentary conditions. In cold years, as during cold periods of the Holocene, some lakes, especially lakes in unfavourable and shadowed landscape positions, experience strongly decreasing sedimentation due to extended or permanent ice coverage, and regional climatic changes can thereby have a strongly diverging effect on lakes in the same region. In addition, lake waters during cold winters, as during cold periods of the Holocene, freeze to greater depths, affecting larger parts of the lake bottom and narrowing the unfrozen deep central part of smaller lakes. Depending on lake basin geometry, many arctic lakes may therefore be affected by turbidity currents and slumping of sediments.

In order to use the huge amount of complex information in lake sediments for terrestrial palaeo-environmental and palaeo-climatic interpretations, it is necessary to take the specific lake appearance and geomorphological setup into consideration and carefully explain and interpret how both lake life cycles and climatic changes have determined the variable sedimentary characteristics observed in a specific lake sediment record

Climatic changes affecting snow coverage on land and ice coverage in near costal waters are considered having the strongest impact on the amount of and access to natural resources and therefore also affecting the living conditions of intuits, periodically living in North East Greenland. Only very few lakes in the near coastal landscapes have the catchment setting to favour an interpretation of lake sediments in relation to changes in snow and ice coverage. Four lakes with small non glaciated catchments have been cored in the study area (Fig. 1.1). Two in the outer coastal region, at Eskimonæs on Clavering Island and close to Germania Havn on Sabine Island, and two in the inner fjord region at Revet on Clavering Island and on Payer land. It is known from lake sediment studies in East Greenland, that the climatic cooling and neoglaciation taking place after the mid Holocene in probably most lakes caused disturbances and strongly changing sedimentary conditions. Strongly decreasing sedimentation rates or even observed hiatuses due to perennial ice covers are observed, and in many lakes repeated sediment slumping often have disturbed and mixed the mostly thin sequences of late Holocene sediments.

The lake at Eskimonæs was cored in 2007, showing undisturbed sediments of about 130 cm covering the period from the early Holocene and indicating some disturbances in the upper part of the sediment cores. Datings showed that sedimentation in this lake started more than 11.000 year BP shortly after the intense warming following the Younger Dryas. But unfortunately the undisturbed sequence only covered about 5000 years, consequently not covering the cultural era of the region, after 4.500 YBP. In 2008 numerous additional corings were carried out in different parts of the lake in order to collect undisturbed lake sediments also covering the younger part of the Holocene. All parts of the lake showed to be affected by slumping, and studies of soils and sediments in the small lake catchment indicated that several incidents of slumping may have occurred during the Holocene, in connection with erosion affecting the lake outlet and the base level.

The lake on Sabine Island was cored in 2007. About 1 m finely layered sediments were collected, obviously representing an undisturbed sequence of the youngest part of the Holocene. Datings showed that the core nearly covered the latest two millennia, and in 2008 additional corings were carried out to collect additional cores at other sites in the lake, and to try to collect deeper cores representing earlier periods in the Holocene. Two additional cores of about 1 m were successfully collected presumably giving more details about the latest two millennia, but due to the compact and clayey nature of the lake sediment it was not possible to penetrate deeper into the lake bottom.

Also in the inner fjord region at Revet and Payer Land only very few lakes are found. The two small near coastal lakes that were chosen, showed to be rather shallow only showing water depths of about 1 m. Lakes that shallow will freeze during winter also causing a permanent freezing of the deeper part of the lake sediment. The permanently frozen sediment (permafrost) was reaches about 30 cm below the present lake bottom. It was possible to collect undisturbed and layered lake sediments cores of about 30 cm from the two lakes. Probably the sediment record will not cover more than the latest 500-1000 years, and dating of the very few plant fragments found in the short cores will determine if it reasonable to carry out further analyses and interpretations of the cores.

Polysequent soils and sediment profiles have been excavated at a number of sites in the near coastal landscapes, in the catchments of the cored lakes and in the vicinity of Inuit settlements. The aim was to document and study changing geomorphological processes during the Holocene, primarily changing nivation, solifluction and landscape erosion. Data from Eskimonæs, Eskimovig and Fladstrand are shown.

*Germania lake on Sabine Island*

Germania lake is located near the coast close to the polynia at Sabine Ø and Hvalros Ø (Fig. 3.22), and was expected to reflect both changing snow coverage in the small lake catchment and changing marine signals due to changing ice coverage and open water conditions. Based on dating of a number of sedimentary shifts in the core, XRF analyses of numerous chemical elements, quantitative analyses of C, S, P, Ca, Mg, K, Na, Fe and Mn and index was calculated to indicate changes from relatively warmer, snow rich conditions connected to more open water in the near coastal Greenland Sea (high index values) to colder periods characterized by very little snow in the landscape and more extensive ice coverage in the Greenland Sea (low index values).

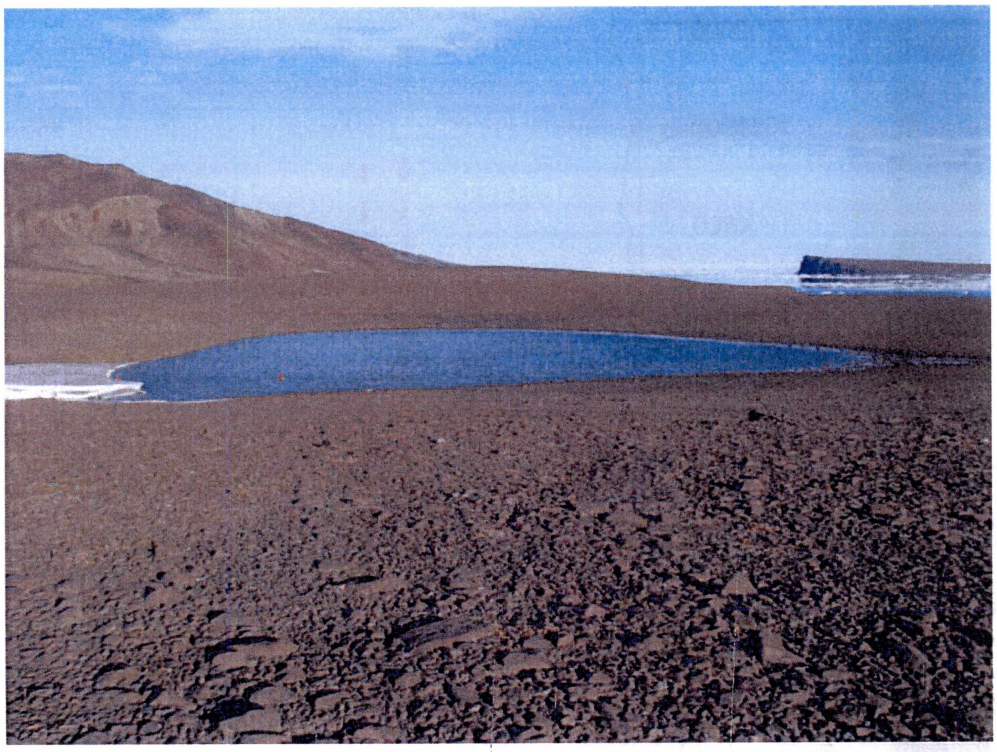

*Figure 3.22. Lake Germania on Sabine Ø. Hvalros Ø and the open water area are seen in the background.*

The index curve is based on the integration of sedimentation rate and normalized values of organic matter content, input of iron and calcium, as well as of tracers indicating increased input from coastal waters like sodium, magnesium and chloride (Fig. 3.23). The index indicate, that the appearance of The Thule Culture Inuit in North East Greenland during the 15$^{th}$ century took place, when the environment changed to more stable conditions characterized by a cold climate, ice rich conditions in coastal waters and only little snow in the landscape. Before the Thule Culture era - in the Germania lake core documented back to around 500 AD - the environment appears to have been both more unstable, showing frequent shifts, and generally showing more snow rich conditions and more open waters at sea.

The medieval warmth, probably mostly representing warmer and more snow rich conditions during winter and spring periods, culminated from the 10$^{th}$ to the 12$^{th}$ century. In the 12$^{th}$ century a cooling set in representing the initial development of the Little Ice Age, and it was followed by nearly 3 centuries showing clearly colder but still quite unstable environments. Preceding the culmination of the medieval warmth, environments also appear unstable, although generally slightly warmer and snow rich than after the medieval maximum. The iron enriched layers in the uppermost part of the core probably have been deposited during periods of extremely cold and dry conditions, being characteristic of the later part of the Little Ice Age during the 18$^{th}$ and 19$^{th}$ century. Lead 210 dating of the topmost sediments show that sedimentation rates and sediment characteristics clearly reflect warmer and more snow rich environments after about 1880 AD.

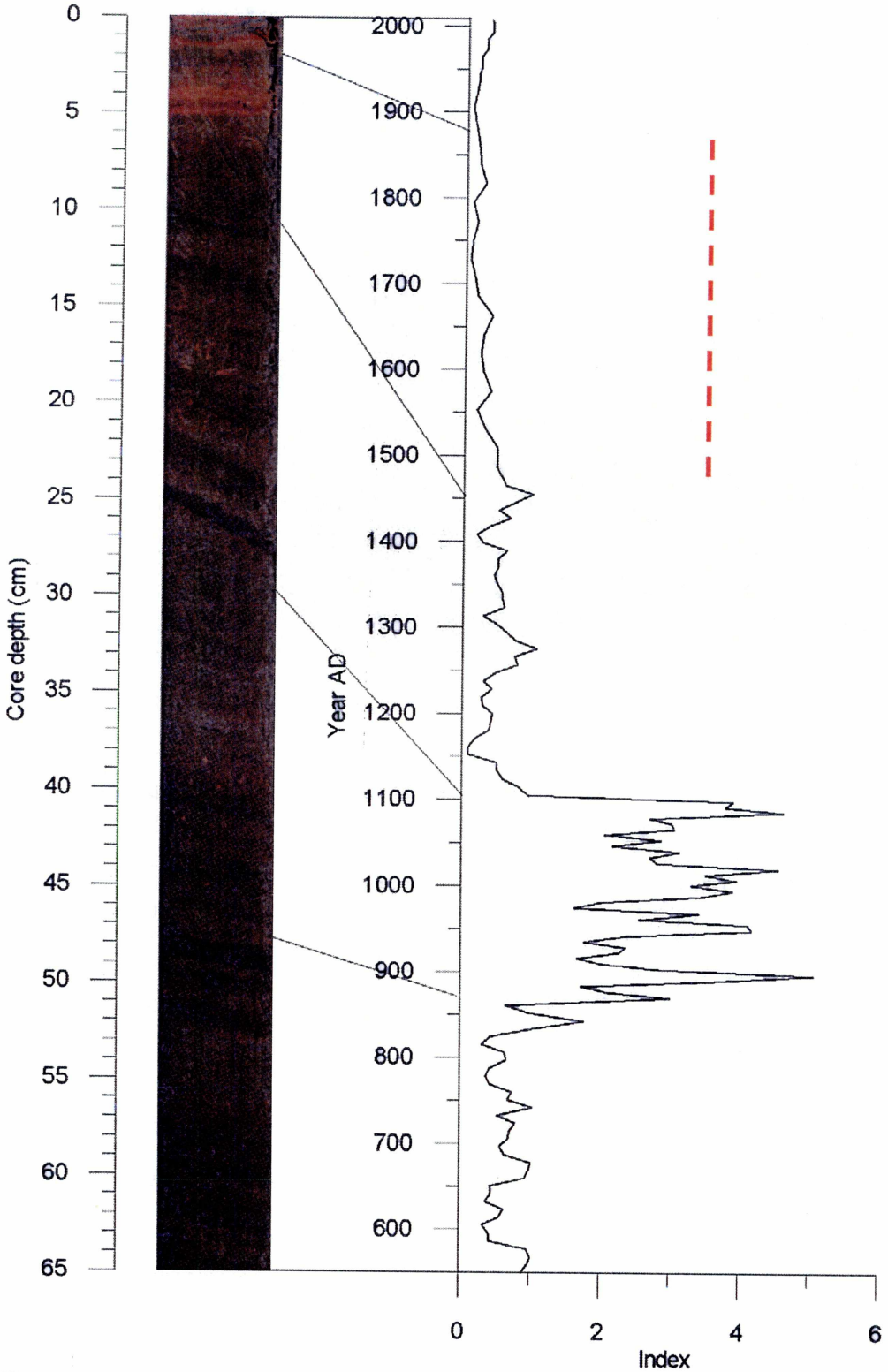


*Figure 3.23 Lake sediment core from Sabine Ø. Low index values represent cold and dry conditions whereas low index values represent more snow rich conditions caused by a stronger influence of warmer and more moist air masses from lower latitudes. The red broken line shows the approximate Thule Inuit Culture era.*

The lake at Eskimonæs

The lake at Eskimonæs (Fig. 3.24) offers from its near coastal position and its geomorphological setting ideal possibilities to reveal environmental changes in the landscape. Unfortunately sediment slumping has affected sediments from the cultural era. Figs. 3.24, 3.25 and 3.26 illustrate the early Holocene sedimentary history of the lake. Data from the Eskimonæs Lake, gives insight in the early Holocene environmental development, immediately following the Younger Dryas and have been the basis for a master project, which will be presented and published separately as a master thesis during the summer of 2009.

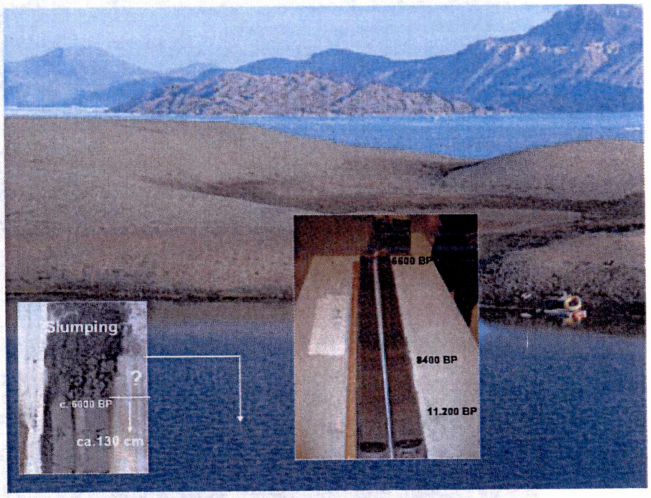


*Figure 3.24. The lake at Eskimonæs. Slumping has affected all sediments from the younger part of the Holocene, whereas finely layered early Holocene sediments are found intact. The undisturbed sediment sequence covers the period about 11.200-6600 BP.*

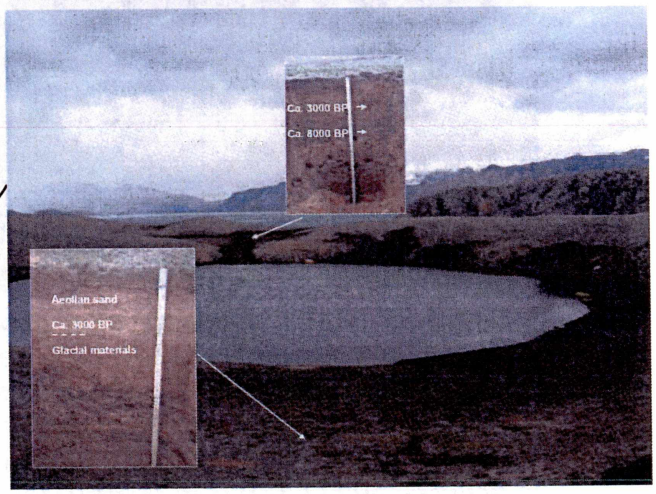


*Figure 3.25. Soils and sediments in the small catchment around the lake at Eskimonæs have been studied and dated using OSL-techniques. After 8000 YBP, and probably following the early Holocene cooling around 8200 sedimentary conditions changes probably caused by base level changes. Again after 3000 YBP a marked change is indicated, also showing increasing niveoaeolian activity*

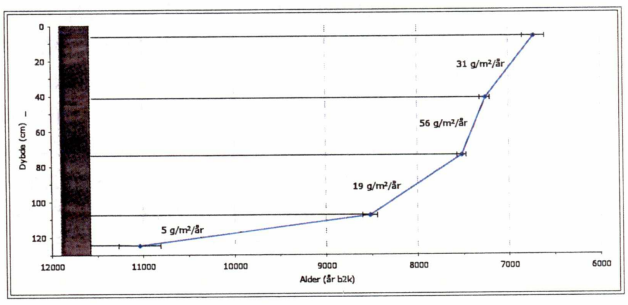


*Figure 3.26. Sedimentation rates during the Early Holocene in the lake at Eskimonæs. During the early part, and before the 8200 BP event, very low rates corroborates the understanding of the early Holocene having dry climates, very low snow coverage and warm high arctic summers. Increasing import of low latitude warmth and moisture and increasing snow fall generally results in higher sedimentation rates.*

Fladstrand.

The Thule Culture settlement at Fladstrand on the south coast of Clavering Island was chosen for archaeological excavations. Wet and moist areas close to the coast and immediately down slope a number of Thule winter houses offered favorable conditions to find well preserved materials, revealing the economy and hunting strategy of The Thule Culture. Soil profiles in the excavated area and at the coast were studied to determine soil-geomorphological processes in the by humans strongly influenced landscape (Fig. 3.27).

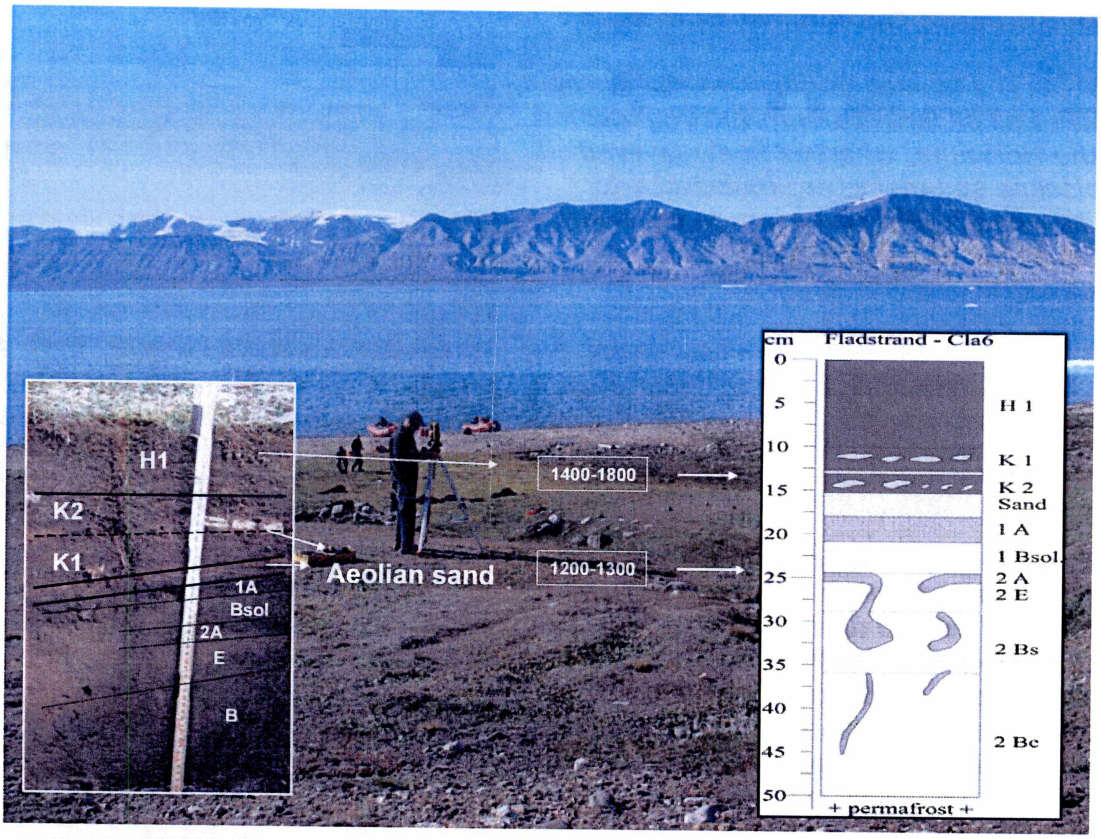


*Figure 3.27. The archaeological observations and datings indicate an early and a later phase during The Thule Culture Era (K1 and K2) from the 15th to the 18th century. The layering of the polysequent soil profile and dating of plant fragments in the solifluction layer (1A and 1Bsol) and in lower culture layer K1 indicates strong climatic impacts on soil-geomorphology. An early Holocene leached and weakly podzolized soil (2A, E & B horizons) indicating warmer conditions, higher precipitation and deeper lying permafrost, has been disturbed/cryoturbated and covered by a thin solifluction layer (1A & Bsol.) Datings indicate, that cryoturbation processes and the covering by niveoaeolian sand not appeared before the start of the Little Ice Age era about 1200 BP. In spite of a generally still colder climate during the Holocene, after the Mid Holocene followed by a neoglaciation in higher lying ice free landscapes, many low lying landscapes remain stable until the beginning of the Little Ice Age, after which permafrost-active layer processes and niveoaeolian activity strongly influenced on soil-geomorphology, for the first time during the Holocene. The little Ice Age obviously represents a unique cold era, following the snow rich medieval period.*

Eskimovig

Close to the Thule Culture settlement at Eskimovig on the south coast of Clavering Island a polysequent soil profile was studied, showing a buried Early Holocene soil covered by solifluction and aeolian materials (Fig. 3.28). $^{14}C$ datings of plant fragments belonging to the period showing solifluction and, materials which cover the Early Holocene leached Brown soil show that this dry and well drained landscape was not influenced by solifluction and niveoaeolian covers before the more severe part of the Little Ice Age. Organic enriched layers in the aeolian cover indicate periods of low niveoaeolian activity, which could represent periods of low snow coverage and less wind blown redistribution of snow and sediment in the landscape. In the lake sediment from Sabine Ø iron enriched layers indicate a number of cold periods with thin snow covers during the 17$^{th}$ and 18$^{th}$ century. In the lake core these are - by linear interpolation from the upper lead 210 dated part of the core - dated to about 1680-1700 AD and 1750-1770 AD. Periods of iron accumulation in lake sediments in Germania Lake correlate well with the humus enriched layers at Eskimovig, and the upper slightly humus enriched layer 5-7 cm below the present land surface could easily correspond to a slightly iron enriched layer in Germania Lake, dated to 1870-1890 AD by lead 210. The Eskimovig soil profile supports the observations from Fladstrand and other sites of unique Holocene cold climate geomorphological processes, restricted to the climatic situation established in the region during the Little Ice Age and after the medieval snow rich period.

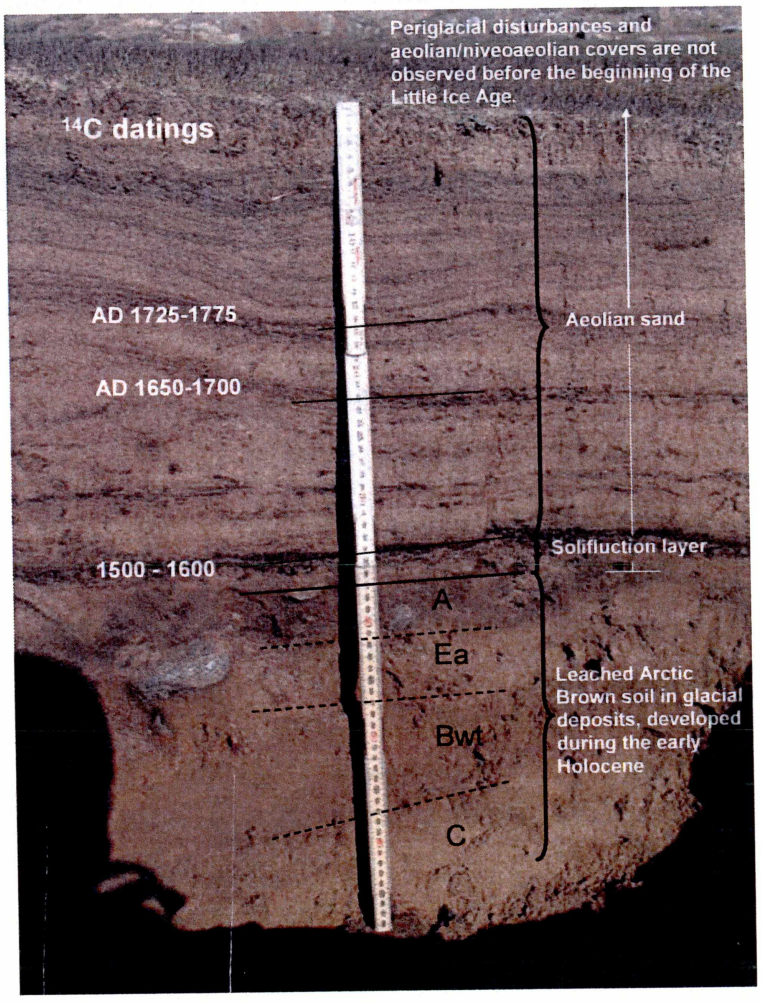


*Figure 3.28. Soil profile at Eskimovig, showing an Early Holocene soil, influenced by periglacial activity during the Little Ice Age.*

Marine cores

In 2008 it was planned to collect short marine sediment cores in the coastal waters between Young Sound and Sabine Ø. The aim was to study sedimentary features related to changes in ice coverage in near coastal waters and also related to changes in snow coverage on land, known to be positively connected to periods of lower ice coverage. The corings were carried out from the Danish naval vessel Vædderen, but due to hard weather conditions during the short stay of Vædderen in the area, only three short cores were collected in a transect outside Sabine Ø (Fig. 3.29). Late August during the passage of the small Danish expedition vessel Active, a short core was collected close to the coast at Germania Havn by Naja Mikkelsen from The Geological Survey of Denmark and Greenland. Near costal marine sediments were found to be mostly very fine grained and very poor in materials suitable for $^{14}C$ dating. From the bottom part of the longest and outermost core in the transect, a very small sample of carbonate material was used for a possible dating. The sample showed to be to small for a proper dating, but fortunately a dating of the Active core, and pronounced similarities in the XRF scanning patterns of the two cores allowed a approximate dating of the bottom part of the core A080814-B (Figs. 3.29 and 3.30). So far X-ray fluorescence spectrometry (XRF) scannings have been carried out on the collected cores. By scanning of the core surface, the geochemical variations can be found throughout the sediment sequence. Variations in different elements are of significance as the differences can indirectly be interpreted in terms of changes in sediment characteristics and depositional environment. Figures 3.30-3.34 show the geochemical variations and correlations between different elements. A first interpretation is presented with respect to possible environmental significance of the element variation.

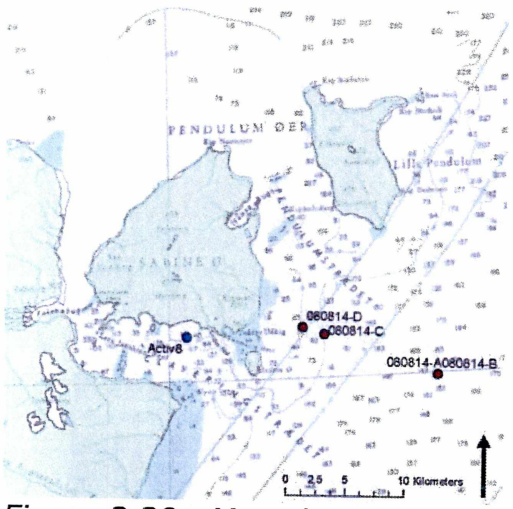


*Figure 3.29. Map showing the sites where the short marine sediment cores were collected.*

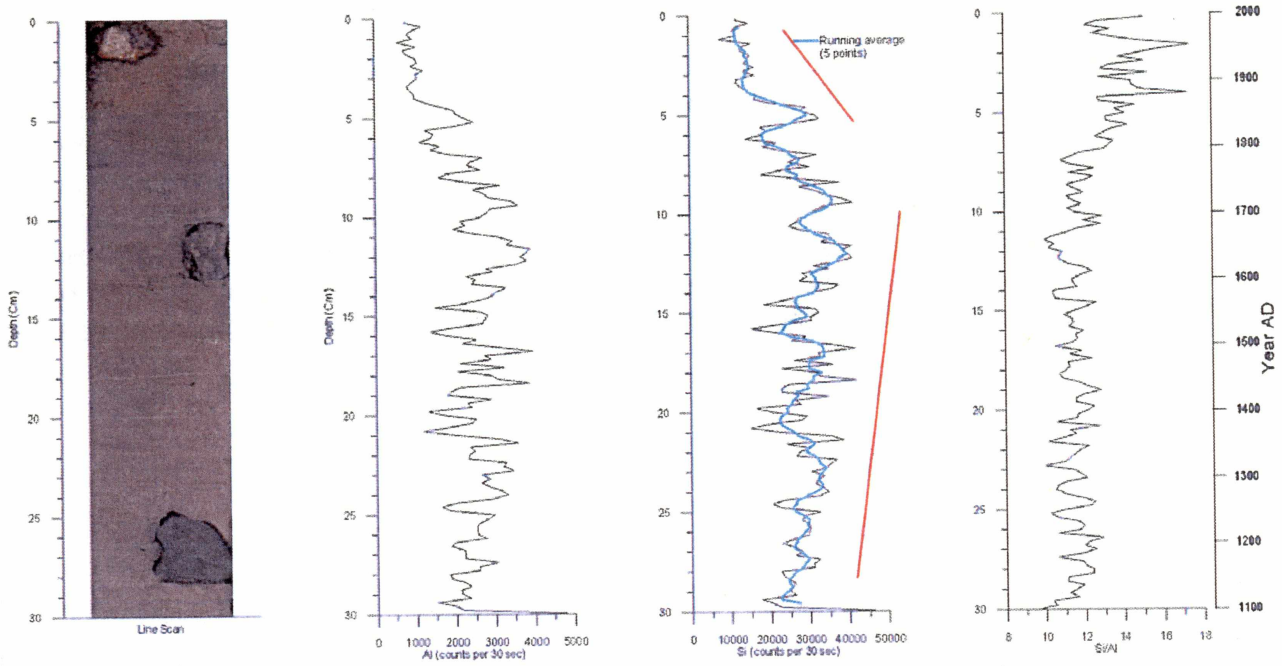


*Figure 3.30. Line scan and aluminium (Al) and silicon (Si) element signals from a XRF scanning of the marine core A080814-B, ca. 15 km. east of Sabine Ø. The Si/Al ratio is also shown.*

Al and Si in the sediment core clearly correlate, and it is also clearly shown that lower values of Al and Si correlate positively with higher Si/Al ratios (Fig. 3.31). This is both seen in the clear sedimentary change after the later part of the 19$^{th}$ century and when looking at more short range variability during the full period covered by the sediment core. In Figures 3.32 and 3.33, Si shows a positive correlation with iron (Fe) and potassium (K) and in Figure 3.33 Si show an inverse relationship with sulphur (S). Consequently, Fe and S do not correlate indicating that sulphur signals probably are related to organic matter contents. XRF data indicate the main characteristic of two main sedimentary trends. One characterized by higher Si/Al ratios, and lower Fe and K values probably indicating coarser grain sizes, and one characterized by lower Si/Al values and higher Si, Al, K and Fe values, probably indicating more fine grained materials. The higher sulphur values following the coarser grain sized could indicate a higher organic matter content.

The visual appearance of the sediment core (Fig. 3.30) corroborates the assumption of a more coarse grained and slightly more organic rich sediment sequence in the uppermost 5 cm, probably representing the sedimentation after the termination of the Little Ice Age (LIA). The coarser grain size and slightly higher organic matter content observed, both after the LIA and during shorter periods in preceding centuries could indicate periods of a stronger, and run off driven land-ocean flux and slightly higher biological production in the near coastal marine environment. More ice free near coastal waters known to be related to higher amounts of snow in near coastal

landscapes could be responsible for the observed shifts from more fine grained to more coarse grained sediments. The niveoaeolian sediments at Eskimovig (Fig. 3.28) presumably indicate cold periods with less snow in the landscape around 1650 and around 1750, both periods also showing marine sediments indicating more ice and less snow. Further analyses of grain size distributions, mineralogy, organic matter content, biological proxies, lead 210 dating of the youngest sediments, and hopefully a few $^{14}C$ datings of the marine sediment core are planned, to allow a more detailed and stronger interpretation of the marine sediments as indicators of environmental change in the near coastal region.

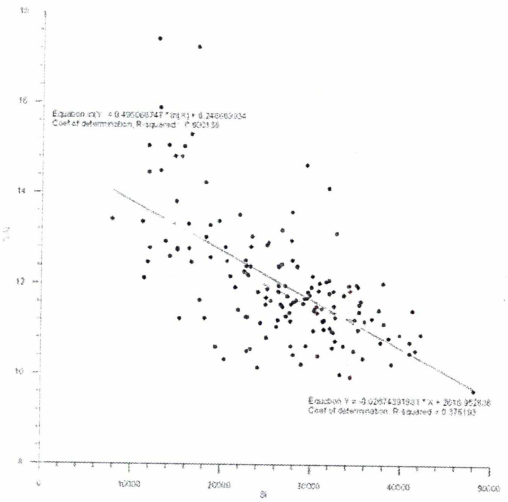

*Figure 3.31. XRF based data showing the relationship between the Si signal and the Si/Al ratio.*

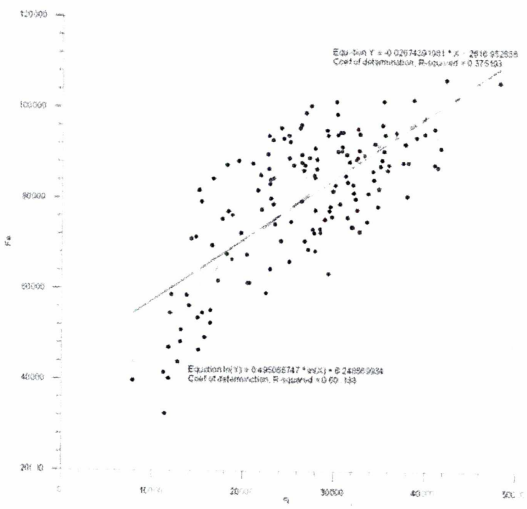

*Figure 3.32. XRF based data showing the relationship between the Si and Fe values*

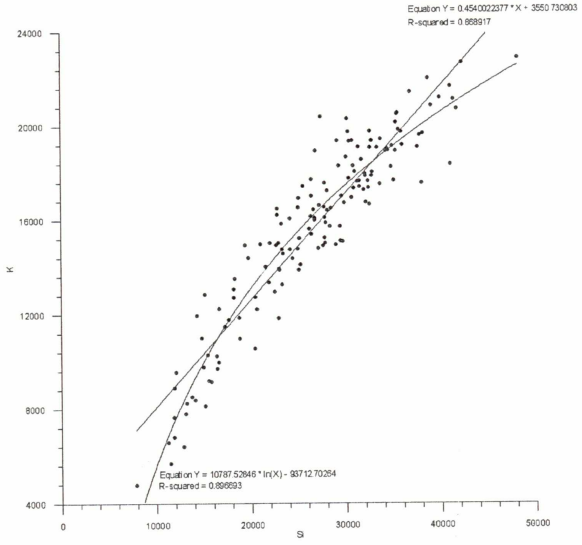


*Figure 3.33. XRF based data showing the relationship between the Si and K values*

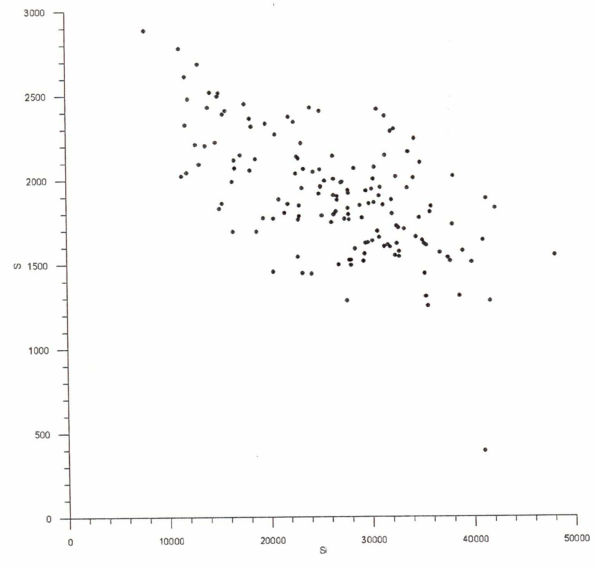


*Figure 3.34. XRF based data showing the relationship between the Si and K values.*

## 4. Geoark activities at visited sites

The GeoArk team visited many sites on Clavering Ø, Wollaston Forland, Sabine Ø and Hvalros Ø during their expeditions in 2007 and 2008.

Morphological observations and topographic measurements of archeological sites were often made with leveling instruments. We used both traditional leveling instruments (Topcon) and differential GPS instruments (Trimble). The latter were using two satellites-receiving antennas ('basis station' and 'rover' station) to measure topography with an accuracy of about 1 cm in all directions. A summary of all Topcon and GPS measurements is presented in Table 4.1 (2007) and Table 4.2 (2008)

Table 4.1. Summary of all Topcon and GPS measurements (RTK) in 2007

| Date | Method | Day of Year | Location | Objective |
|---|---|---|---|---|
| 2007_08_07 | Topcon | 219 | Eskimonæs | Morphology |
| 2007_08_08 | Topcon | 220 | Eskimonæs | Morphology |
| 2007_08_09 | Topcon | 221 | Fladstrand | Morphology and archeology |
| 2007_08_10 | Topcon | 222 | Eskimonæs | Morphology and archeology |
| 2007_08_11 | GPS | 223 | Eskimonæs | Morphology |
| 2007_08_16 | Topcon | 228 | Dahls Skær | Morphology |
| 2007_08_17 | Topcon | 229 | Dødemandsbugten | Morphology |
| 2007_08_18 | Topcon | 230 | Strandengnæs | Morphology |
| 2007_08_19 | Topcon | 231 | Dahls Skær | Morphology and archeology |
| | GPS | 231 | Dahls Skær | Morphology and archeology |
| 2007_08_20 | Topcon | 232 | Grønnedal | Morphology |
| 2007_08_22 | GPS | 233 | Dahls Skær | Morphology and archeology |

Table 4.2. Summary of all GPS measurements (R8-RTK) in 2008

| Date | Day of Year | Location | Remarks |
|---|---|---|---|
| 2008_07_29 | 211 | Revet | Morphology |
| 2008_07_31 | 213 | Revet | Morphology |
| 2008_08_02 | 215 | Eskimonæs | Morphology |
| 2008_08_05 | 218 | Eskimonæs | Morphology and archeology |
| 2008_08_06 | 219 | Dødemandsbugten | Morphology and archeology |
| 2008_08_07 | 220 | Bådsted | Morphology and archeology |
| | 220 | Holmevig | Morphology and archeology |
| 2008_08_08 | 221 | Eskimonæs | Morphology |
| | 221 | Eskimovig | Morphology and archeology |
| 2008_08_09 | 222 | Eskimonæs | Morphology |
| 2008_08_13 | 226 | Hvalros Ø | Morphology and archeology |
| 2008_08_15 | 228 | Hvalros Ø | Morphology and archeology |
| 2008_08_16 | 229 | Hvalros Ø | Morphology and archeology |
| 2008_08_17 | 230 | Sabine Ø / Hansabugt | Archeology |
| 2008_08_19 | 232 | Hvalros Ø | Morphology and archeology |
| 2008_08_20 | 233 | Hvalros Ø | Morphology and archeology |
| 2008_08_21 | 234 | Hvalros Ø | Morphology and archeology |
| 2008_08_27 | 240 | Grønnedal | Morphology |
| 2008_08_28 | 241 | Zackenberg | Morphology |
| 2008_08_29 | 242 | Zackenberg | Morphology |
| 2008_08_30 | 243 | Henningelv, Grønnedal | Morphology and archeology |
| | 243 | Kap Berghaus | Morphology and archeology |
| 2008_09_01 | 245 | Zackenberg | Morphology |

The nearshore area was also surveyed with the use of an echosounder and gps positioning system, operated from our Zodiac vessel. These observations were mainly used to describe cross-shore profiles in front of sandy pocket beaches facing the fjord, like Eskimonaes, or in front of major delta systems, like Zackenberg (see Appendix A). A summary of the observations is presented in Table 4.3. The locations of all leveling and echosounding observations are presented in Fig. 4.1.

Table 4.3. Summary of all soundings in 2007 and 2008

| Date | Hour | Day of Year | Location | Tide Table |
|---|---|---|---|---|
| 2007_08_10 | 16-17 | 222 | Eskimonæs | Finsch Øer |
| 2007_08_16 | 18:30 | 229 | Dahls Skær | Finsch Øer |
| 2008_08_04 | 10 | 217 | Falskenæs, Granatdal | Finsch Øer |
| | 16 | 217 | Hallebjergene | Finsch Øer |
| 2008_08_06 | 10-11 | 219 | Dødemandsbugten | Finsch Øer |
| 2008_08_31 | 11-13 | 244 | Zackenberg | Zackenberg |

All soundings are recorded in foot and transformed to m (1 foot = 0.3048 m).

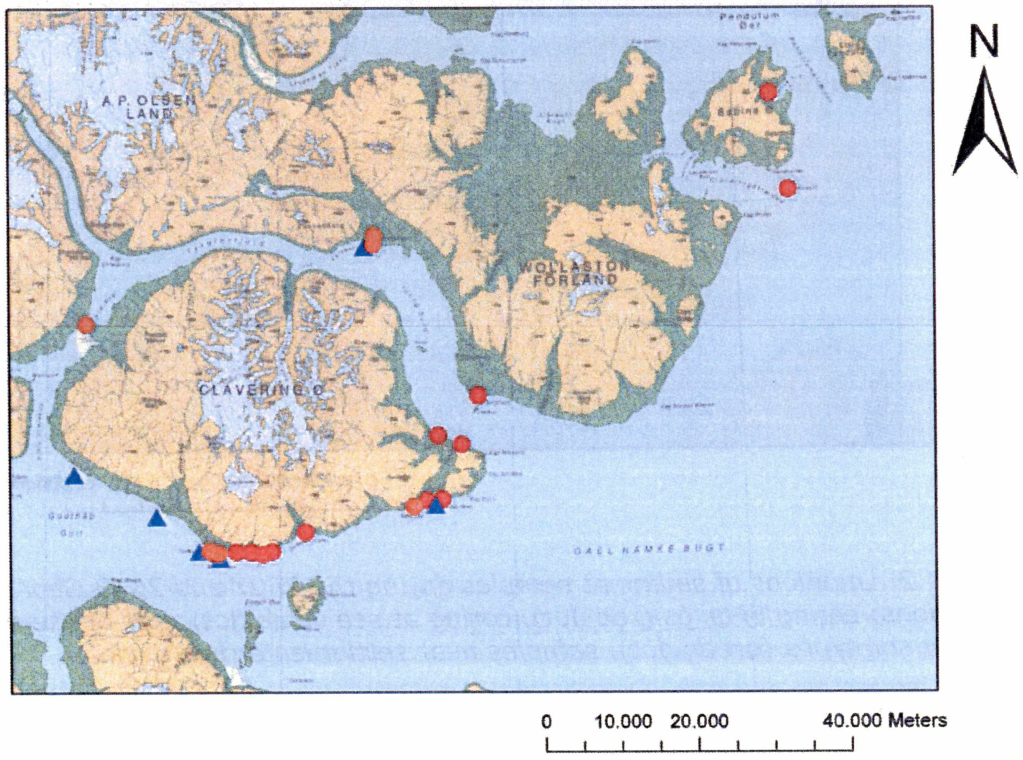


*Figure 4.1. Locations of all leveling and echosounding observations during the 2007 and 2008 GeoArk expeditions: leveling of morphology and archeology (red dot), leveling of morphology only (orange dot), sounding (blue triangle).*

Different sediment samples were taken during the two expeditions in 2007 and 2008. The basic sampling program that served as basis for the analysis and results described in Chapter 3 included sediment coring in lakes, dug pits in different soil types and on the beaches, and sediment coring in the Ocean. Besides, some extra sediment samples under settlements were taken to date the Thule Culture settlements with OSL (see Appendix C). The locations of all these activities are preented in Fig. 4.2.

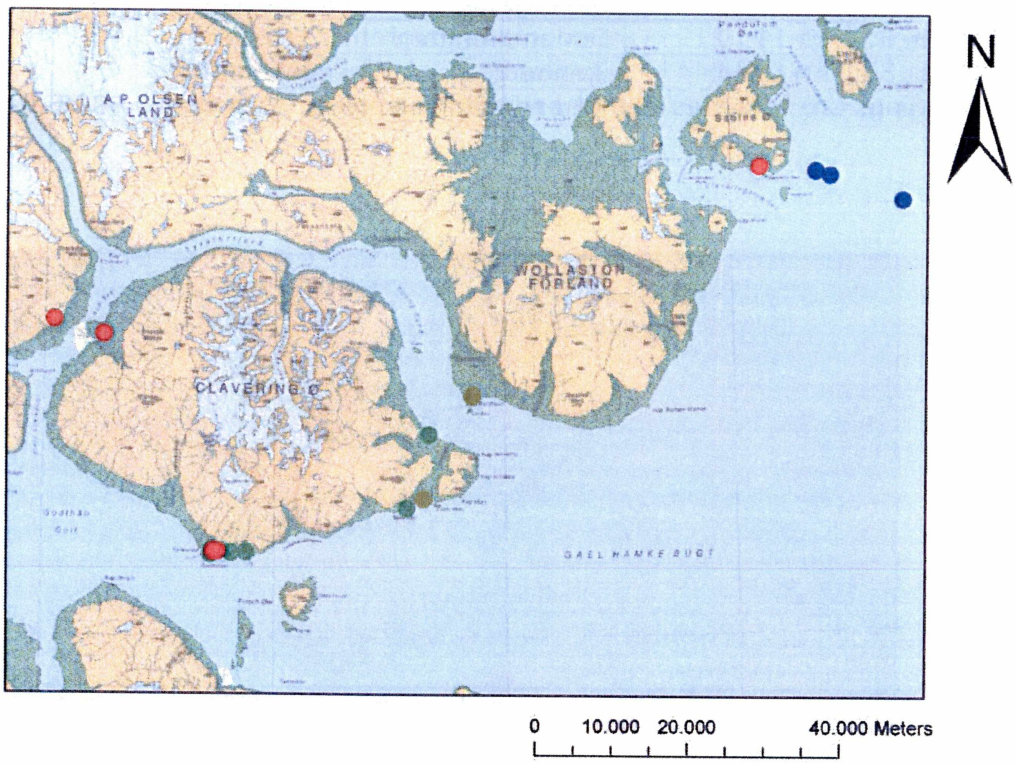


*Figure 4.2. Locations of sediment samples during the 2007 and 2008 GeoArk expeditions: coring in lakes (red dot), coring at sea (blue dot), pits at the beach and in different soil types (green dot), samples near settlements (brown dot).*

## 5. Final remarks

The coastal environments of North-East Greenland have been favorable to settle Inuits from the Thule Culture. Most of the winter settlements were located along the southern shoreline of Clavering Ø where pocket beaches and small creeks were relatively stable, and where solifluction processes were less than in the other areas, partly because of the lack of sediment. Besides, these shorelines were also well protected against the dominant northerly winds in the winter. Spring and summer settlements were probably less coupled to specific coastal environments and more related to the location of polynya. However, most of these spring- and summer settlements (tent-rings) were found on the basalt headlands and on former beach ridges. These relatively stable units were alternating with coastal areas with abundant sediment and lots of solifluction processes. Major deltas in the area, like Lerbugten and Zackenberg, were too dynamic to serve as a safe location for settlements.

The effects of variable High Arctic climates on flora and fauna have been huge, and the generally cold and ice rich but also highly variable conditions, basically established after 4500 BP and also characterizing our present, have strong influences on the amount of and excess to natural resources. Obviously, the immigration of humans to Greenland around 4500 BP, flourishing cultural periods and several periods of deserted cultural landscapes during the 4500 year long history of humans in Greenland have been affected by the changing environmental conditions. The IPY-GeoArk project indicates that stable cold periods, landscapes of low snow coverage and ice rich coastal waters, e.g. characteristic for the Thule era in the Young Sound region(c. 1400-1800), have favored Inuit's in their excess to both terrestric and marine game species in the High Arctic. Somewhat warmer but also unstable periods, showing more frequent and longer periods of enhanced snow coverage and low summer ice coverage in coastal waters, e.g. characterizing the era from AD 0 until the 1400, including the maximum medieval warmth from about AD 900-1100, seem to have caused a desolation of the High Arctic coastal landscapes.

## References

Hansen, B.U., Sigsgaard, C., Rasmussen, L., Cappelen, J., Hinkler, J., Mernild, S.H., Petersen, D., Tamstorf, M.P., Rasch, M., Hasholt, B., 2008. Present-day climate at Zackenberg. Advances in Ecological Research 40, 111-149.

Hinkler, J., 2005. From digital cameras to large-scale sea-ice dynamics. A snow-ecosystem perspective. PhD thesis. University of Copenhagen, Institute of Geography and National Environmental Research Institute (NERI). Department of Arctic Environment. 184 pp.

Kaufmann, L.H., 2009. Polynya dynamics and variability inferred from satellite imagery and historical data. BSc thesis. University of Copenhagen, Department of Geography and Geology. 63 pp.

Koch, L., Haller, J., 1971. Geological Map of East Greenland $72^0$-$76^0$ N.Lat (1:25000). Meddelelser om Grønland 183, 26 pp. and 13 maps.

## Appendix A. Geomorphological monitoring of the Zackenberg delta

## GeoBasis & GeoArk activities in 2008 (with Charlotte Sigsgaard)

### 1. Coastal dynamics

The GeoBasis program has a long tradition of monitoring the coastal dynamics at the Zackenberg delta in NE Greenland (see Sigsgaard, 2005, Chapter 8). Their monitoring program is focused on cliff recession rates along the shore of Zackenbergdalen and along the present day river, and on the evolution of cross-shore profiles at a beach and spit system in front of a former delta lobe. A map showing the monitoring sites in the coastal zone is presented in Fig. A1.1.

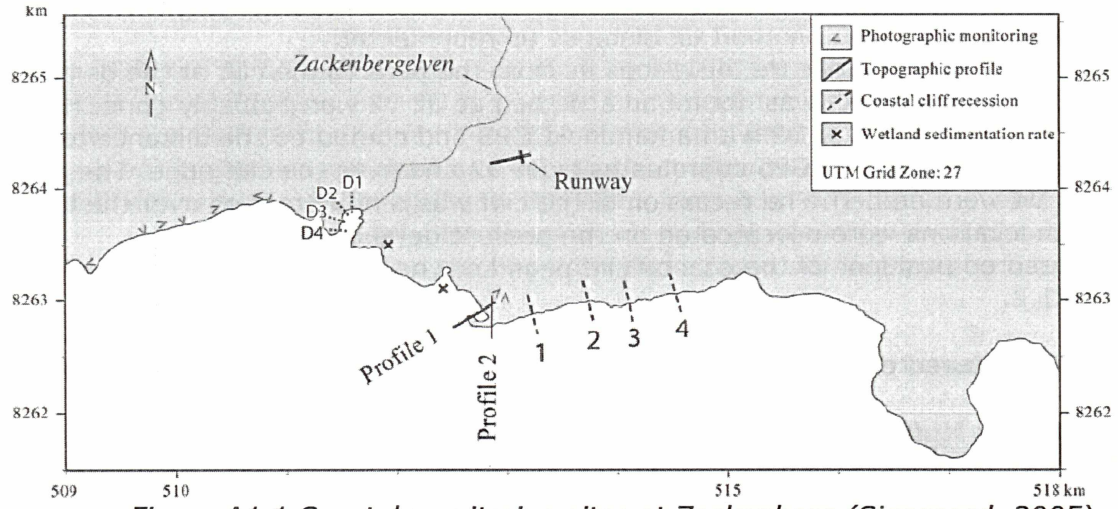


*Figure A1.1 Coastal monitoring sites at Zackenberg (Sigsgaard, 2005)*

The next sections give a brief summary of data measured in 2008. Levelings were made with a Real-Time-Kinematic GPS system. The base station was placed over well-known coordinates at the Zackenberg station (UTM, N:8264536, E:512683, Z:82.816, height: 34.78 m a.s.l.). The data include the standard monitoring parameters for the GeoBasis program (section 1.1 and 1.2) and additional data for the analysis of the delta dynamics over the last decades (section 1.3).

### 1.1 Coastal cliff positions

The coastal retreat rates along the south coast of Zackenbergdalen (coastal cliff) and along the western shore of the present delta (delta cliff) are normally measured in 4 sites each (Fig. A1.1). Table A1.1 presents the measured distances between the reference pegs and the edge of the cliff in 2008.

Table A1.1 Cliff positions at the coastal cliff sites and the delta cliff sites in 2008

| Location | Distance peg – cliff (m) | Remarks |
|---|---|---|
| *Coastal cliff* | | |
| Line 1: C1 | 19.9 | |
| Line 2: C2 | 19.0 (19.0, 20.8, 21.4) | Orientation peg is gone |
| Line 3: C3 | 18.3 | |
| Line 4: C4 | 15.9 | |
| *Delta cliff* | | |
| Line 1: D1 | - | Peg was not found |
| Line 2: D2 | 14.4 | Estimated value |
| Line 3: D3 | - | Peg was eroded |
| Line 4: D4 | - | Peg was eroded |

The orientation peg at location C2 was gone. We measured the cliff edge at this location at three sites and used the shortest distance as representative.
We were not able to measure the distances from the pegs to the cliff at the delta very accurate. The peg at D1 was not found and the peg at D2 was probably gone. Here, we estimated the position of D2 with a handhold GPS and computed the distance towards the cliff edge, using RTK-GPS coordinates from D2 and from the cliff edge. The pegs at D3 and D4 were eroded. The recession of the cliff was tens of meters over the last years and both locations were now located on the present delta plain.
The measured positions of the coastal cliff pegs and the delta cliff pegs are presented in Table A1.2.

Table A1.2 Measured positions (UTM) of the coastal cliff pegs and delta cliff pegs in 2008 (29-08-2008)

| Location | Northing | Easting | Height (m a.s.l.; top peg) |
|---|---|---|---|
| Line 1: C1 | 8263011.797 | 513270.730 | 6.540 |
| Line 2: C2 | 8263079.662 | 513747.771 | 3.040 |
| Line 3: C3 | 8263065.533 | 514026.070 | 2.948 |
| Line 4: C4 | 8263122.847 | 514399.420 | 2.960 |
| Line 2: D2 | 8264018.274 | 511525.331 | 20.029 |

The data of the cliff and delta pegs were stored in the file: cliffrecession2008.txt.
A summary of photos of the cliffs is given in Table A1.3.

Table A1.3 Summary of cliff photos in 2008 (29-08-2008)

| Location | File code | Remark |
|---|---|---|
| C3 | ZackC3a2008.jpg | East facing |
| C3 | ZackC3b2008.jpg | West facing |
| C4 | ZackC4a2008.jpg | East facing |
| C4 | ZackC4b2008.jpg | West facing |
| D2 | ZackD2x2008.jpg | At about estimated pos D2 |

## 1.2 Beach profiles

Profile 1 (Fig. A1.2) was about 275 m long and crossed a curved sandy spit on the old delta front. The prominent ridge with a height of 1.2 m at about 250 m was the present spit where we observed a lot of overwash features. The other sandy ridge at about 220 m was a former curved spit. This ridge was sheltered by the present day spit. The area between the former curved spit and the beach was very flat and shallow and a lot of fine sediments were deposited here. Profile 2 (Fig. A1.3) was about 140 m long and crossed an aggrading coastal plain with sandy beach ridges. These beach ridges could be easily distinguished in the field. The height of these ridges ranged from 0.20 to 0.30 m.
Peg P1b was the origin in Fig. A1.2 and peg P2a in Fig. A1.3, respectively (see Sigsgaard, 2005). We didn't correct our measured heights, since our height measurements were in the same range as those described by Sigsgaard (2005; see Table A1.4 for a comparison).

Table A1.4 Position (UTM) and height of the pegs in profile 1 (P1) and profile 2 (P2).

| Peg | Northing* | Easting* | Height* (m asl) | Northing | Easting | Height (m asl) | Marker in the field* |
|---|---|---|---|---|---|---|---|
| P1a | 8262971 | 512861 | 6.39 | 8262969 | 512859 | 6.406 | Iron peg on gravel plateau |
| P1b | 8262952 | 812830 | 5.12 | 8262953 | 512830 | 5.084 | Iron peg on gravel plateau |
| P1c | 8262946 | 512816 | | | | | Peg on driftwood |
| P1d | 8262866 | 512668 | 0.98 | 8262864 | 512667 | 0.895 | Wooden peg, inner barrier |
| P2a | 8262974 | 512899 | 6.13 | 8262971 | 512897 | 6.194 | Iron peg on gravel plateau |
| P2b | 8262934 | 512904 | | 8262933 | 512903 | 1.696 | Peg on driftwood |
| P2c | 8262867 | 512914 | 0.99 | 8262866 | 512912 | 1.007 | Iron peg on beach ramp |

*Data out of Tables 8.3 and 8.4 in Sigsgaard (2005)

Coastal profile data were stored in the files: Profile1280808.txt and Profile2290808.txt. ZackP1x2008.jpg is a photo of profile 1, made on 28 August 2008 and ZackP2x2008.jpg is a photo of profile 2, made on 29 August 2008.

All original data and an extensive explanation were stored in the excel-file: coast_delta_zackenberg_2008.xls.

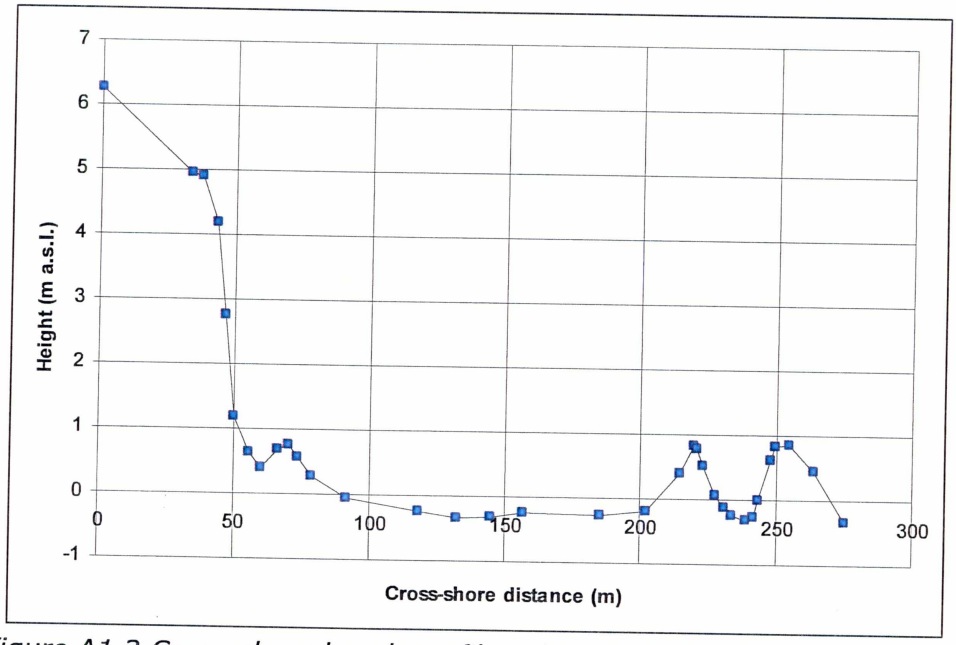


*Figure A1.2 Cross-shore beach profile 1 (28-08-2008; Day-of-year 241)*

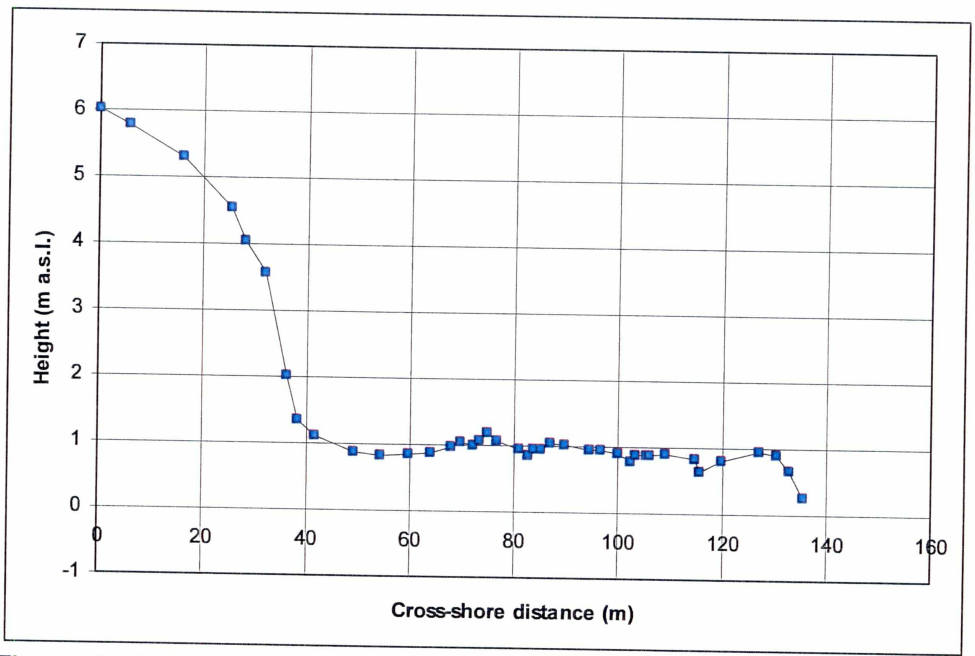


*Figure A1.3 Cross-shore beach profile 2 (29-08-2008; Day-of-year 242)*

## 1.3 Additional data measured on the delta

Additional data measured on the delta include (Fig. A1.4):

- Profile over the present watershed between the new delta lobe and the old delta lobe (Fig. A1.5; long dark blue line in the center of Fig. A1.4). This profile was measured in order to see if the river is also discharging in the old delta lobe during high discharge events. However, there was no evidence in the field that this occurred;
- High water line (level of 28 August 2008; yellow line in Fig. A1.4). The water line was measured in order to see changes in coastal features. Besides, the volume of the spit can be estimated in combination with profile data (section 1.2). Major changes occurred at the spit in the eastern part of the old delta. The spit extended about 125 m to the west and it migrated a bit further inland (about 2 m) over the last 6 years. This cross-shore shift can probably also be seen in an analysis of the profiles 1 and 2 over the last years;
- Salt marsh line (green line in Fig. A1.4). This line was measured to border the tidal area of the old delta. Besides, it also indicated the oldest part of the new delta, where the dynamics are more tidal than fluvial at the moment;
- Coastal cliff line (red line in Fig. A1.4). This line was measured in order to have a spatial idea of the present day cliffs. The measured lines can be used with other information (satellite images and data in 1.1) to determine the cliff erosion rates. Besides, the volumes eroded can be estimated by assuming a coastal cliff retreat with a constant slope. The cliff between the old and the new delta was eroding on the eastern site (no vegetation cover; high water mark on the toe of the cliff). Spectacular erosion rates were observed near the western cliff on the new delta. Retreat rates of 125 m over the last 6 years were observed and cliff erosion pegs were gone (D3 and D4, section 1.1).
- Cross-shore profile near location C1 (Fig. A1.6; see Fig. A1.1 for location): This additional profile was made to estimate cliff heights and shape in this area. Data can be used to estimate eroded volumes over time, assuming a constant shape during the cliff retreat;
- Cross-shore profiles on the delta front (between red dots in Fig. A1.4). The cross-shore profiles were made with a zodiac boat, using an echosounder and a regular GPS system. The profiles are used to have an idea of the delta front and can be used to compute the wave transformation and wave induced sediment transport on the delta. Spit formation rates and spit orientations can so also be better understand.
- Depth contour of -5 m on the delta front. Echosoundings showed that there was a very steep slope between -5 and -15 m water depth. For this reason, the spatial pattern of the delta front was mapped by measuring the -5 m depth contour. A first glance at Fig. A1.4 (light blue dots) reveals that the -5 m depth contour follows the present day shoreline, and there is not a prominent delta shape lobe into the fjord observed.

All original data and an extensive explanation were stored in the excel-file: coast_delta_zackenberg_2008.xls.

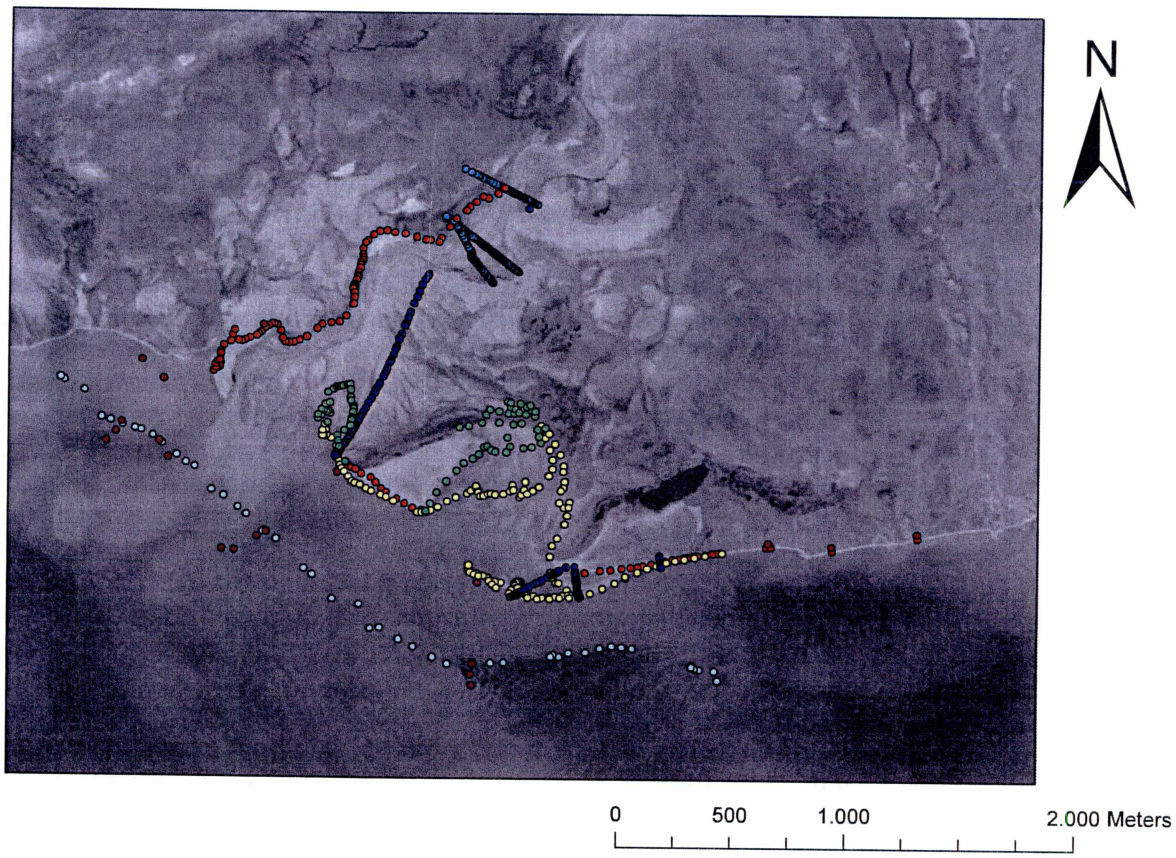


*Figure A1.4 Map with all measurements in the Zackenberg area. Profiles over the central part of the delta and along the shore (dark blue lines, from west to east: border new and old delta; profile 1; profile 2, profile C1), high water line (yellow), salt marsh line (green), coastal cliff line (red), coastal cliff pegs (dark red), sounding markers (dark red at sea), -5 m depth contour (light blue at sea), and Zackenberg river profiles (light blue at land in the north of the Figure).*

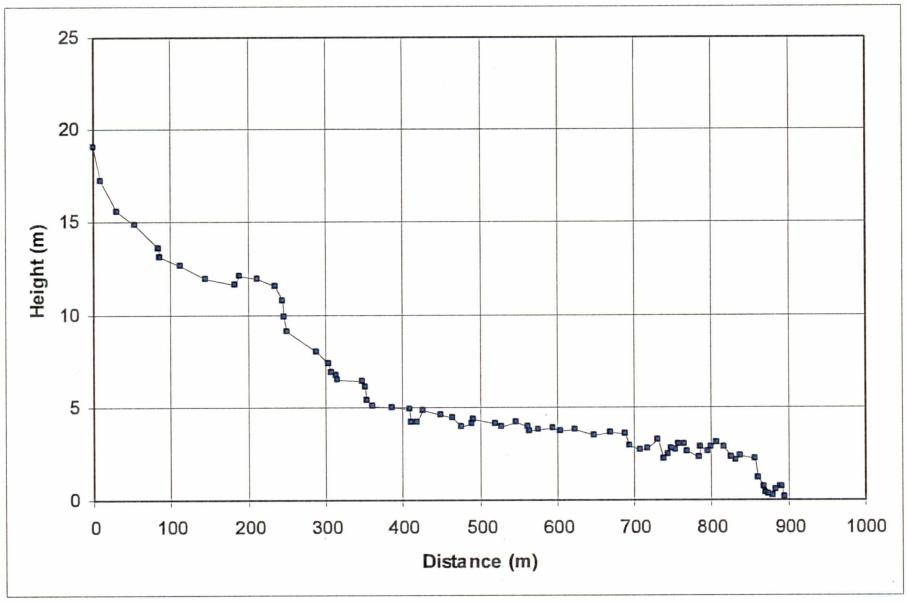


*Figure A1.5 Cross-delta profile (28-08-2008; Day-of-year 241)*

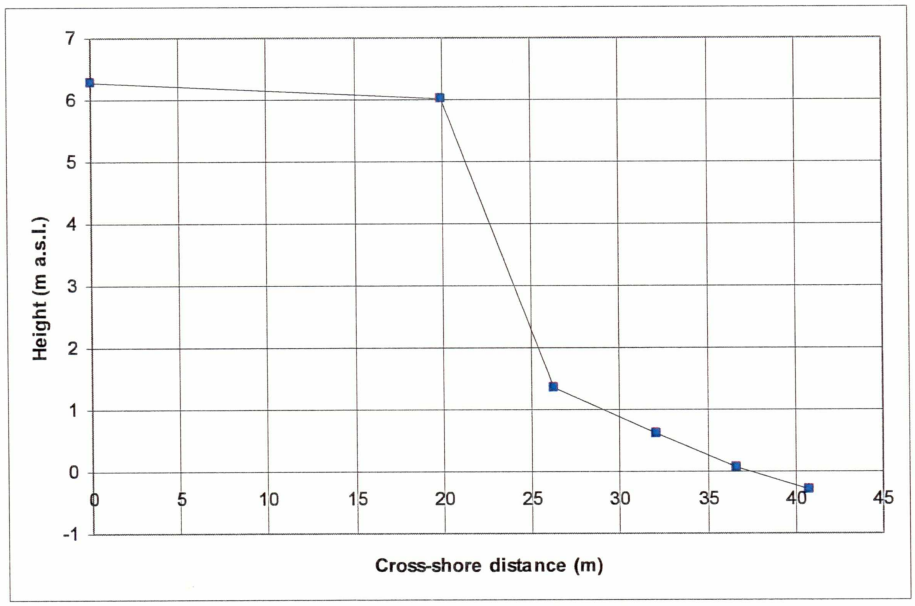


*Figure A1.6 Cross-shore beach profile C1 (28-08-2008; Day-of-year 241)*

## 2. Zackenberg river profiles

Three cross-river sections were measured with an RTK-GPS on 1 September 2008. The locations of the cross-river profiles are presented in Fig. A1.4. The profiles are presented in Figs. A2.1 (northern profile, also regularly used for water discharge measurements), A2.2 (central profile) and A2.3 (southern profile). These cross-river sections are regularly monitored in the GeoBasis program.

All original data and an extensive explanation were stored in the excel-file: river_zackenberg_2008.xls.

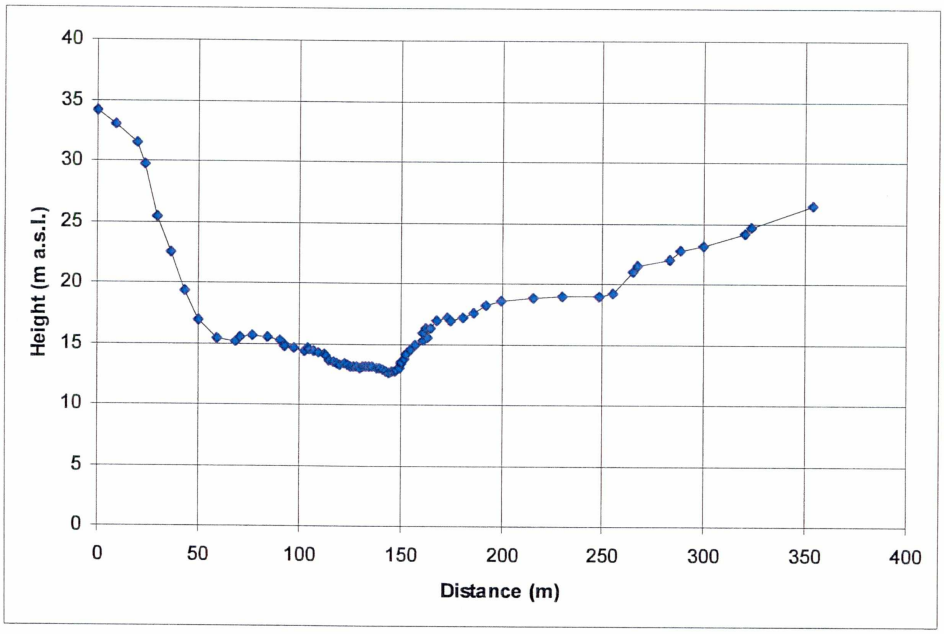


*Figure A2.1 Northern river profile (01-09-2008; Day-of-year 245)*

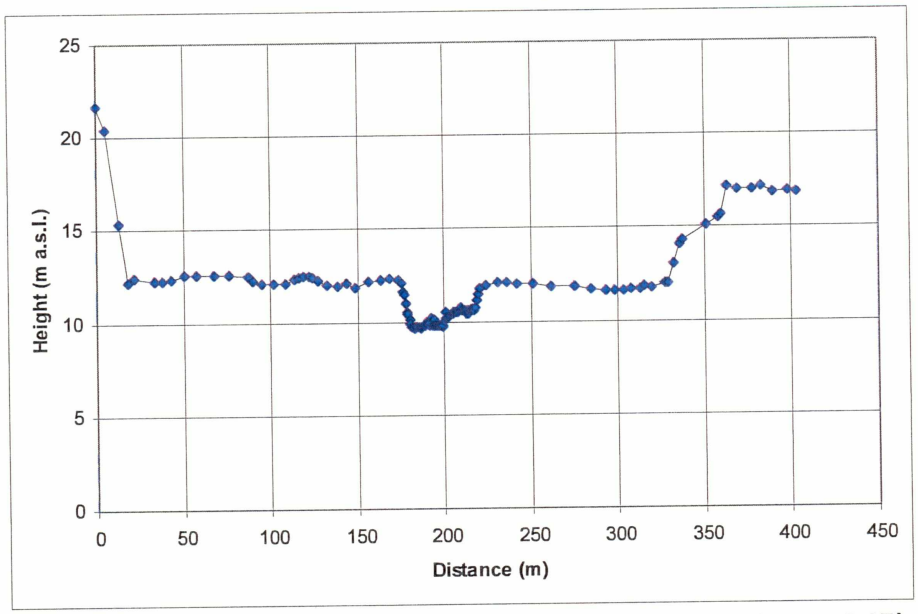


*Figure A2.2 Central river profile (01-09-2008; Day-of-year 245)*

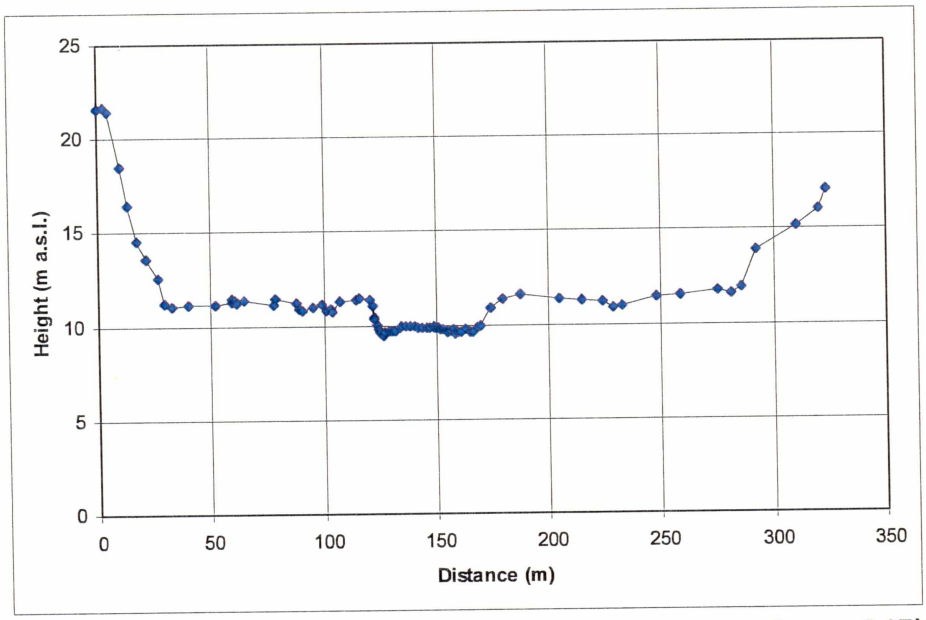


*Figure A2.3 Southern river profile (01-09-2008; Day-of-year 245)*

## References

Sigsgaard, C., 2005. GeoBasis. Guidelines and sampling procedures for the geographical monitoring programme of Zackenberg Basic. National Environmental Research Institute & Institute of Geography, University of Copenhagen. 108 pp.

## Appendix B. Wiggle-matching technique for combining cores

### *Introduction*

A sedimentary sequence in a natural environment is often studied by analyzing a series of vertical cores. These cores contain high-resolution vertical information, typically in the order of mm, on e.g., grain size characteristics, organic content, chemical content, etc.

Quite often, a complete vertical sedimentary sequence is composed of a series of sub-cores, each representing a certain depth interval. Ideally, these sub-cores do have an overlap in the vertical sense. In that case, the whole sedimentary history can be described with the use of one composed core. This note contains a description of a wiggle-matching technique that is used to compose one vertical core out of a number of sub-cores.

### *Data*

Sub-cores describing a vertical sedimentary sequence in a high-arctic lacustrine environment on Clavering Island, NE Greenland were used (Fig. B.1). The sub-cores were typically 0.2m to 1.0m long. The total length of the composed core was always representing the sedimentary layers over the permafrost layer in the area and never exceeded 1.5m. Chemical properties of the sublayers were measured with an XRF-scanner and the vertical resolution of the data was 0.002m. The vertical profiles of the S, Si, K, Fe and Ca content in the sub-cores were used in the present study (see Fig. B.2 for an example).

### *Methods*

The wiggle-matching technique was executed in four steps: 1) data smoothing, 2) choice of data window, 3) computation of the optimal linear correlation coefficient between the cores, based on a least-square fitting method between the data windows in the sub-cores.

Data smoothing was executed to reduce the high frequency spiky character of the measured vertical distribution of the chemical properties. Two methods were tested to smooth the data: 1) a moving average method with a 5-point running-average box filter, and 2) a spectral method, based on a simple fast Fourier transform (FFT) and its inverse, actually acting as a low pass filter.
The moving-average technique was directly operating on the vertical distribution. The size of the running average box influenced the variability of the measured series: small values of this box gave a high variation and higher values resulted in lower variations over depth. The size of the box also influenced the final length of the sub-core. In case of a small overlap between the sub-cores, the box size needed to be small, always below the expected size of the overlap. A 5-point running-average box represented averaging over 0.01m in our measured series. The averaged value was automatically placed at the last value of the box, in our case at the deepest value in the sub-core. An adjustment of 0.005m in an upward direction was applied in our case to place the moving-average value at the central position in the box.

The spectral method was based on a FFT technique. Actually, data was transformed (FFT), the higher frequencies were set to zero (low-pass filter), and a new depth-series was computed with an inverse FFT transformation. The spectral method was also very effective in reducing the high-frequency spiky character of the originally measured series. However, it was not so successful in describing the very low-frequency variations, due to the limited amount of data in one sub-core (tapering-effect). This was especially the case when these variations occurred at the start and end of the depth-series.

The choice of the data window in the sub-cores was the next step, just after data smoothing. The data window should of course be smaller than the proposed overlap between sub-cores (upper limit). Besides, it should be large enough in order to represent enough layers on which a statistical correlation could be computed (lower limit). We used a fixed data window in the upper part of the lower (deepest) sub-core and varied the data window over depth in the upper sub-core (just above it; Fig. B.3). The upper part of the fixed data window in the lower core was normally set at about 0.01m below the top of the sub-core. This was done to reduce the impact of boundary pollution in the depth-series. For each position of the data window in the upper sub-core we computed a linear correlation coefficient between the chemical properties of the sub-cores, using a least-square fitting method. This resulted in a vertical distribution of the correlation coefficients for a specific data window (Fig. B.4). The depth of the maximum value for the correlation coefficient represented the depth in the upper sub-core where the upper limit of the data window was found (see Fig. B.3).

In summary, we started with the computation of the smoothed time-series. Most of the time, we used the moving average method. Then, we estimated the expected overlap between the sub-cores, based on our notes we made during coring. Thereafter, we chose different data window sizes and computed the correlation coefficients between the different sub-cores. The depth of the maximum correlation probably resembled the start in the overlap between the sub-cores.

***Results***

Sub-cores from two locations on Clavering Island, NE Greenland, were used to create two composed cores. These cores were further used to study the sedimentary sequence and climate change over the last part of the Holocene in a high-arctic lacustrine environment. The coring at the first location (UTM 27 North: 492005, 8223243) resulted in three sub-cores (Fig. B.5). The expected overlap between the sub-cores is large and could be over 0.2-0.4m. The coring at the second location (UTM 27 North: 492014, 8223147) also resulted in three sub-cores. However, the expected overlap between these sub-cores was much smaller, with an expected overlap of 0.05m between the upper and middle sub-core and of 0.03m between the middle and lower sub-core.

Fig. B.2 gives an example of the chemical element (K) of the sub-cores in location 1. The data was smoothed with both the 5-point running-average box filter (left panel) and the spectral method (right panel). In this specific case, both methods could be used to smooth the depth-series. All results for the successive chemical elements are shown in Appendix B.1. The smoothened depth-series (moving-average method) was further used.

The data window in the sub-cores was set to different sizes: 0.10m, 0.15m, 0.20m and 0.30m (see Table B.1). This was large enough to have enough data in the window and smaller than the maximum expected overlap between the sub-cores (see Table B.1). For all these cases, the vertical distribution of the linear correlation coefficient was computed. An example of this distribution is given in Fig. B.4. Further examples for different elements and a data window of 0.30m are shown in Appendix B.2. All maximum correlation coefficients for five different chemical elements on location 1 are presented in Table B.1. There is a clear convergence towards two levels over overlap, one for the upper and central sub-cores and one for the central and lower sub-cores. The upper and central sub-core correlated well with a data window of 0.30m, and the central and lower sub-core correlated well with a data window for 0.20m (see Appendix B.3). The latter had to be smaller, since our observations during coring indicated less overlap. We also computed the correlation between the upper and lower core (Appendix B.4). The correlation coefficients in Table B.1 differ a lot. In the case of sub-core 1 and 2, the maximum correlation coefficients were found with a data window of 0.30m. This meant that in choosing large windows, the correlation was still better. This trend was however certainly not observed comparing the sub-cores 2 and 3. An increase of window size decreased the correlation. This could be due to two aspects: 1) the size of the data window was too large, compared to the expected overlap interval, and 2) the correlation maximum was not a single peak in the depth profile, but showed multiple maxima (see Appendix B.2 and B.3: Element Fe). The overlap between the upper and the lower core, neglecting the middle core is also striking. Looking to the different elements, there is often a distinct peak, but the levels differ. In general, there is overlap between -0.05 m (lower core) and -0.39 m (upper core), if we apply the distinct maximum in the Fe series (has still multiple maxima). However, different rates of compaction in the two cores make it difficult to apply the technique (see spacing of light stripes in both cores), where similar compaction rates are assumed.

The final result showing the overlapping parts in the sub-cores is summarized in Table B.2 and graphically presented in Fig. B.6. These depth values were related to the original files and were corrected for the shift in depth that was introduced by using a 5-point running-average box.

***Discussion and concluding remarks***

The described wiggle-matching technique is a method to compose one core out of a series of sub-cores, using statistical tools. In our case, the matching is executed vertical depth profiles of measured chemical properties. The choice of the specific chemical elements is based on the stability of the element in the environment and the general applicability of these elements in other studies. Luckily, we found a convergence of depth-values towards the same overlap area, using different elements (S, Si, K and Ca). The other element applied (Fe) did not show similar patterns. We decided to neglect the outcome of the wiggle-matching based on this element, because the depth-profile of the correlation coefficient showed much more peaks, and the absolute value of the correlation coefficient maxima were less than in the other elements.

The wiggle-matching technique in this study is applied to chemical properties of the sub-cores. However, a similar technique could be applied to other properties with a high resolution over depth (order of mm), like grain size values, organic contents, or color properties (intensities of the separate RGB band or ratios between them).

A successful application of the model still needs additional information about the sub-cores. First, an estimation of the expected overlap, observed while taking the sub-cores, will help to define the 1) expected data window used, and 2) to choose the upper and lower position of the fixed data window in the lower sub-core. For instance, if the expected overlap is in the order of 0.05m, the data window can never exceed 0.05m, but will probably much smaller, because the lower 0.01m in the upper sub-core and the upper 0.01m in the lower sub-core are preferable left out of the analysis, due to boundary effects in estimating the chemical properties.

The success of the wiggle-matching is also based on the least-square fit. Linear correlation coefficients are the simplest ones and can be easily used in our study, because we computed them on the same chemical element in the sub-cores. However, the correlation coefficients between the data windows in different sub-cores never reached the value 1 (complete correlation). This can be caused by different aspects: 1) differences in compaction of the layers in the sub-cores while taking the samples, 2) measuring errors of the chemical properties in the sub-cores while doing the XRF scans, 3) etc.

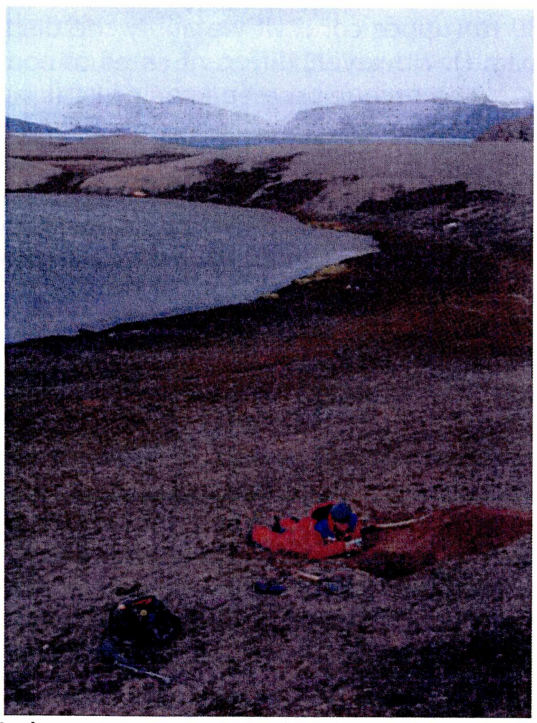

*Figure B.1. High-arctic lacustrine environment on Clavering Island, NE Greenland.*

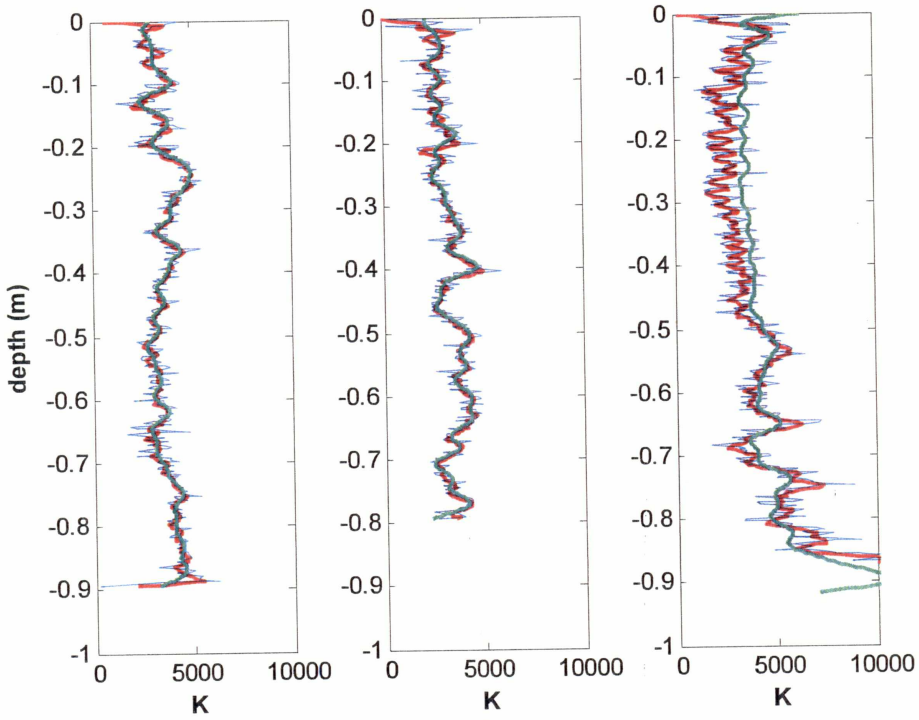


*Figure B.2. Vertical distribution of chemical element K in three sub-cores (left, center and right panels; blue lines) with the 5-points moving average smoothing (red lines) and with the spectral smoothing (green lines).*

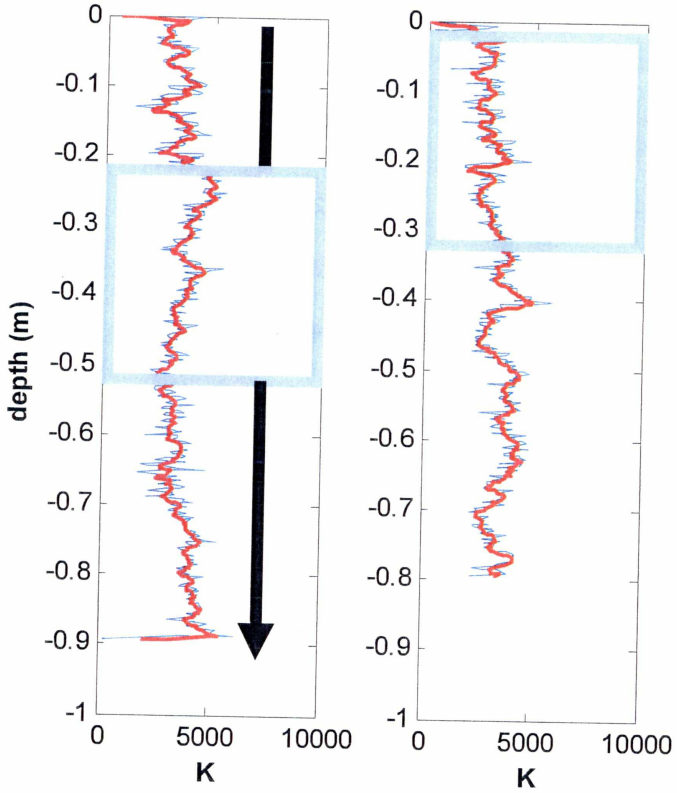


*Figure B.3. Definition sketch of the data window handling in two sub-cores. Window sizes are fixed (here 0.3m), window in the upper core (left panel) varies over depth, while window in the lower core is at a fixed depth (right panel, from 0.025m till 0.325m).*

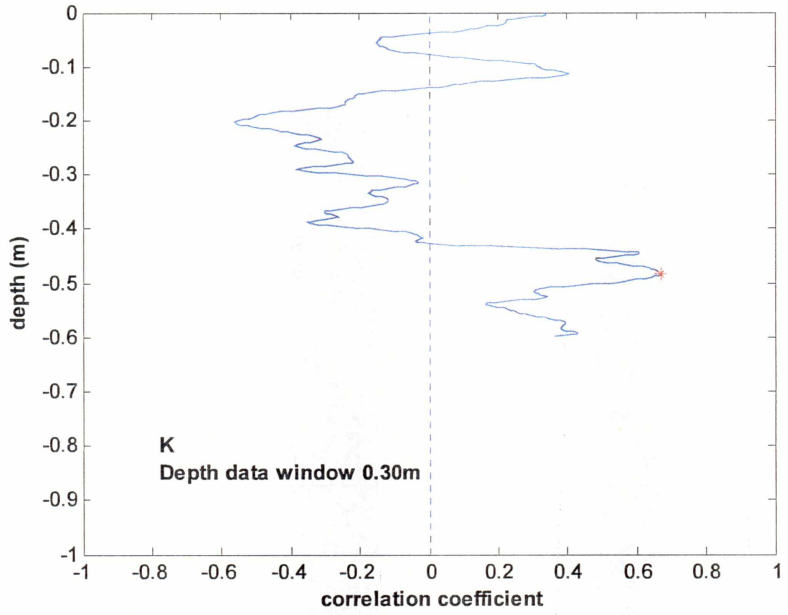


*Figure B.4. Example of the vertical distribution of the correlation between two sub-cores (1-2), based on the K element. Red star is maximum correlation. Depth value is the upper value of the data window in the upper core.*

Core 1A, upper core

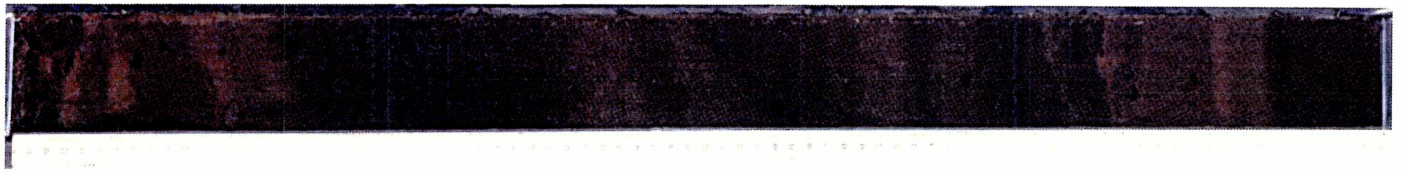

Core 2A, middle core

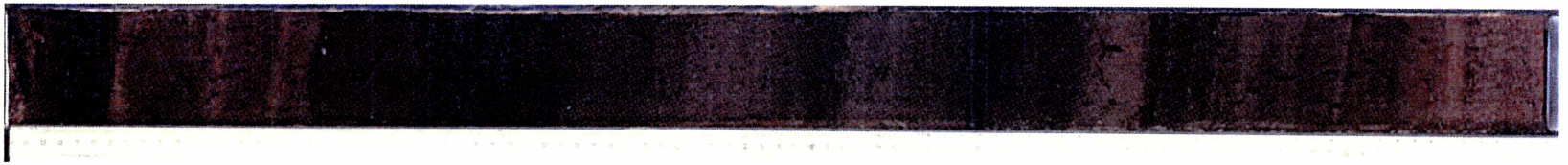

Core 3A, lower core

*Figure B.5. Photograph of the three sub-cores at Clavering Island, NE Greenland. Left is top, right is bottom.*

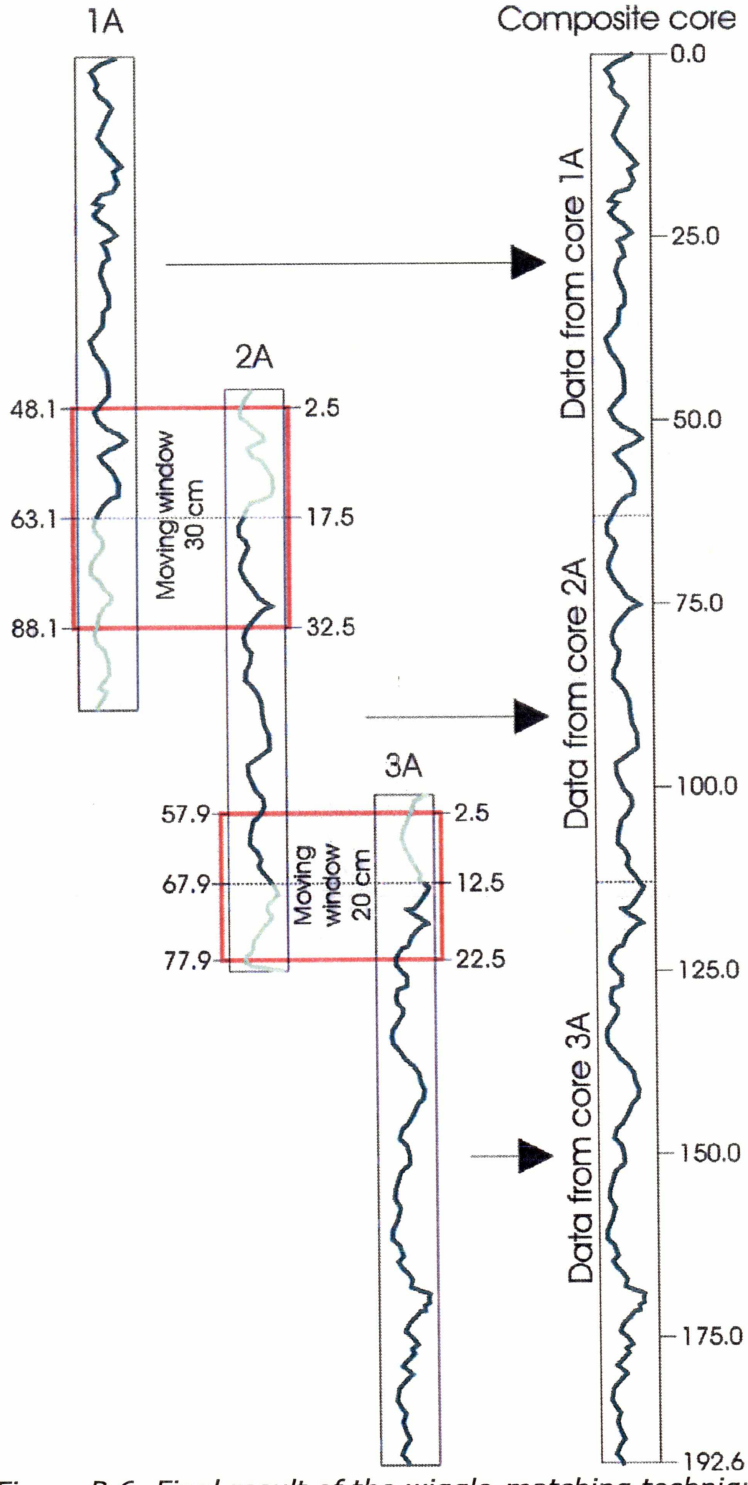


*Figure B.6. Final result of the wiggle-matching technique*

*Table B.1. Maximum correlation depth values and correlation coefficient values for different chemical elements, with different data window sizes, at one location on Clavering Island, NE Greenland.*

Sub-core 1 (upper sub-core, variable depth) and 2 (middle sub-core, fixed with upper level at 0.025m)

| Element | Max. Depth (m) | Correlation | Data window size | Depth interval (m) |
|---|---|---|---|---|
| Si | -0.748 | 0.6571 | 50 | 0.10 |
| K | -0.402 | 0.6653 | 50 | 0.10 |
| Ca | -0.620 | 0.7328 | 50 | 0.10 |
| S | -0.352 | 0.6461 | 50 | 0.10 |
| Fe | -0.444 | 0.8556 | 50 | 0.10 |
| Element | Max. Depth (m) | Correlation | Data window size | Depth interval (m) |
| Si | -0.164 | 0.6717 | 100 | 0.20 |
| K | -0.114 | 0.5292 | 100 | 0.20 |
| Ca | -0.488 | 0.6025 | 100 | 0.20 |
| S | -0.614 | 0.5331 | 100 | 0.20 |
| Fe | -0.442 | 0.5526 | 100 | 0.20 |
| Element | Max. Depth (m) | Correlation | Data window size | Depth interval (m) |
| Si | -0.486 | 0.6717 | 150 | 0.30 |
| K | -0.484 | 0.6725 | 150 | 0.30 |
| Ca | -0.486 | 0.8255 | 150 | 0.30 |
| S | -0.528 | 0.7796 | 150 | 0.30 |
| Fe | -0.444* | 0.3313 | 150 | 0.30 |

* Multiple maxima over depth

*Table B.1, continued.*

Sub-core 2 (middle sub-core, variable depth) and 3 (lower sub-core, fixed with upper level at 0.025m)

| Element | Max. Depth (m) | Correlation | Data window size | Depth interval (m) |
|---|---|---|---|---|
| Si | -0.138 | 0.7629 | 50 | 0.10 |
| K | -0.630 | 0.6547 | 50 | 0.10 |
| Ca | -0.584 | 0.6779 | 50 | 0.10 |
| S | -0.646 | 0.7278 | 50 | 0.10 |
| Fe | -0.292 | 0.7404 | 50 | 0.10 |
| Element | Max. Depth (m) | Correlation | Data window size | Depth interval (m) |
| Si | -0.618 | 0.6656 | 75 | 0.15 |
| K | -0.618 | 0.5051 | 75 | 0.15 |
| Ca | -0.584 | 0.6073 | 75 | 0.15 |
| S | -0.032 | 0.5629 | 75 | 0.15 |
| Fe | -0.074 | 0.6338 | 75 | 0.15 |
| Element | Max. Depth (m) | Correlation | Data window size | Depth interval (m) |
| Si | -0.582 | 0.6053 | 100 | 0.20 |
| K | -0.584 | 0.3992 | 100 | 0.20 |
| Ca | -0.584 | 0.5479 | 100 | 0.20 |
| S | -0.032* | 0.4965 | 100 | 0.20 |
| Fe | -0.074* | 0.5981 | 100 | 0.20 |
| Element | Max. Depth (m)** | Correlation | Data window size | Depth interval (m) |
| Si | -0.008 | 0.3726 | 150 | 0.30 |
| K | -0.492 | 0.2867 | 150 | 0.30 |
| Ca | -0.306 | 0.2628 | 150 | 0.30 |
| S | -0.010 | 0.3677 | 150 | 0.30 |
| Fe | -0.294 | 0.3408 | 150 | 0.30 |

* Multiple maxima over depth; ** probably outside the expected overlap

*Table B.1, continued.*

Sub-core 1 (upper sub-core, variable depth) and 3 (lower sub-core, fixed with upper level at 0.02m)

| Element | Max. Depth (m) | Correlation | Data window size | Depth interval (m) |
|---|---|---|---|---|
| Si | -0.226* | 0.7107 | 100 | 20 |
| K | -0.362* | 0.7473 | 100 | 20 |
| Ca | -0.344 | 0.6441 | 100 | 20 |
| S | -0.318 | 0.5884 | 100 | 20 |
| Fe | -0.360* | 0.6716 | 100 | 20 |

* Multiple maxima over depth; ** probably outside the expected overlap

Sub-core 1 (upper sub-core, variable depth) and 3 (lower sub-core, fixed with upper level at 0.05m)

| Element | Max. Depth (m) | Correlation | Data window size | Depth interval (m) |
|---|---|---|---|---|
| Si | -0.340* | 0.7115 | 100 | 20 |
| K | -0.260* | 0.5142 | 100 | 20 |
| Ca | -0.356 | 0.6748 | 100 | 20 |
| S | -0.348 | 0.6009 | 100 | 20 |
| Fe | -0.390* | 0.6356 | 100 | 20 |

* Multiple maxima over depth; ** probably outside the expected overlap

*Table B.2. Computed optimal overlap values between sub-cores in two locations on Clavering Island.*

| | Depth core 1 (m) | Depth core 2 (m) | Method | Cores |
|---|---|---|---|---|
| Location 1 | -0.481 (-0.481 - -0.781) | -0.025 (-0.025 - -0.325) | Wiggle-matching, data window 0.30m | Upper-Middle |
| | -0.579 (-0.579 - -0.779) | -0.025 (-0.025 - -0.225) | Wiggle-matching, data window 0.20m | Middle-Lower |
| | -0.35 | -0.02 (-0.02 - -0.22) | Wiggle-matching, data window 0.20m | Upper-Lower |
| | -0.36 | -0.05 (-0.05 - -0.25) | Wiggle-matching, data window 0.20m | Upper-Lower |
| Location 2 | - | - | Estimated overlap < 0.05m | Upper-Middle |
| | - | - | Estimated overlap < 0.03m | Middle-Lower |

**Appendix B.1.**
Vertical distribution of chemical elements in three sub-cores (left, center and right panels; blue lines) with the 5-points moving average smoothing (red lines) and with the spectral smoothing (green lines).

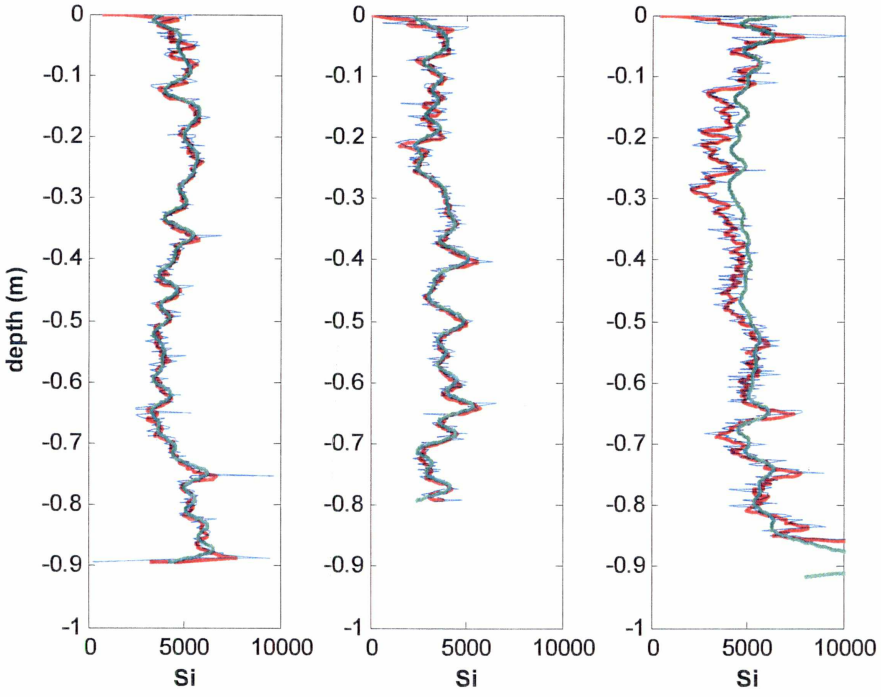

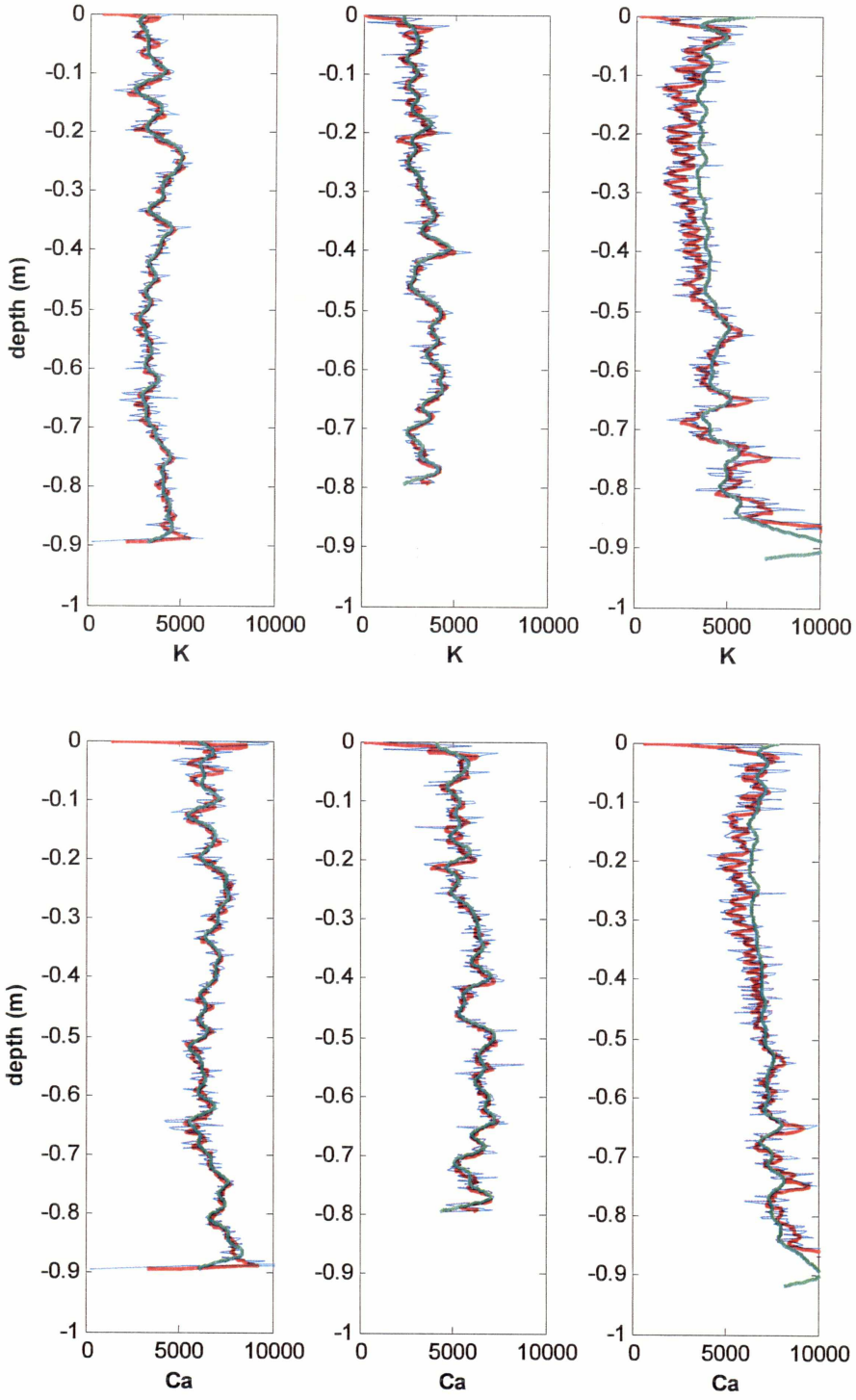
depth (m)
0
-0.1
-0.2
-0.3
-0.4
-0.5
-0.6
-0.7
-0.8
-0.9
-1
0
5000
10000
K
Ca

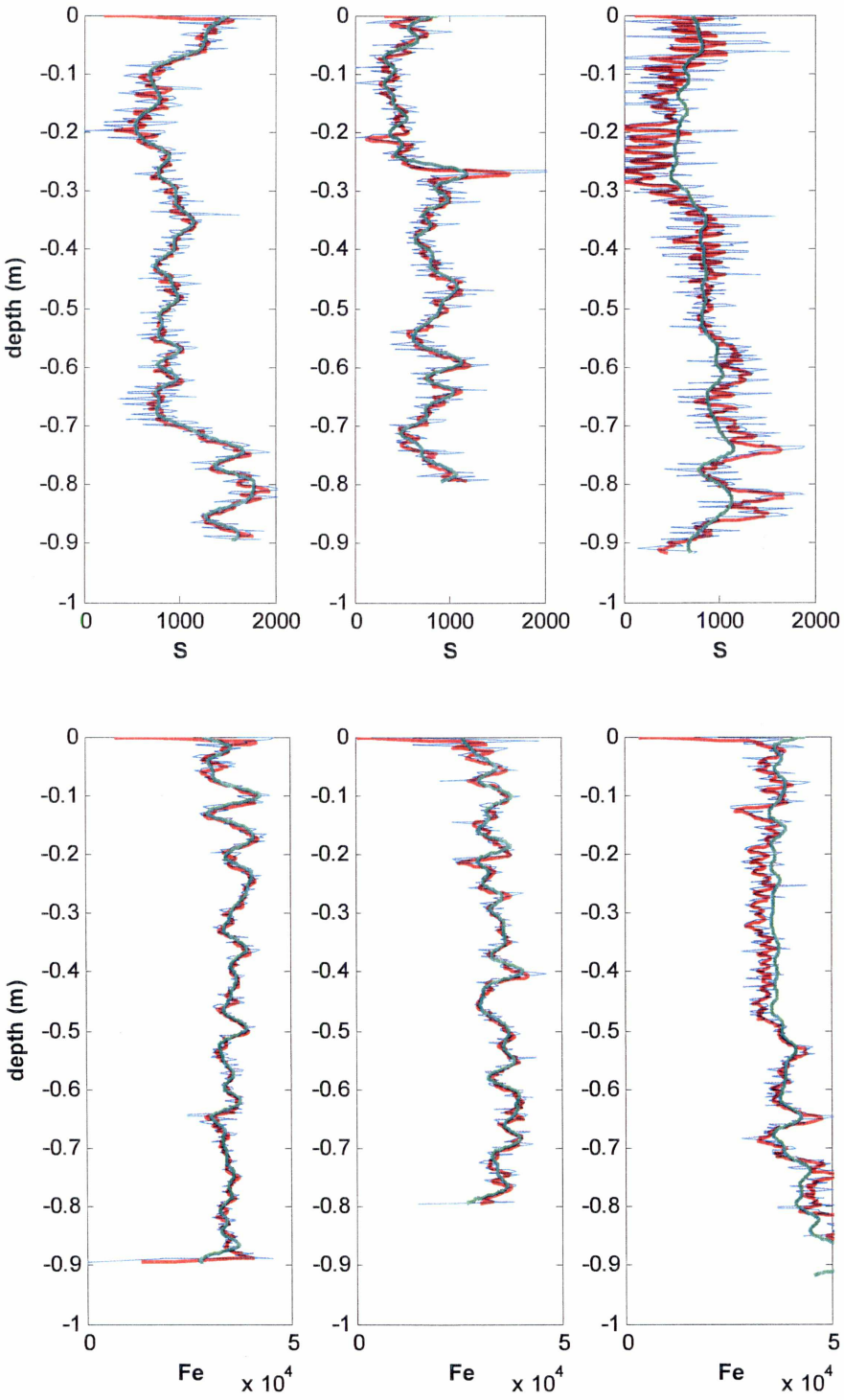
depth (m)
0
-0.1
-0.2
-0.3
-0.4
-0.5
-0.6
-0.7
-0.8
-0.9
-1
0
1000
2000
S
0
5
Fe
x 10^4

**Appendix B.2.**
Vertical distribution of the correlation between two sub-cores (1-2; upper and middle). Red star is maximum correlation. Depth value is the upper value of the data window in the upper core.

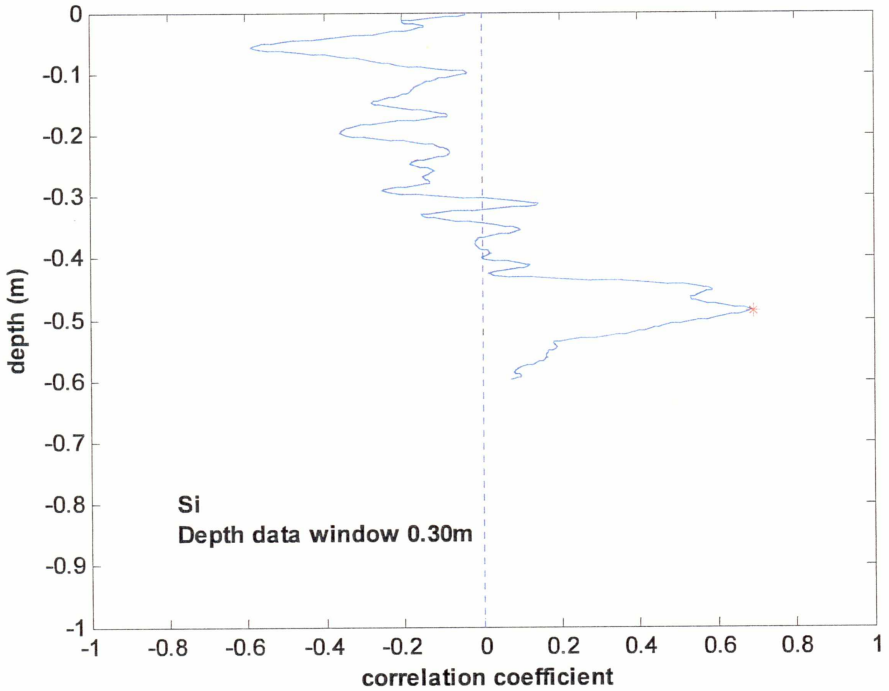

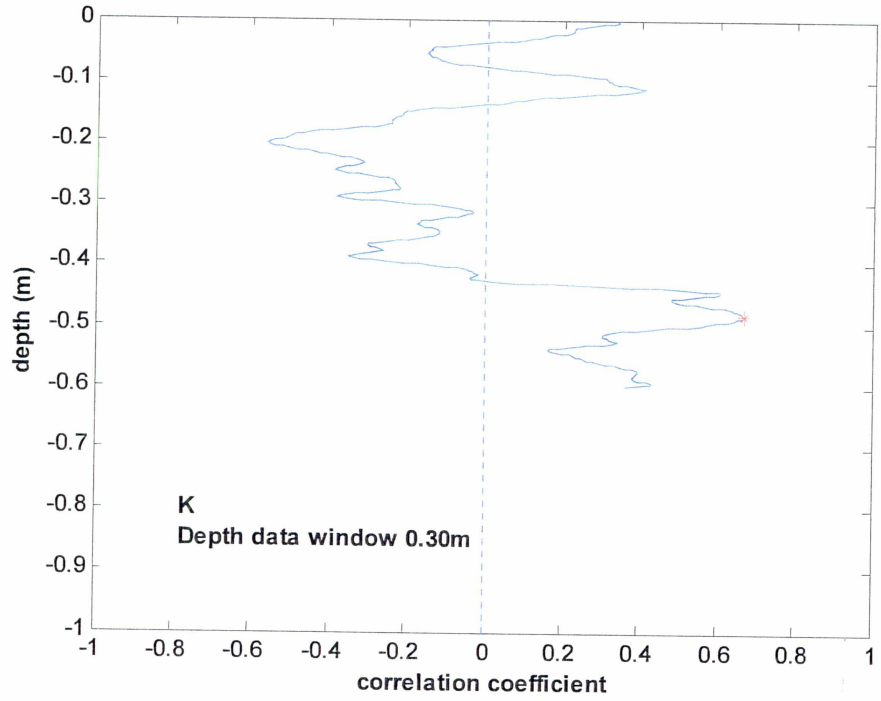
depth (m)
0
-0.1
-0.2
-0.3
-0.4
-0.5
-0.6
-0.7
-0.8
-0.9
-1
-1
-0.8
-0.6
-0.4
-0.2
0
0.2
0.4
0.6
0.8
1
correlation coefficient
K
Depth data window 0.30m

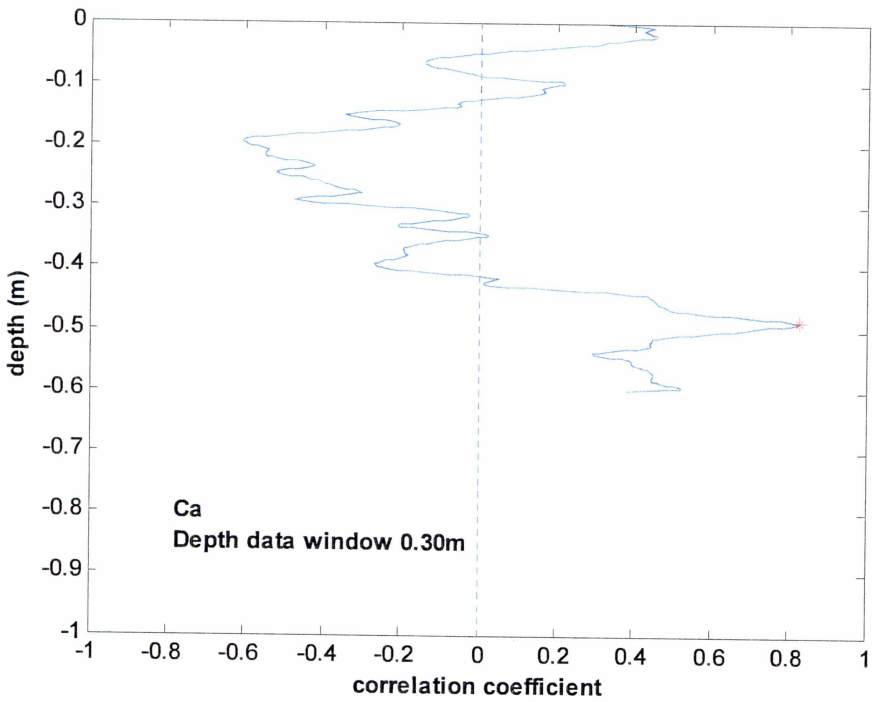
depth (m)
0
-0.1
-0.2
-0.3
-0.4
-0.5
-0.6
-0.7
-0.8
-0.9
-1
-1
-0.8
-0.6
-0.4
-0.2
0
0.2
0.4
0.6
0.8
1
correlation coefficient
Ca
Depth data window 0.30m

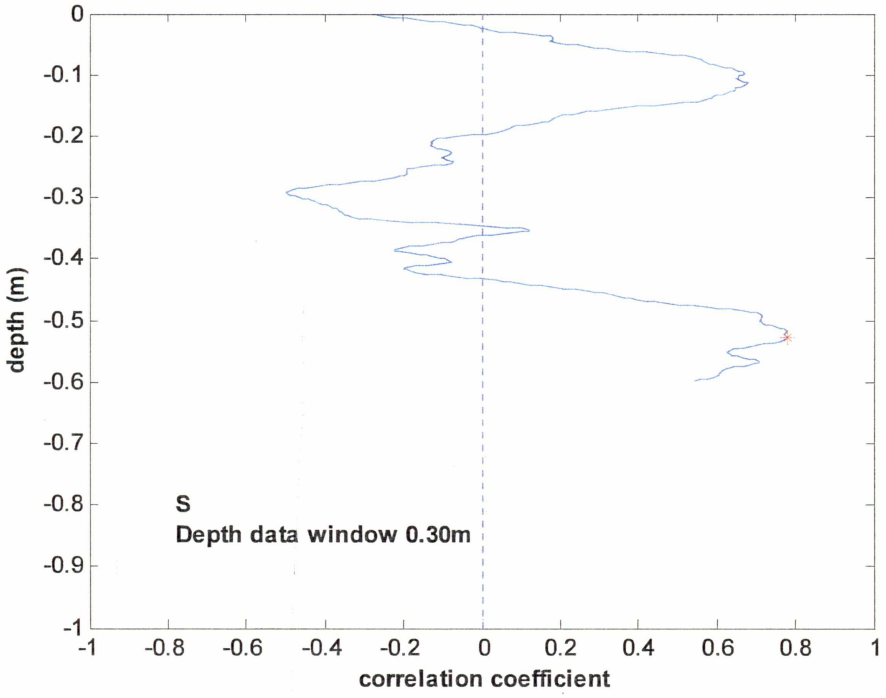
depth (m)
0
-0.1
-0.2
-0.3
-0.4
-0.5
-0.6
-0.7
-0.8
-0.9
-1
S
Depth data window 0.30m
-1
-0.8
-0.6
-0.4
-0.2
0
0.2
0.4
0.6
0.8
1
correlation coefficient

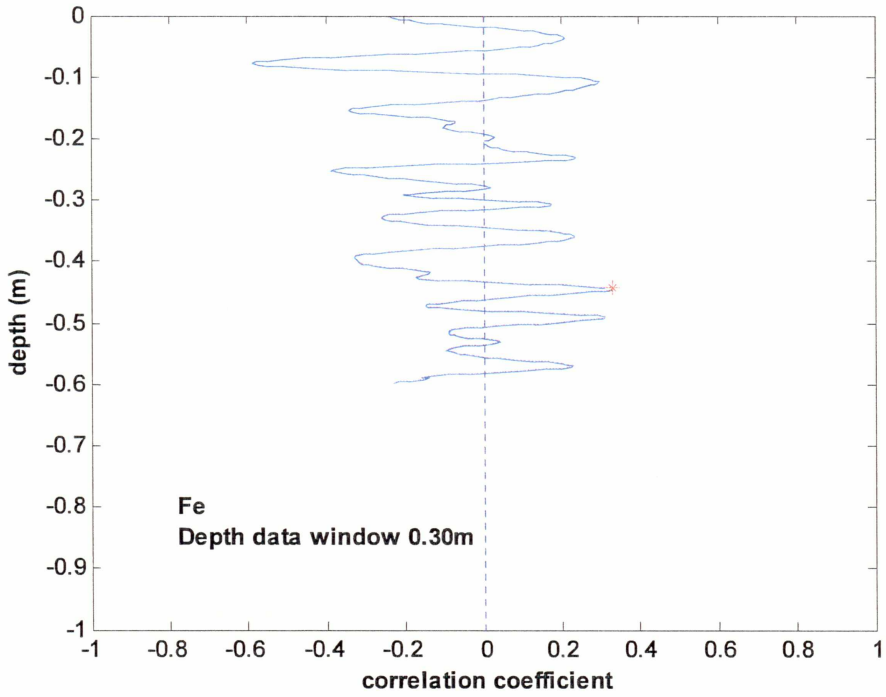
depth (m)
0
-0.1
-0.2
-0.3
-0.4
-0.5
-0.6
-0.7
-0.8
-0.9
-1
Fe
Depth data window 0.30m
-1
-0.8
-0.6
-0.4
-0.2
0
0.2
0.4
0.6
0.8
1
correlation coefficient

**Appendix B.3.**
Vertical distribution of the correlation between two sub-cores (2-3; middle and lower). Red star is maximum correlation. Depth value is the upper value of the data window in the middle core.

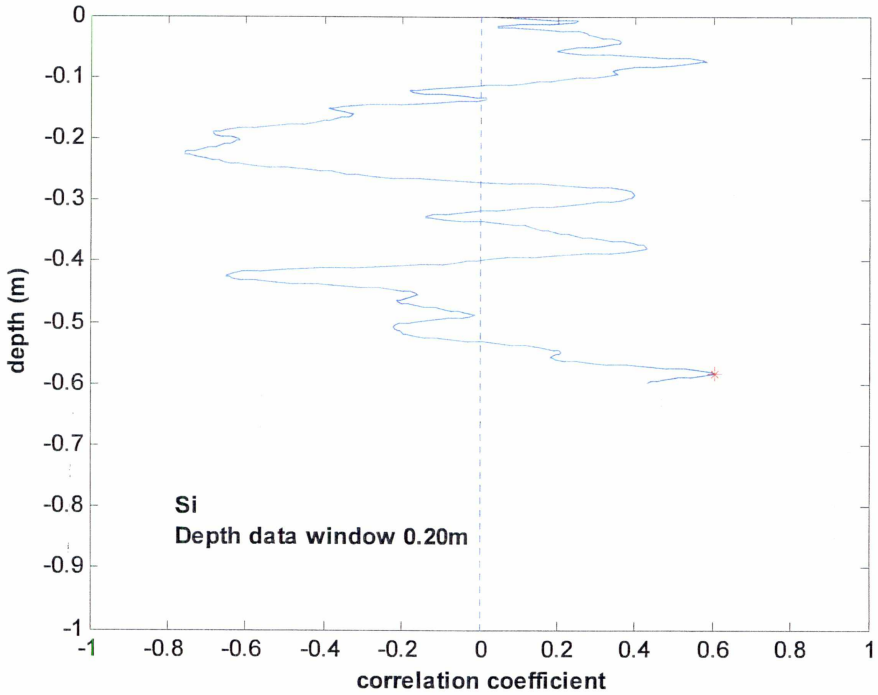

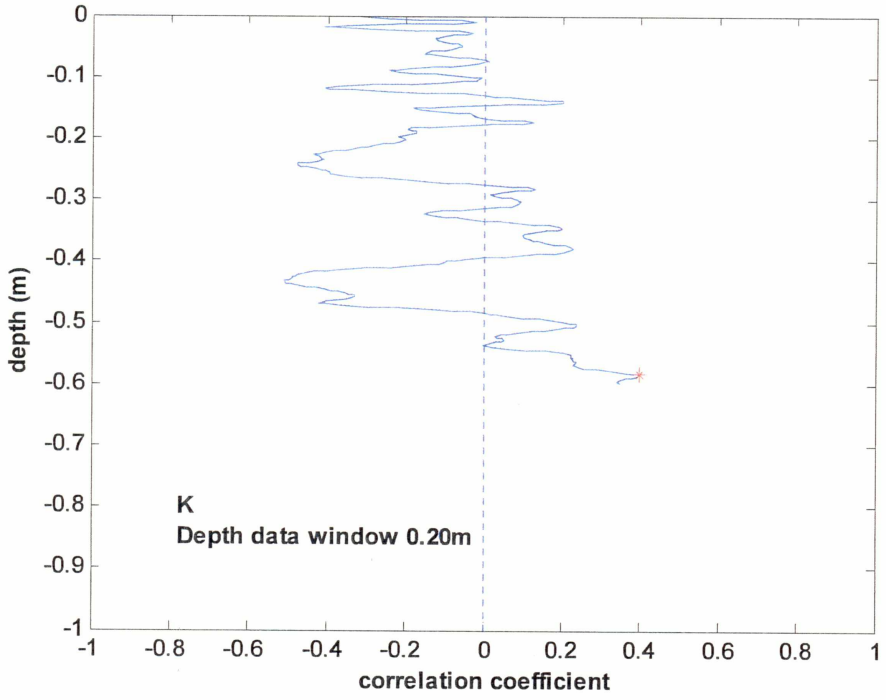
depth (m)
0
-0.1
-0.2
-0.3
-0.4
-0.5
-0.6
-0.7
-0.8
-0.9
-1
-1
-0.8
-0.6
-0.4
-0.2
0
0.2
0.4
0.6
0.8
1
correlation coefficient
K
Depth data window 0.20m

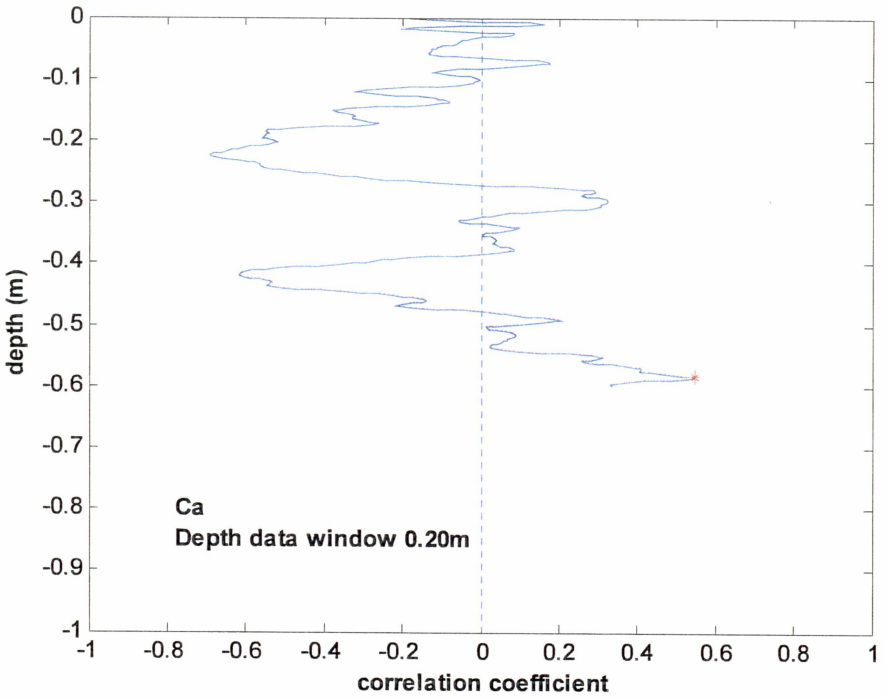
depth (m)
0
-0.1
-0.2
-0.3
-0.4
-0.5
-0.6
-0.7
-0.8
-0.9
-1
-1
-0.8
-0.6
-0.4
-0.2
0
0.2
0.4
0.6
0.8
1
correlation coefficient
Ca
Depth data window 0.20m

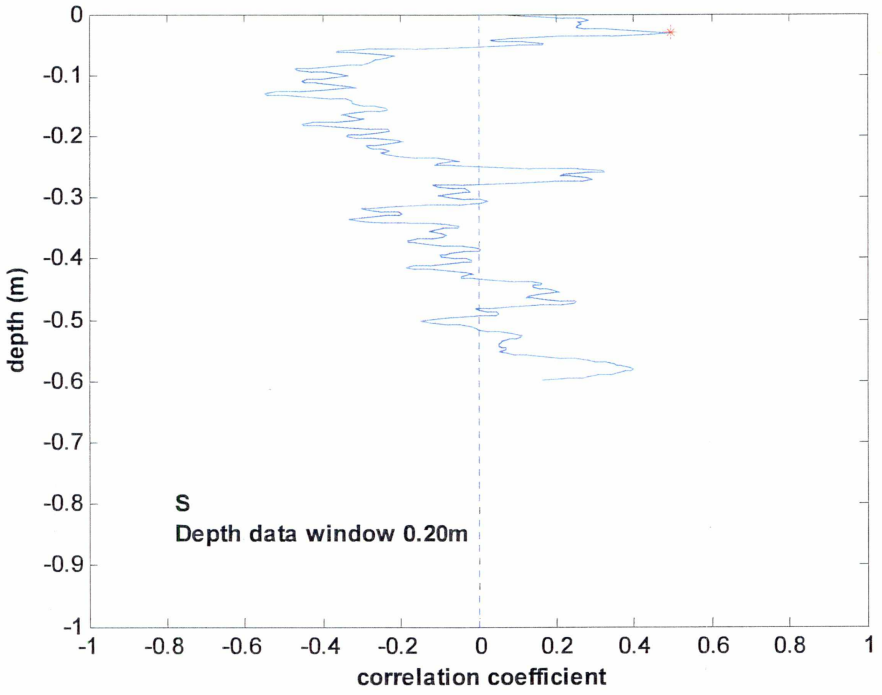
depth (m)
0
-0.1
-0.2
-0.3
-0.4
-0.5
-0.6
-0.7
-0.8
-0.9
-1
-1
-0.8
-0.6
-0.4
-0.2
0
0.2
0.4
0.6
0.8
1
correlation coefficient
S
Depth data window 0.20m

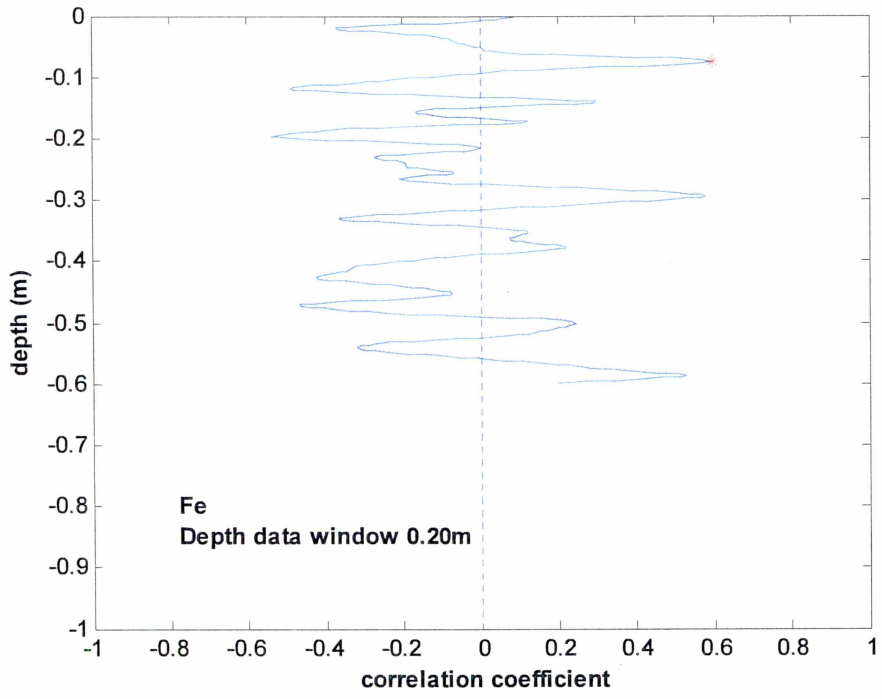
depth (m)
0
-0.1
-0.2
-0.3
-0.4
-0.5
-0.6
-0.7
-0.8
-0.9
-1
-1
-0.8
-0.6
-0.4
-0.2
0
0.2
0.4
0.6
0.8
1
correlation coefficient
Fe
Depth data window 0.20m

**Appendix B.4.**
Vertical distribution of the correlation between two sub-cores (1-3; upper and lower). Red star is maximum correlation. Depth value is the upper value of the data window in the upper core. Core 3 (lower core) window is from -0.05 m until -0.25 m.

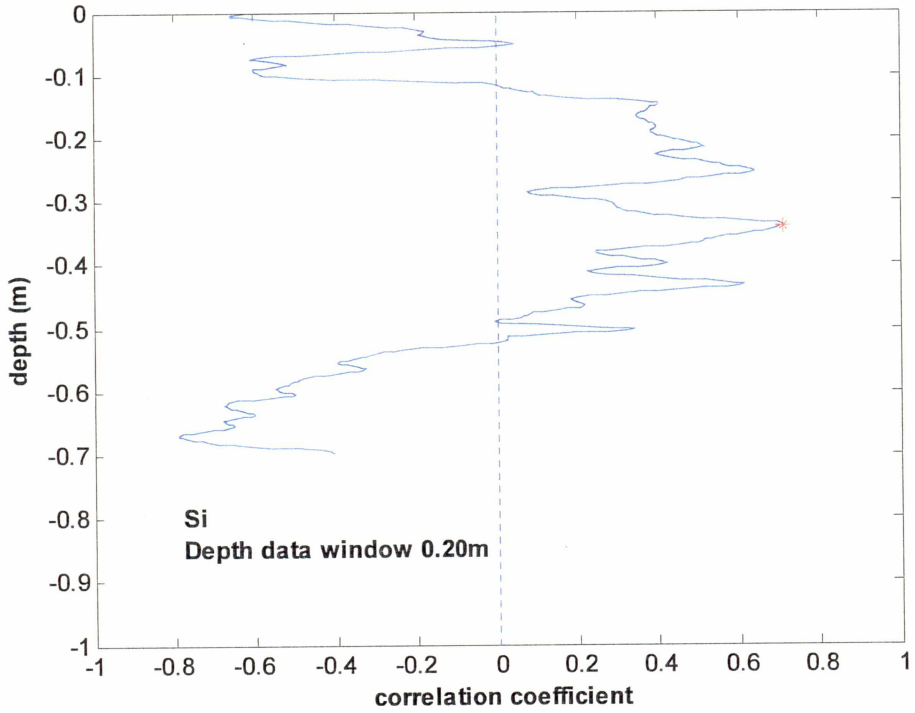

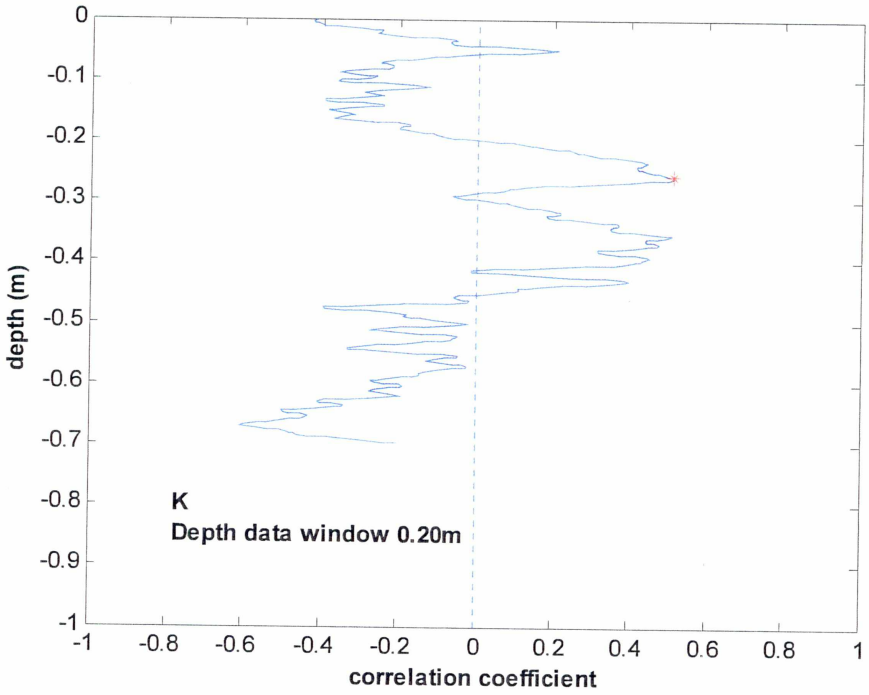
depth (m)
0
-0.1
-0.2
-0.3
-0.4
-0.5
-0.6
-0.7
-0.8
-0.9
-1
-1
-0.8
-0.6
-0.4
-0.2
0
0.2
0.4
0.6
0.8
1
correlation coefficient
K
Depth data window 0.20m

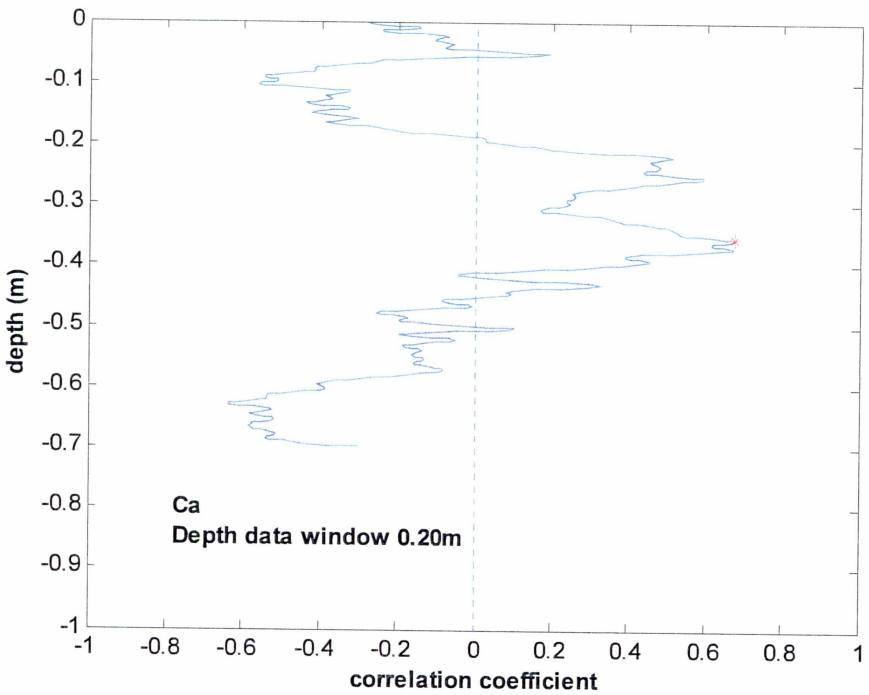
depth (m)
0
-0.1
-0.2
-0.3
-0.4
-0.5
-0.6
-0.7
-0.8
-0.9
-1
-1
-0.8
-0.6
-0.4
-0.2
0
0.2
0.4
0.6
0.8
1
correlation coefficient
Ca
Depth data window 0.20m

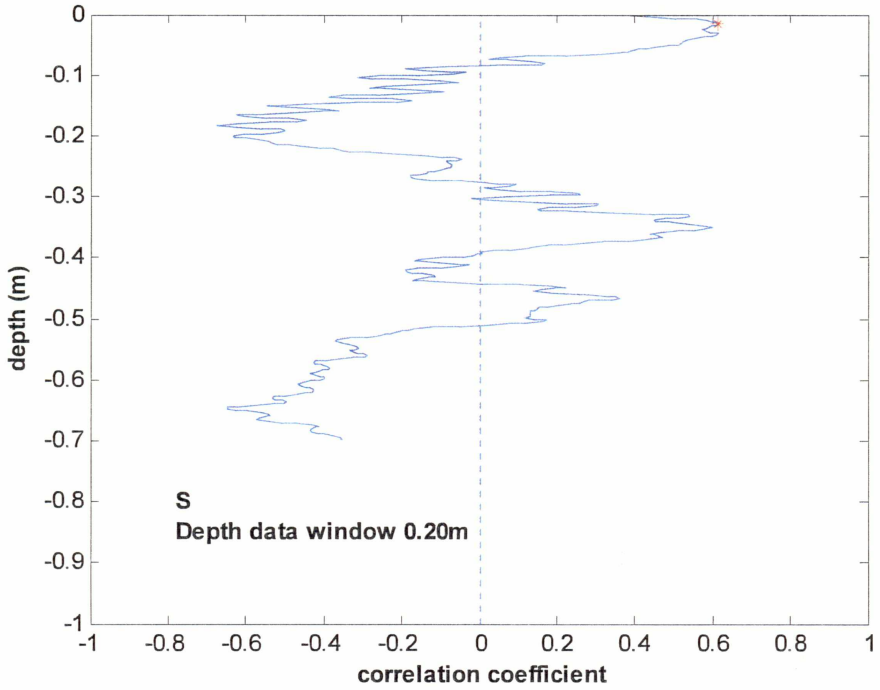
depth (m)
0
-0.1
-0.2
-0.3
-0.4
-0.5
-0.6
-0.7
-0.8
-0.9
-1
-1
-0.8
-0.6
-0.4
-0.2
0
0.2
0.4
0.6
0.8
1
correlation coefficient
S
Depth data window 0.20m

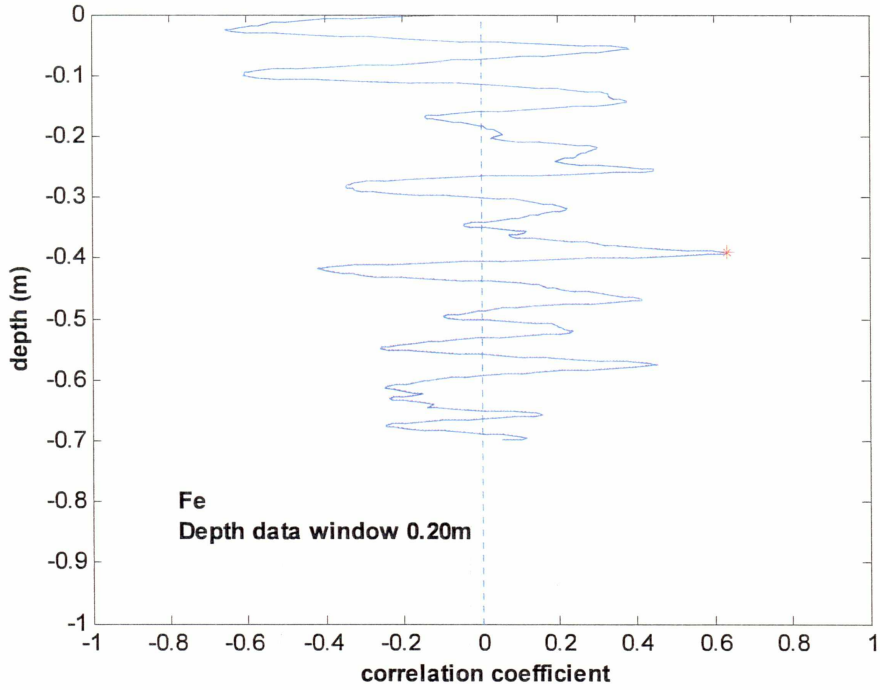
depth (m)
0
-0.1
-0.2
-0.3
-0.4
-0.5
-0.6
-0.7
-0.8
-0.9
-1
-1
-0.8
-0.6
-0.4
-0.2
0
0.2
0.4
0.6
0.8
1
correlation coefficient
Fe
Depth data window 0.20m

**Appendix B.5.**
Vertical distribution of the correlation between two sub-cores (1-3; upper and lower). Red star is maximum correlation. Depth value is the upper value of the data window in the upper core. Core 3 (lower core) window is from -0.02 m until -0.22 m.

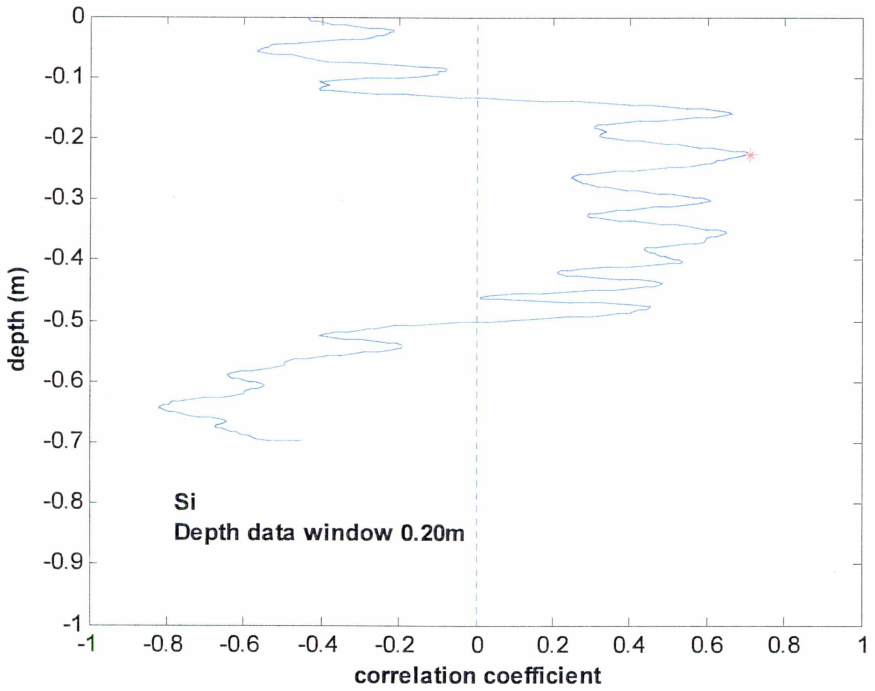

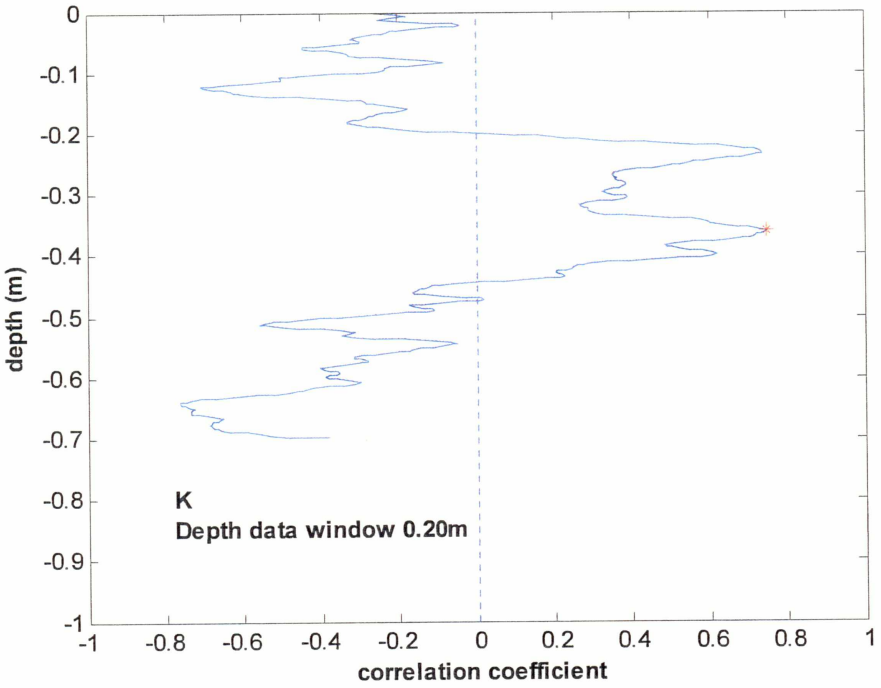
depth (m)
0
-0.1
-0.2
-0.3
-0.4
-0.5
-0.6
-0.7
-0.8
-0.9
-1
-1
-0.8
-0.6
-0.4
-0.2
0
0.2
0.4
0.6
0.8
1
correlation coefficient
K
Depth data window 0.20m

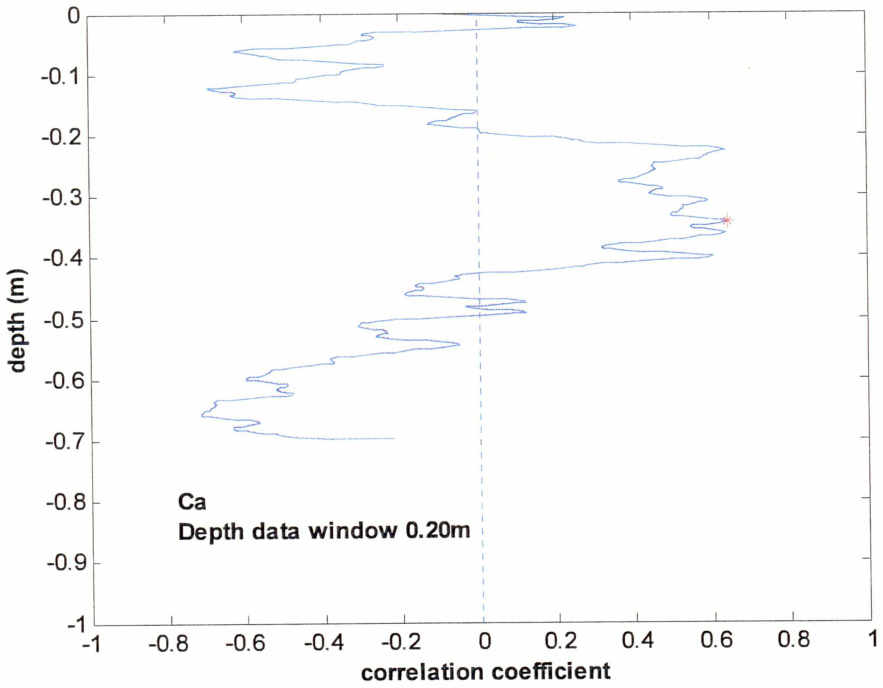
depth (m)
0
-0.1
-0.2
-0.3
-0.4
-0.5
-0.6
-0.7
-0.8
-0.9
-1
-1
-0.8
-0.6
-0.4
-0.2
0
0.2
0.4
0.6
0.8
1
correlation coefficient
Ca
Depth data window 0.20m

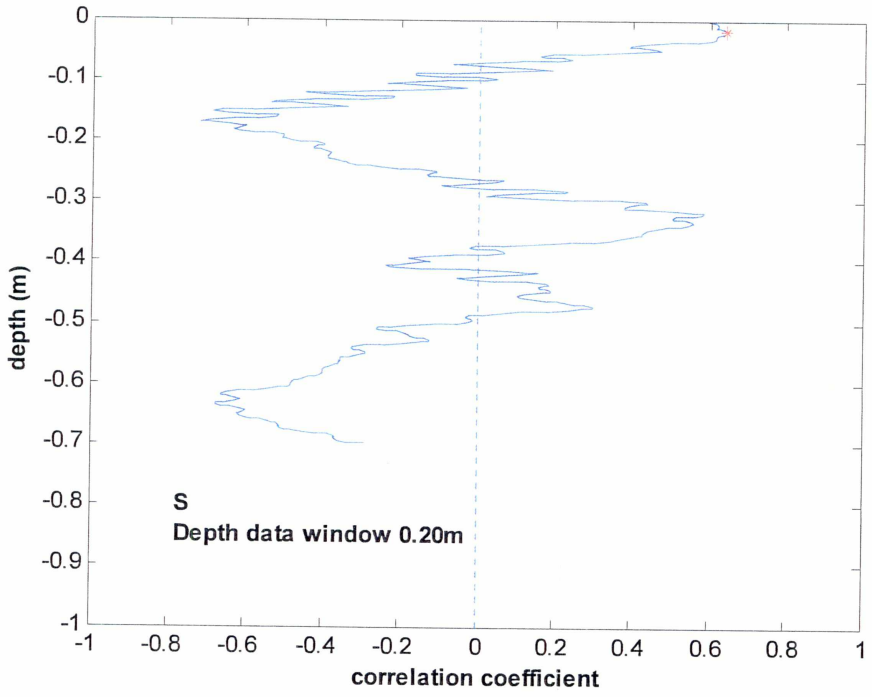
depth (m)
correlation coefficient
S
Depth data window 0.20m

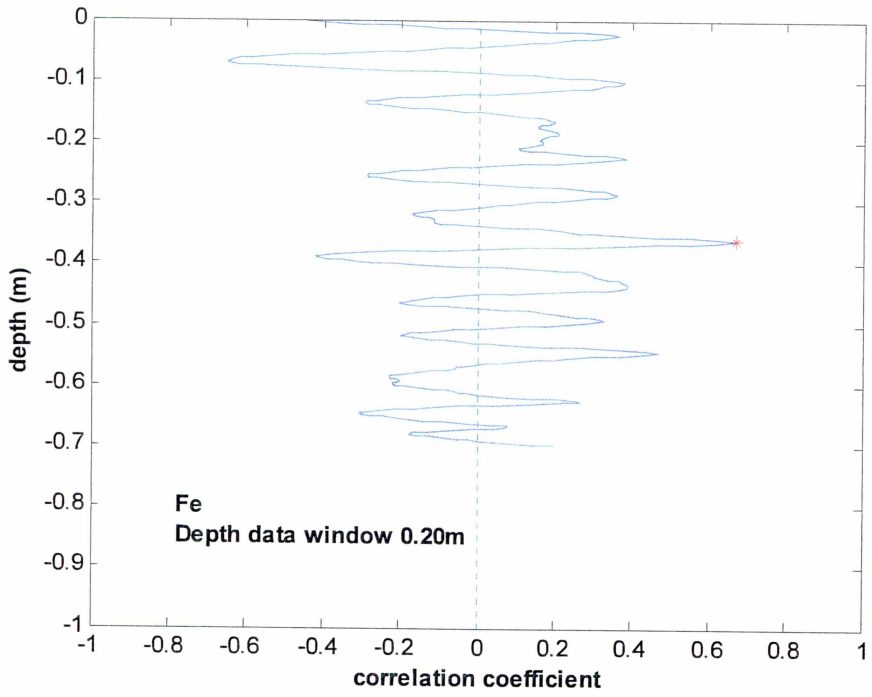
depth (m)
correlation coefficient
Fe
Depth data window 0.20m

## Appendix C. OSL dating of Eskimo settlement structures

Optical stimulated luminescence dating (OSL) can be used to determine the time of burial and covering of sediments. In the GeoArk project OSL has been used in the near coastal landscapes to date coastal landforms under the influence of a changing sea level, a changing climate influencing on wind and wave activity and changing net sediment budgets. As part of the GeoArk project, it was planned as an experiment to use OSL-techniques to date the coverage of beach sediments by larger flat stones used in Eskimo settlement structures. Both Thule Eskimo tent structures and Palaeo Eskimo tent structures were included in the experiment. Samples were collected in small plastic tubes of sediments immediately below flat stones, used by the Eskimos to fit up the area covered by the tent (Fig. C1). In 2007 the experimental samplings took place in three structures at Dahls Skær (Figs. C2, C3, C4 and C5). To confirm the results from 2007 repeated samplings were carried out in 2008 in two neighboring structures to site 2 and 3 at Dahls Skær. Also in 2008, additional sampling was carried out in 2 tent structures at Kap Berghaus (Figs. C6 and C7) and one tent structure on Hvalros Ø. At Kap Berghaus a parallel sampling was carried out at each site, one of the beach ridges close to the tent structure but not affected by tent stones and one of the surface materials just below a larger placed tent stone. The results from the 2007 sampling, and preliminary calculations based on the 2008 sampling are presented below, and indicate a promising potential to use OSL dating for the approximate dating of settlement structures on beach ridges. Obviously an improved sampling technique could be developed, allowing sampling of a more narrow depth interval immediately below placed stones. The obtained ages presumably are slightly too high and have to be considered as maximum ages for the settlement structures.

*Figure C1. Sampling of beach ridge sediments under placed flat stone in the interior of a Palaeo Eskimo tent ring at Dahls Skær.*

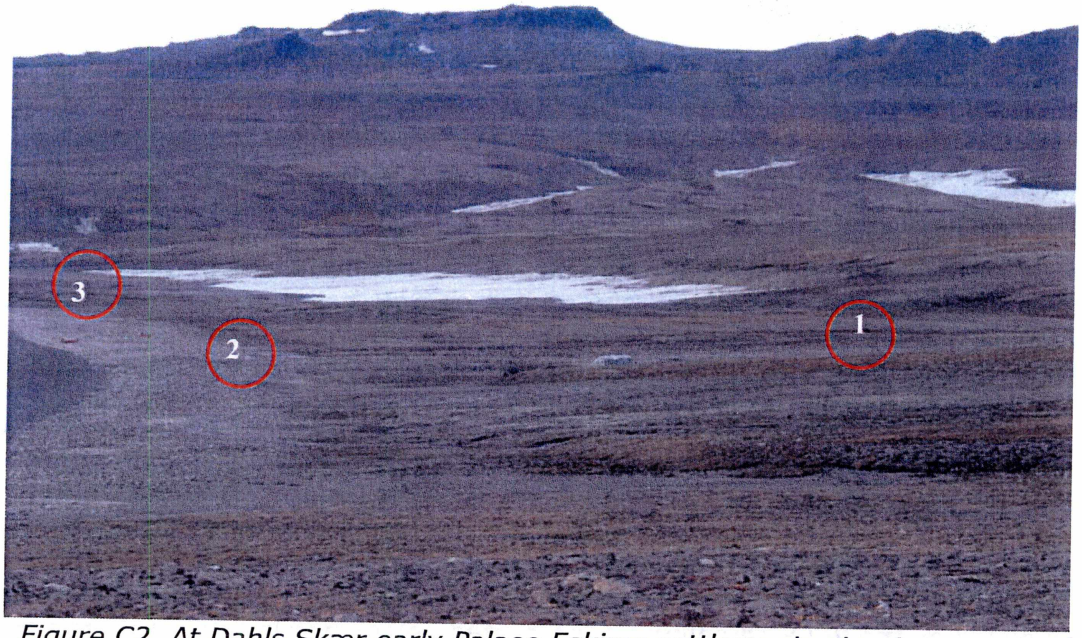


*Figure C2. At Dahls Skær early Palaeo Eskimo settlements structures were observed on the uppermost beach ridges (locality 1 and Fig. C3.). At locality 2 (Fig. C4.) large Thule Culture tent rings were found in the wet depression affected by periodic wash over, just behind the present beach ridge. In the western part of the bay at Dahls Skær (locality 3 and Fig. C5) close to a small stream, a small number of settlement structures were located. The structures were quite distinct and appeared to have a Palaeo Eskimo origin, which was confirmed by archaeological finds. But displacements of stones seem to have taken place, probably evidencing Thule Culture activity, including the appearance of play feature like structures inside the small settlement areas.*

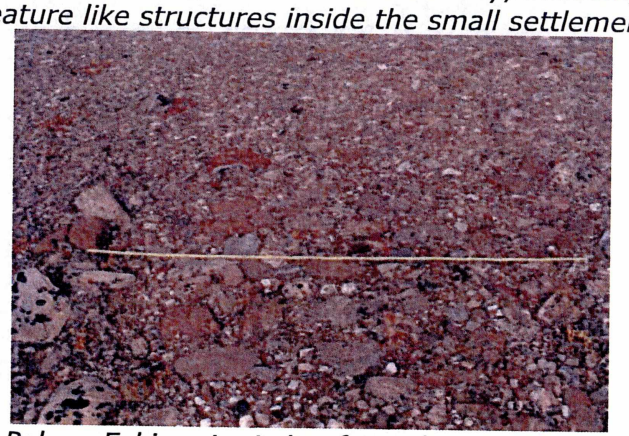

*Figure C3. Early Palaeo Eskimo tent ring from the uppermost beach ridge in the Dahls Skær bay. OSL dating confirm the structure to belong to the Inuit pioneer era in North East Greenland, and show a maximum age of the tent ring of 5100 YBP ± 600 YBP.*

*Figure C4. Thule Culture tent ring from the lowermost part of the beach ridge plain. The area is presently wet during summers and affected by periodic wash over from the sea. Two neighboring tent rings have been sampled in 2007 and 2008 and dated by OSL. Dating confirm the tent rings to belong to the Thule era and show maximum ages of 720 YBP ± 150 Y (2007) and 740 YBP ± 210 Y (2008). Both tent rings seem to belong to the Thule pioneer era in the early 15$^{th}$ century.*

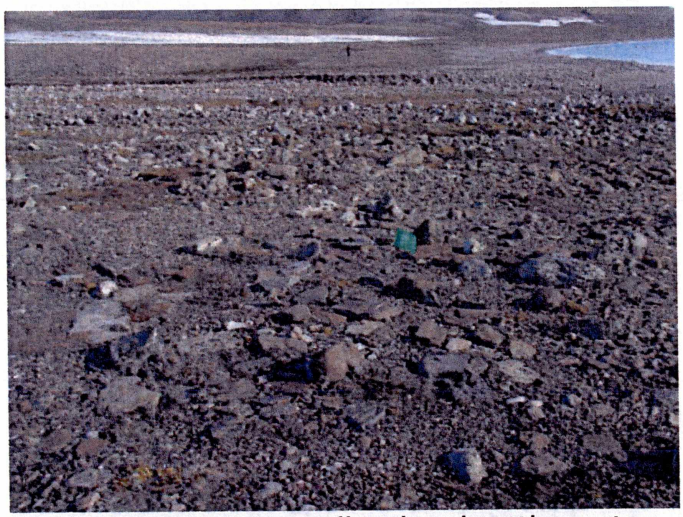

*Figure C5. Settlement structure in a small isolated settlement area in the western part of the Dahls Skær bay. Evidence of both Palaeo Eskimo (Dorset/Sarqaq) and Thule Culture activity are found in the specific structures and in the small settlement area as such. An OSL dating from 2007 show an age of 1520 YBP ± 150 Y, whereas preliminary OSL calculations of a sample from a neighboring structure in 2008 indicate and age of 400-500 YBP. The 2007 dating could represent a Palaeo Eskimo signature in spite of the present understanding, that Palaeo Eskimos neither from the north nor from the south are known to be present in East Greenland at that time, and nearly all Greenland is regarded being desolated 0 AD and for the following millennium. The 2008 age of 400-500 YBP could represent the Thule Culture signature through displacements of stones.*

*Figure C6. At Kap Berghaus to sets of sampling for OSL dating were carried out. One representing a beach ridge (background sample site) and one representing a structure of flat stones placed in the interior of a tent ring on the beach ridge (foreground). The shown beach ridge in this lower part of the beach ridge plain at Kap Berghaus (4-5 m a.s.l.) show an OSL age of approximately 5800 YBP, indicating the position of the sea level at that time. Data and age for the settlement structure are still to be calculated and concluded.*

*Figure C7. A lower lying beach ridge at Kap Berghaus ( 2-3 m. a.s.l.) show an OSL age of approximately 4500 YBP, and the preliminary calculations of a sample from a Sarqaq tent ring, indicate that the arrival of the Sarqaq culture in the area, presumably from the south, took place during the Inuit pioneer phase in Greenland, shortly after 4500 YBP.*